Dissertation

zur Erlangung des Doktorgrades

der Fakultät für Chemie und Pharmazie der

Ludwig-Maximilians-Universität München

Molecularly targeted imaging and radionuclide therapy

of non-thyroidal tumors following viral and non-viral

sodium iodide symporter (NIS) gene delivery

vorgelegt von

Kathrin Klutz

aus Aalen

2010

# Table of Contents

# 1. Introduction

## The sodium iodide symporter (NIS)

### The sodium iodide symporter and its role as therapy gene

The sodium iodide symporter (NIS) represents an intrinsic plasma membrane glycoprotein with 13 transmembrane domains localized at the baslolateral membrane of thyroid follicular cells that mediates the active transport of iodide in the thyroid gland (Fig. 1). Cloning and molecular characterization of the NIS gene (Spitzweg and Morris, 2002b) allowed investigation of its expression and regulation in thyroidal and nonthyroidal tissues (Spitzweg *et al.*, 1998; Spitzweg *et al.*, 1999b; Spitzweg *et al.*, 2000a;



**Fig. 1**: Schematic illustration of the sodium iodide symporter (NIS). With permission reproduced from Spitzweg *et al.*, 2001c.

Spitzweg *et al.*, 2001b; Spitzweg and Morris, 2002b; Unterholzner *et al.*, 2006; Willhauck *et al.*, 2008c), its pathophysiological role in benign and malignant thyroid disease as well its potential role in diagnosis and therapy of cancer outside the thyroid gland (Spitzweg *et al.*, 1999a; Spitzweg *et al.*, 2000a; Spitzweg and Morris, 2002b).

NIS-mediated iodide transport is inhibited by the $Na^+/K^+$-ATPase inhibitor ouabain, as well as thiocyanate ($SCN^-$) and perchlorate ($ClO_4^-$) (Spitzweg and Morris, 2002b). TSH is the main stimulatory regulator of thyroidal NIS expression as well as of its proper membrane targeting, acting through the adenylate cyclase-cAMP mediated pathway (Spitzweg and Morris, 2002b).

NIS represents one of the oldest and most successful targets for molecular imaging and targeted radionuclide therapy. Functional NIS expression in differentiated thyroid carcinomas allows not only postoperative localization and ablation of the thyroid remnant as well metastases, but also provides the possibility of subsequent postablative ^{131}I total body scanning that can diagnose local and metastatic residual and recurrent disease followed by ^{131}I ablation, thereby improving the prognosis of thyroid cancer patients significantly and making thyroid cancer one of the most manageable cancers (Spitzweg *et al.*, 2001c; Spitzweg and Morris, 2002b). Thyroidal NIS expression therefore provides the molecular basis for the most effective form of systemic anticancer radiotherapy available to the clinician today.
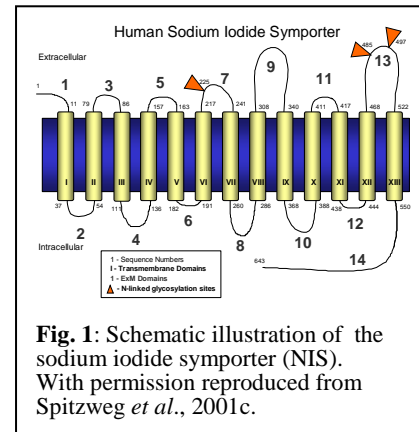
Cloning of the NIS gene in 1996 has provided us with a powerful new reporter and therapy gene, that allowed the development of a promising cytoreductive gene therapy strategy based on NIS gene transfer in extrathyroidal tumors followed by radioiodine application (Fig. 2). Many of the characteristics of NIS suggest that it represents an ideal therapy gene due to several advantages:

### 1. High degree of efficacy

NIS is already being used clinically as molecular basis of $^{131}$I therapy, an already approved anticancer therapy in thyroid cancer with a well-understood therapeutic window and safety profile.



**Fig. 2**: The role of the NIS gene as diagnostic and therapeutic gene.
With permission reproduced from Spitzweg *et al*., 2007a

### 2. High bystander effect

NIS gene therapy is associated with a substantial bystander effect based on the crossfire effect of the beta-emitter $^{131}$I with a path length of up to 2.4 mm. A bystander effect is desirable for any kind of gene therapy strategy, because it reduces the level of transduction efficiency required for a therapeutic response.

### 3. Dual function of NIS as a diagnostic and therapeutic gene

In its role as reporter gene NIS allows direct, non-invasive imaging of functional NIS expression by $^{123}$I-scintigraphy, $^{123}$I-SPECT- or $^{124}$I-PET-imaging, as well as exact dosimetric calculations before proceeding to therapeutic application of $^{131}$I.

### 4. High degree of specificity

Native expression of NIS outside the thyroid is very low not causing significant morbidity after $^{131}$I application, as known from the extensive experience with $^{131}$I therapy in thyroid cancer.

### 5. Normal human gene and protein

NIS as a normal human gene and protein implies that its expression in cancer cells is unlikely to be toxic or to elicit a significant immune response that could limit its efficacy.

In their pioneer studies C. Spitzweg and J.C. Morris chose prostate cancer as the initial tumor model and used the prostate-specific antigen (PSA) promoter to achieve prostate-

specific iodide accumulation, which resulted in a significant therapeutic effect after application of $^{131}$I, even in the absence of iodide organification (Spitzweg *et al.*, 1999c; Spitzweg *et al.*, 2000b; Spitzweg *et al.*, 2001a; Kakinuma *et al.*, 2003). In preparation of the first phase I clinical study on $^{131}$I therapy of locally recurrent prostate cancer after local NIS gene transfer, these data were confirmed in extensive biotoxicity and efficacy studies in rats and in a preclinical large animal model in beagle dogs after intraprostatic injection of a replication-incompetent adenovirus without significant toxicity outside the prostate and thyroid gland (Dwyer *et al.*, 2005b). After further extensive preclinical evaluation in several tumor models by various groups including our own, NIS has been characterized as a promising target gene for the treatment of non-thyroid cancers following selective NIS gene transfer into tumor cells which allows therapeutic application of radioiodine (Spitzweg *et al.*, 1999c; Spitzweg *et al.*, 2000b; Spitzweg *et al.*, 2001a; Spitzweg *et al.*, 2001c; Spitzweg and Morris, 2002b; Kakinuma *et al.*, 2003; Dingli *et al.*, 2004; Cengic *et al.*, 2005; Dwyer *et al.*, 2005a; Scholz *et al.*, 2005; Dwyer *et al.*, 2006a; Dwyer *et al.*, 2006b; Spitzweg *et al.*, 2007; Willhauck *et al.*, 2007; Willhauck *et al.*, 2008b; Willhauck *et al.*, 2008c; Hingorani *et al.*, 2010a; Li *et al.*, 2010; Penheiter *et al.*, 2010; Trujillo *et al.*, 2010).
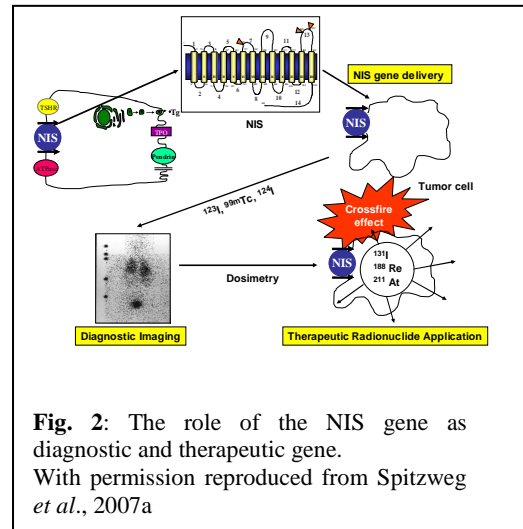
As logical consequence of these pioneer studies in the NIS gene therapy field, the next crucial step towards clinical application of the promising NIS gene therapy concept, has to be the evaluation of gene transfer methods that own the potential to achieve sufficient tumor-selective transgene expression levels not only after local or regional but also after systemic application to be able to reach tumor metastases.

Only a limited number of studies have investigated systemic NIS gene delivery approaches with the aim of NIS-targeted radionuclide therapy of metastatic disease. An oncolytic measles virus encoding human NIS was applied systemically in a multiple myeloma mouse model and allowed to enhance the oncolytic potency of the virus after $^{131}$I application (Dingli *et al.*, 2004). In a more recent study, an oncolytic vesicular stomatitis virus (VSV) was designed to express NIS to be able to monitor virus replication by $^{123}$I scintigraphic imaging in addition to stimulation of the oncolytic potency by the combination with $^{131}$I therapy, which was successfully investigated in a multiple myeloma mouse model after systemic vesicular stomatitis virus application (Goel *et al.*, 2007).

**Iodide organification and alternative radionuclides**

Following NIS transduction the achieved radiation dose responsible for a therapeutic effect of trapped $^{131}$I is determined by a variety of factors, including the rate of iodide uptake and

efflux, the rate of radiocative decay, as well as the possibility of iodide recirculation. In contrast to extrathyroidal tumors, in the thyroid gland thyroid peroxidase-catalyzed oxidation and incorporation of iodide into tyrosyl residues along the thyroglobulin backbone, a process called iodide organification, increases the effective half-life and therefore therapeutic efficacy of accumulated radioioidine (Spitzweg and Morris, 2002b). Many studies demonstrating a therapeutic effect of ^{131}I and alternative radionuclides such as [188]Re and [211]At following NIS gene transfer in various non-organifying tumor models (Spitzweg *et al.*, 1999c; Spitzweg *et al.*, 2000b; Spitzweg *et al.*, 2001c; Petrich *et al.*, 2006; Willhauck *et al.*, 2007 Dadachova *et al.*, 2005; Willhauck *et al.*, 2008a), clearly demonstrate that iodide organification is not a mandatory requirement for a therapeutic effect of [131]I. In addition, in non-thyroidal tumors with rapid iodide efflux, therapeutic efficacy of NIS-targeted radionuclide therapy can be significantly enhanced by application of alternative radionuclides, such as the beta-emitter [188]Re or the alpha-emitter [211]At, that are known to be also transported by NIS, but offer the possibility of higher energy deposition in a shorter time period due to their higher energy and shorter half-life ([188]Re: physical half-life 16.7 h, E = 0,764 MeV, path length 23-32 mm; [211]At: physical half-life 7,2 h, high linear energy transfer 97 keV/μm) as compared to [131]I (physical half-life 8 d, E = 0,134 MeV, therapeutic range 2.6-5 mm), which has convincingly been demonstrated by several groups, including our own studies in the prostate cancer model (Dadachova *et al.*, 2005; Petrich *et al.*, 2006; Willhauck *et al.*, 2007; Willhauck *et al.*, 2008a).

**The sodium iodide symporter and its role as reporter gene**

Cloning of NIS has provided us not only with a powerful therapeutic gene, but also with one of the most promising reporter genes available today. NIS has many characteristics of an ideal reporter gene, as it represents a non-immunogenic protein with a well-defined body biodistribution and expression, that mediates the transport of readily available radionuclides, such as ^{131}I, ^{123}I, ^{125}I, [124]I, ^{99m}Tc, [188]Re or [211]At, and allows signal amplification by the accumulation of the radionuclide.

The field of gene therapy has made considerable strides in the last decade by the development of new vectors and an increasing repertoire of therapeutic genes. Non-invasive monitoring of the *in vivo* distribution of viral and non-viral vectors, as well as monitoring of the biodistribution, level and duration of transgene expression have been recognized as critical elements in the design of clinical gene therapy trials. The need for this technology is

further highlighted by the advent of replication-competent viruses for cancer gene therapy where it is critically important to monitor biodistribution, replication and elimination *in vivo*.

Several investigators have studied the potential of NIS as novel reporter gene in various applications, demonstrating that *in vivo* imaging of radioiodine accumulation correlates well with the results of *ex vivo* gamma counter measurements as well as NIS mRNA and protein analysis (Spitzweg *et al.*, 1999c; Spitzweg *et al.*, 2001a; Spitzweg and Morris, 2002b; Dingli *et al.*, 2003b; Kakinuma *et al.*, 2003; Scholz *et al.*, 2005; Spitzweg *et al.*, 2007; Willhauck *et al.*, 2007; Willhauck *et al.*, 2008b).

Furthermore, in several studies NIS was successfully used as a reporter gene to monitor *in vivo* biodistribution of replication-competent viral vectors, including oncolytic measles virus in liver cancer and myeloma xenograft models, oncolytic vesicular stomatitis virus in a myeloma xenograft model, as well as oncolytic adenovirus in a colon cancer xenograft model using conventional $^{123}$I- or $^{99m}$Tc-gamma camera imaging or $^{99m}$Tc-SPECT/CT fusion imaging (Blechacz *et al.*, 2006; Goel *et al.*, 2007; Merron *et al.*, 2007).

Taken together, the pioneer work in the prostate cancer model by J. C. Morris and C. Spitzweg (Spitzweg *et al.*, 1999c; Spitzweg *et al.*, 2000b; Spitzweg *et al.*, 2001a; Kakinuma *et al.*, 2003) and consecutive work in other tumor models by several groups including our own has convincingly demonstrated the gene therapy and oncology communities the enormous potential of NIS as novel reporter and therapy gene that has paved the way for the development of an innovative and potentially curative cytoreductive gene therapy strategy.

## Cancer Gene Therapy

Cancer gene therapy represents one of the most rapidly evolving areas in preclinical and clinical cancer research. Two of the most important problems to overcome are lack of selectivity of the existing vectors and low efficiency of gene transfer. Cancer gene therapy is the transfer to and expression of genetic material in malignant human cells for a therapeutic purpose. This relatively narrow definition can be extended to include gene delivery to tumor and normal immune cells for modulating antitumor immune response. The term gene therapy encompasses a range of approaches, including corrective gene therapy to restore the normal function of a deleted or mutated gene (usually a tumor suppressor gene) or negate the effect of a tumor promoting gene (oncogene), cytoreductive gene therapy to deliver an

exogenous gene that causes cell death and immunomodulatory gene therapy to induce gene expression that enhances immune responses against tumor tissues. Identifying and elaborating sophisticated selective gene therapy systems may amount to nothing unless genes can be targeted to a significant fraction of clonogenic cells. To date most studies have focused on locoregional gene delivery by direct injection or infusion, a technique with limited relevance to clinical situations such as metastatic disease in which systemic delivery systems are needed. For this reason vector development represents an extremely active field of investigation (Verma and Somia, 1997). Vectors for gene therapy can be considered under the headings of viral and non-viral systems.

**Viral vector systems**

Viruses are attractive vehicles for gene delivery since they have evolved specific and efficient means of entering human cells and expressing their genes. The main challenge for viral vector development lies in harnessing the targeting efficiency of viruses, while abrogating their ability to cause infection and disease. Modifying the viral genome to remove sequences required for viral replication and pathogenicity represents a means of achieving these goals. The removed viral coding sequences can be replaced with exogenous therapeutic genes. Such genetically engineered viruses theoretically retain wild-type viral cellular tropism and ensure transgene expression in the target cell population without causing ongoing infection. Attempts to alter the natural tropisms of viruses by manipulating the viral components that mediate cell binding and internalization represent a means of redirecting viruses specifically to chosen target cells (Krasnykh *et al.*, 1996). To date most viral vector development has focused on retrovirus, adenovirus, adeno-associated virus, herpes simplex virus and pox virus.

The use of adenoviruses has emerged as a powerful approach for increasing transduction efficiency and therapeutic efficacy in cancer gene therapy.

Adenoviruses are double strand DNA viruses. More than 40 adenovirus serotypes in 6 groups (A to F) have been identified. Group C viruses (serotypes Ad2 and Ad5) have been most extensively evaluated as candidates for gene delivery (Zhang *et al.*, 1999)**.** However, up to 70% of the general population have neutralizing antibodies to Ad2 and Ad5 that accelerate adenovirus clearance after initial administration. Adenoviruses enter cells by binding to the coxsackievirus- (CAR) and adenovirus receptor, which facilitates interaction of viral arginine-glycine-aspartate (RGD) sequences with cellular intergrins. After internalization the virus escapes from cellular endosomes, partially disassembles and

translocates to the nucleus, where viral gene expression begins. Clearly administering replicating adenoviruses in patients with cancer, of whom many are immune suppressed, raises important safety concerns. Therefore, efforts have been made to render adenovirus incapable of replication (so-called replication defective adenovirus). It has been achieved by deleting one or more of the early adenovirus genes E1 to E4. Replication defective adenoviruses have a number of potential advantages as vectors for targeted gene delivery, as they can be produced in high titers ($10^{10}$ to $10^{11}$ infectious units per ml), they can infect nondividing cells, and gene expression occurs without integration into the host genome. Furthermore, the use of replication-competent adenoviruses has emerged as a powerful approach for increasing transduction efficiency and therapeutic efficacy by an additional oncolytic effect due to selective virus replication (oncolytic virotherapy). The first example of conditionally replicative adenovirus was ONYX 015, targeting cancer cells with a defective p53 pathway (Everts and Van Der Poel, 2005). Tumor-selective replication of adenoviruses has also been achieved by the application of tissue- or tumor-specific promoters to drive the expression of genes essential for viral replication, such as E1A. This has been investigated in a variety of tumor models, including prostate cancer using the prostate-specific antigen (PSA) or rat probasin promoter to drive E1 expression, and in liver cancer using the AFP promoter (Everts and Van Der Poel, 2005). Overall, replicating adenovirus-based gene therapy vectors are the most widely used platform for gene delivery offering high promise for cancer treatment, and have already been used safely in human clinical trials (Everts and Van Der Poel, 2005). The major hurdles of effective oncolytic virotherapy, in particular after systemic application, have been antiviral immune responses, inefficient viral spread within the tumor and significant virus pooling in the liver, reducing the levels of viable virus reaching the tumor resulting in limited transduction efficiency. In order to enhance the antitumor effect of oncolytic virotherapy the combination with conventional anticancer strategies, such as chemotherapy, radiotherapy, or gene therapy as a multimodal cancer therapy approach has been the major focus of studies in the recent years.

**Non-viral vector systems**

Delivering genes to target organs with synthetic vectors is a vital alternative to virus-based methods. For systemic delivery polycationic molecules are used to condense DNA into sub-micrometer particles termed polyplexes, which are efficiently internalized into cells, while DNA is protected from nucleases. Several polycations, like polyethylenimine (PEI), bear an intrinsic endosomolytic mechanism, which allows the transition of the polyplexes from the

endosome to the cytoplasm (Meyer and Wagner, 2006). Non-viral gene delivery systems are characterized by ease of synthesis, lower immunogenicity and greater flexibility. In recent years they have also been significantly improved in terms of toxicity profiles, tumor-selectivity and transduction efficiency, and therefore represent highly promising gene delivery vehicles for systemic gene therapy approaches.

Since these non-viral systems do not show selectivity to specific target cells, they can either be used in a more universal way or their surface may be chemically or biologically modified for specific targeting. Moreover, they offer an enhanced biosafety profile since they can be generated protein-free or non-immunogenic or humanized protein / peptides resulting in lower immunogenicity. A further benefit of synthetic transfer systems is that they can easily be synthesized in large quantities at rather low cost and offer a higher loading capacity for DNA. However, the major drawback of synthetic vectors is their limited transduction efficacy compared to viral vectors after *in vivo* application, which is currently mainly compensated by the application of larger quantities of vector formulation.

Most synthetic vectors are generally based on formulations of chemically defined, positively charged polymers (polycations or cationic lipids), which interact electrostatically with the negatively charged nucleic acids. The resulting "polyplexes" or "lipoplexes" protect DNA from degradation and are positively charged themselves due to an excess of polymer used to form compact nanosized complexes suitable for cell entry. Cell entry mainly occurs due to interaction with the negatively charged cell membranes followed by endocytosis of polyplexes.

Over the last decades a huge variety of polymers, mainly cationic polymers or cationic lipids have been investigated to generate synthetic gene carriers. To date, systemic administration of polycationic polymers has often resulted in toxic responses, which is mostly linked to the positive surface of the vectors making them incompatible for clinical applications. The existing synthetic cationic systems can be divided in two groups: non-degradable and degradable polymers. Non-degradable polymers like linear- (LPEI) or branched polyethylenimine (BPEI) are "static" structures, which cannot be degraded, metabolized and eliminated by the body. In consequence they can accumulate in cells or organs leading to undesired and uncontrollable long-term toxicity in living systems. In this thesis a novel class of branched polycations based on oligoethylenimine (OEI)-grafted polypropylenimine dendrimers (G2-HD-OEI) were used for systemic NIS gene delivery in a syngenic neuroblastoma (Neuro 2A) mouse model (Klutz *et al.*, 2009) and human hepatocellular carcinoma (HCC) xenograft mouse model (HuH7). Low toxicity in

association with high transfection efficiency was observed in different tumor cell lines *in vitro* using this polymers. Further, polyplexes formed by these biodegradable polymers prevented aggregation with erythrocytes and toxic side effects after systemic administration *in vivo* (Russ *et al.*, 2008a).

A main approach in gene therapy is the efficient and specific delivery of therapeutic genetic material into selected cells in order to prevent the unspecific toxicity. The addition of specific targeting ligands to polyplexes may enhance transfection efficiency and allows a more specific delivery of therapeutic genes. For this purpose, a number of ligands targeting to specific cellular receptors have been exploited, including carbohydrates, proteins, peptides, vitamins or antibodies. For example an anti-CD3-antibody was covalently coupled to PEI for specific delivery of polyplexes to a CD3 expressing T cell leukaemia cell line (Kircheis *et al.*, 1997) or RGD-PEI conjugates were used for gene delivery to integrin expressing endothelial tumor cells (Kunath *et al.*, 2003). Promising results were obtained with transferrin coupled polyplexes, which led to several-hundred-fold increase in transfection efficiency in selected cell lines (Kircheis *et al.*, 1997). Further, mannose was applied for targeting of mannose receptor on dendritic cells (Kircheis *et al.*, 1997), and galactose for targeting of the asioaloglycoprotein receptor on hepatocytes (Zanta *et al.*, 1997).

The epidermal growth factor receptor (EGFR) is upregulated in a broad range of epithelial tumors, such as liver cancer, and has therefore been evaluated as a target structure for gene delivery vectors (De Bruin *et al.*, 2007). EGF, the natural ligand of the EGFR, has strong growth promoting properties by activation of the receptor tyrosine kinase via phosphorylation and thereby represents a strong tumor promoting agent. Therefore, a synthetic ligand with high receptor affinity which does not activate the receptor tyrosine kinase is required to function as a feasible ligand to target gene delivery vectors to EGFR-expressing tumor cells. In this context, Li *et al.* discovered a new EGFR ligand by phage display library analysis called GE11 (Sequence: CYHWYGYFPQNVI) which showed high affinity towards EGFR with no significant activation potential at the receptor tyrosine kinase (Li *et al.*, 2005).

In the current study, we evaluated the efficacy of novel synthetic nanoparticle vectors based on linear polyethylenimine (LPEI), shielded by attachment of polyethylene glycol (PEG) and coupled with the synthetic EGFR-specific peptide GE11 for targeting the NIS gene to human hepatocellular carcinoma (HCC) cells.

# Aims of the thesis

Currently available data clearly demonstrate the enormous potential of NIS as a novel reporter and therapy gene. As logical consequence of the pioneer work in the prostate cancer model by J.C. Morris and C. Spitzweg and the consecutive work in other tumor models in the NIS gene therapy field, the next crucial step towards clinical application of the promising NIS gene therapy concept, has to be the evaluation of gene transfer methods that own the potential to achieve sufficient tumor-selective transgene expression levels not only after local or regional but also after systemic application to be able to reach tumor metastases.

The fist aim of the thesis was to explore the potential of a replication-deficient adenovirus for local NIS gene transfer *in vitro* and *in vivo* in a HCC (HepG2) xenograft mouse model. Further, we compared the therapeutic efficacy of $^{131}$I and $^{188}$Re after local adenoviral NIS gene transfer in this HCC xenograft model.

The second aim of the thesis was to characterize the biodistribution of functional NIS expression after systemic NIS gene transfer using branched polycations based on oligoethylenimine (OEI)-grafted polypropylenimine dendrimers for tumor-specific NIS gene delivery in a syngenic neuroblastoma (Neuro2A) mouse model and human hepatocellular carcinoma (HCC) xenograft mouse model (HuH7). Based on the *in vivo* imaging and *ex vivo* biodistribution analysis data, therapeutic efficacy of $^{131}$I was analyzed.

The third aim of the thesis was to further enhance tumor selectivity by the application of novel nanoparticle vectors based on linear polyethylenimine (LPEI), shielded by polyethylene glycol (PEG), and coupled with the synthetic peptide GE11 as an EGFR-specific ligand for targeting the NIS gene to EGFR-expressing human HCC (HuH7) cells. Biodistribution of functional NIS expression and the therapeutic efficacy of $^{131}$I were analyzed after systemic, EGFR-targeted NIS gene delivery.

Based on the role of NIS as a potent and well characterized reporter gene allowing non-invasive imaging of functional NIS expression by $^{123}$I-scintigraphy and $^{123}$I-SPECT-CT imaging, these studies allowed detailed characterization of *in vivo* vector biodistribution as well as localization, level and duration of transgene expression, an essential prerequisite for exact planning and monitoring of clinical gene therapy trials with the aim of individualization of the NIS gene therapy concept in the clinical setting.

# 2. Chapter 1

# Comparison study of $^{131}$I and $^{188}$Re therapy in liver cancer after tumor-specific *in vivo* sodium iodide symporter (NIS) gene transfer

# Abstract

We recently reported therapeutic efficacy of $^{131}$I in hepatocellular carcinoma (HCC) cells stably expressing the sodium iodide symporter (NIS) under the control of the tumor-specific alpha-fetoprotein (AFP) promoter. In the current study we investigated the efficacy of adenovirus-mediated *in vivo* NIS gene transfer followed by $^{131}$I and $^{188}$Re administration for the treatment of HCC xenografts. We used a replication-deficient adenovirus carrying the *h*NIS gene linked to the mouse AFP promoter (Ad5-AFP-NIS) for *in vitro* and *in vivo* NIS gene transfer. Functional NIS expression was confirmed by *in vivo* γ-camera imaging, followed by analysis of NIS protein and mRNA expression. Human HCC (HepG2) cells infected with Ad5-AFP-NIS concentrated 50% of the applied activity of $^{125}$I, which was sufficiently high for a therapeutic effect in an *in vitro* clonogenic assay. Four days after intratumoral injection of Ad5-AFP-NIS (3 x $10^9$ PFU) HepG2 xenografts accumulated 14.5% ID/g $^{123}$I with an effective half-life of 13 h (tumor absorbed dose 318 mGy/MBq $^{131}$I). In comparison, 9.2% ID/g $^{188}$Re was accumulated in tumors with an effective half-life of 12.8 h (tumor absorbed dose 545 mGy/MBq). After adenovirus-mediated NIS gene transfer in HepG2 xenografts administration of a therapeutic dose of $^{131}$I or $^{188}$Re (55.5 MBq) resulted in a significant delay in tumor growth and improved survival, with $^{188}$Re being mildly more potent than $^{131}$I. In conclusion, a therapeutic effect of $^{131}$I and $^{188}$Re was demonstrated in HepG2 xenografts after tumor-specific adenovirus-mediated *in vivo* NIS gene transfer.

# Introduction

Hepatocellular carcinoma (HCC) is a common cancer with increasing incidence world wide. It is estimated that only about 5% of HCC patients are suitable for liver transplantation (Jelic, 2009) and surgical resection rates vary between 9% and 27% (Lee *et al.*, 1982; Lai *et al.*, 1995). However, the majority of patients have unresectable disease that is generally considered incurable, for which the direction of treatment is palliative. Despite novel treatment strategies including cryosurgery, percutaneous ethanol injection, radiofrequency thermal ablation and chemoembolization, the prognosis of patients suffering from advanced HCC has remained poor. Therefore, the development of alternative therapeutic approaches, including gene therapy, is required to improve the management of these patients.

In order to investigate an innovative gene therapy approach, in an earlier study we examined the feasibility of $^{131}$I therapy of HCC following stable transfection with the sodium iodide symporter (NIS) using a mouse alpha-fetoprotein (AFP) promoter construct to target NIS expression to HCC cells (Willhauck *et al.*, 2008b). NIS mediates the active transport of iodide across the basolateral membrane of benign and malignant thyroid cells and represents the molecular basis for the diagnostic and therapeutic application of radioiodine, which has been successfully used for over 70 years in the treatment of thyroid cancer patients (Spitzweg *et al.*, 2001c; Hingorani *et al.*, 2010a). Since its cloning in 1996 NIS has been characterized as a novel promising target gene for the development of a novel gene therapy strategy based on selective NIS gene transfer into tumor cells followed by diagnostic and therapeutic application of radioiodine (Dai *et al.*, 1996; Smanik *et al.*, 1996; Spitzweg and Morris, 2001). The capacity of the NIS gene to induce radioiodine accumulation in non-thyroidal tumors has been investigated in a variety of tumor models by several groups including our own (Spitzweg *et al.*, 1999c; Spitzweg *et al.*, 2000b; Spitzweg and Morris, 2002b; Kakinuma *et al.*, 2003; Dingli *et al.*, 2004; Cengic *et al.*, 2005; Dwyer *et al.*, 2005a; Scholz *et al.*, 2005; Dwyer *et al.*, 2006a; Dwyer *et al.*, 2006b; Willhauck *et al.*, 2007; Willhauck *et al.*, 2008a; Willhauck *et al.*, 2008b; Hingorani *et al.*, 2010a; Li *et al.*, 2010; Penheiter *et al.*, 2010; Trujillo *et al.*, 2010). Taken together, the potential of NIS as a novel reporter and therapy gene for the treatment of extrathyroidal tumors has been convincingly demonstrated. In order to achieve tumor selectivity with maximal tumor-specific cytotoxicity and minimal side effects in healthy organs, functional NIS gene expression can be transcriptionally targeted by application of tissue- or tumor-specific

promoters (Hart, 1996; Peerlinck *et al.*, 2009). In our earlier study, we applied a mouse AFP promoter construct consisting of the basal promoter and the enhancer I and demonstrated tumor-specific iodide uptake activity in a hepatocellular carcinoma cell line (HepG2) stably transfected with the human NIS gene under the control of the AFP promoter, which resulted in an up to 93% cell killing after $^{131}$I exposure in an *in vitro* clonogenic assay. After application of a therapeutic $^{131}$I dose (55.5 MBq) the amount of accumulated radioiodide in xenografts derived from stably transfected NIS expressing HCC cells was high enough to significantly inhibit tumor growth (Willhauck *et al.*, 2008b).

To further improve the NIS gene therapy concept towards a possible clinical application, in the current study we developed a replication-deficient adenovirus carrying the human NIS gene linked to the same AFP promoter construct (Ad5-AFP-NIS) that allows *in vivo* NIS gene delivery.

Because extrathyroidal tumors are not able to organify iodide after NIS gene transfer, the limited iodide retention time may hamper therapeutic efficacy of $^{131}$I therapy. The application of $^{188}$Rhenium, which is also transported via NIS, but characterized by a shorter physical half-life and decay properties superior to $^{131}$I may provide a powerful tool to enhance therapeutic efficacy of NIS-mediated radionuclide therapy. $^{188}$Re has already been successfully used by our own group to enhance the therapeutic efficacy of NIS-mediated radionuclide therapy in a prostate cancer xenograft model. We showed significant therapeutic efficacy with a tumor volume reduction of 85% after $^{188}$Re application as compared to 73% after $^{131}$I treatment (Willhauck *et al*., 2007). In addition, Dadachova *et al*. demonstrated a more pronounced growth inhibiting effect in NIS-expressing mammary tumors in a transgenic mouse model after application of $^{188}$Re (Dadachova *et al.*, 2005).

In the current study, we therefore examined accumulation and therapeutic efficacy of $^{131}$I in direct comparison with $^{188}$Re in a HCC xenograft mouse model after tumor-specific, adenovirus-mediated *in vivo* NIS gene transfer.

# Materials and Methods

*Cell culture*

The human HCC cell line (HepG2; ATCC-HB-8065) and the human prostate cancer cell line (LNCaP; ATCC-CRL-1740) were cultured in RPMI (Invitrogen Life Technologies Inc., Karlsruhe, Germany) supplemented with 10% fetal bovine serum (v/v) (PAA; Colbe, Germany) and 1% penicillin/streptomycin (v/v). The human melanoma cell line (1205 Lu, kindly provided by Meenhard Herlyn, The Wistar Institute, Philadelphia, USA) was grown in MCDB 153 medium (Invitrogen Life Technologies Inc.) supplemented with 20% Leibovitz´s L-15 medium (v/v) (Invitrogen Life Technologies Inc.), 2% fetal bovine serum (v/v), 5 µg/ml insulin (Sigma, Munich Germany) and 1% penicillin/streptomycin (v/v). Cells were maintained at 37 °C and 5% $CO_2$ in an incubator with 95% humidity. The cell culture medium was replaced every second day and cells were passaged at 85% confluency.

*Recombinant adenovirus production*

A replication-deficient human recombinant type 5 adenovirus (Ad5) carrying the human NIS gene linked to a mouse AFP promoter construct consisting of the basal promoter and enhancer element I (Willhauck *et al.*, 2008b) (kindly provided by Markus Geissler, Esslingen, Germany) was developed in collaboration with ViraQuest Inc. (North Liberty, IA, USA) (Ad5-AFP-NIS). The human NIS cDNA was cut from the pcDNA plasmid (kindly provided by Sissy M. Jhiang, Ohio State University, Columbus, OH, USA) using *EcoRI* and cloned into the shuttle vector (pVQAd-AscI-NpA). The AFP promoter construct was cloned into the pVQAd-AscI-NpA using *Kpn I* and *Xho I*. The resulting shuttle vector construct contains the full-length NIS cDNA coupled to the AFP promoter.

As controls, a replication-deficient adenovirus carrying the NIS cDNA under the control of the unspecific cytomegalovirus (CMV) promoter generated as described previously (Ad5-CMV-NIS) (Spitzweg *et al.*, 2001a) and an empty virus (Ad5-control) were used.

*Adenovirus-mediated NIS gene transfer in vitro*

For *in vitro* infection experiments, HepG2 or control cells (LNCaP and 1205 Lu) ($1.5 \times 10^5$ cells/ml in 12-well plates) were washed and incubated with OptiMEM (Invitrogen Life Technologies Inc.) containing Ad5-AFP-NIS (60 MOI = multiplicity of infection) for 2.5 h. Medium was replaced by fresh culture medium and virus-infected cells were further

maintained for 4 days, before iodide accumulation was measured (see below) to determine levels of functional NIS protein expression. All adenoviral infections were carried out at least in triplicates.

### $^{125}$I uptake assay

Following infection with Ad5-AFP-NIS or Ad5-control, iodide uptake of HepG2 or control cells was determined at steady-state conditions (Weiss *et al.*, 1984) as described previously (Spitzweg *et al.*, 1999c). Results were normalized to cell viability and expressed as cpm/A 490 nm.

### Cell viability assay

Cell viability was measured using the commercially available MTS-assay (Promega Corp., Mannheim, Germany) according to the manufacturer´s recommendations as described previously (Unterholzner *et al.*, 2006).

### Clonogenic assay

HepG2 cells were infected with Ad5-AFP-NIS (60 MOI) as described above. Four days following infection, cells were incubated for 7 h with 29.6 MBq (0.8 mCi), 14.8 MBq (0.4 mCi) or 7.4 MBq (0.2 mCi) $^{131}$I in Hank´s balanced salt solution supplemented with 10 µM NaI and 10 mM HEPES (pH 7.3) at 37 °C. After incubation with $^{131}$I, a clonogenic assay was performed as described previously (Mandell *et al.*, 1999; Spitzweg *et al.*, 2000b).

### Establishment of xenograft tumors in nude mice

HepG2 and 1205 Lu xenografts were established in 5 weeks old female CD-1 nu/nu mice (Charles River, Sulzfeld, Germany) by subcutaneous injection of 1 x 10$^7$ HepG2 cells suspended in 100 µl PBS and 100 µl Matrigel Basement Membrane Matrix (Becton Dickinson, Bedford, MA, USA) or 1.5 x 10$^6$ 1205 Lu cells suspended in 100 µl PBS into the flank region. LNCaP xenografts were established in male CD-1 nu/nu by subcutaneous injection of 1 x 10$^6$ cells suspended in 250 µl PBS and 250 µl of Matrigel Basement Membrane Matrix (Becton Dickinson, Bedford, MA, USA) into the flank region. Animals were maintained under specific pathogen-free conditions with access to mouse chow and water *ad libidum*. The experimental protocol was approved by the regional governmental commission for animals (Regierung von Oberbayern, Munich, Germany).

*Adenovirus-mediated NIS gene delivery in xenograft tumors in nude mice*

Experiments started when tumors had reached a size of 3-5 mm. After a 10-day pretreatment with L-T4 (l-thyroxine, Sanofi-Aventis, Frankfurt am Main, Germany) (5 mg/l) in their drinking water to maximize radioiodine uptake in the tumor and reduce iodide uptake by the thyroid gland, animals were anesthetized with ketamine (Hameln pharmaceuticals, Hameln, Germany) (100 µg/g) and xylazine 2% (v/v) (Bayer, Leverkusen, Germany) (10 µg/g). Thereafter, $3 \times 10^9$ PFU (diluted with PBS to a total volume of 100 µl) of the recombinant Ad5-AFP-NIS or Ad5-control were injected at five different injection sites directly into the tumor using tuberculin syringes with a 30-gauge x 0.5-inch needle. The needle was moved to various sites within the tumor during injection to maximize the area of virus exposure. To investigate tumor specificity of the virus construct in the case of virus leakage, a cohort of tumor-bearing mice received $3 \times 10^9$ PFU of either the non-specific Ad5-CMV-NIS or the tumor-specific Ad5-AFP-NIS systemically via tail vein injection.

*Radionuclide uptake studies in vivo*

Four days after intratumoral or intravenous injection of Ad5-AFP-NIS, Ad5-control or Ad5-CMV-NIS, mice received 18.5 MBq (0.5 mCi) $^{123}$I or 111 MBq (3 mCi) $^{188}$Re intraperitoneally (i.p.) and radionuclide biodistribution was monitored by serial imaging on a gamma camera (Forte, ADAC Laboratories, Milpitas, CA, USA) equipped with a VXHR (Vantage Extra High Resolution) collimator ($^{123}$I) or a medium-energy general purpose (MEGP) collimator ($^{188}$Re) as described previously (Willhauck *et al.*, 2007; Willhauck *et al.*, 2008a). Regions of interest were quantified and expressed as a fraction of the total amount of applied radionuclide per gram tumor tissue. The retention time within the tumor was determined by serial scanning after radionuclide injection and dosimetric calculations were performed according to the concept of MIRD, with the dosis factor of RADAR-group (www.doseinfo-radar.com).

*Analysis of NIS mRNA expression using quantitative real-time PCR*

After infection with Ad5-AFP-NIS total RNA was isolated from HepG2 xenografts using the RNeasy Mini Kit (Qiagen, Hilden, Germany) according to the manufacturer's recommendations. Single stranded oligo (dT)-primer cDNA was generated using Superscript III Reverse Transcriptase (Invitrogen Life Technologies Inc., Karlsruhe, Germany). Following primers were used: *h*NIS (5`-TGCGGGACTTTGCAGTACATT-3´)

and (5`-TGCAGATAATTCCGGTGGACA-3´), GAPDH: (5`-GAGAAGGCTGGGGCTCATTT-3´) and (5`-CAGTGGGGACACGGAAGG-3´). Quantitative real-time PCR (qPCR) was performed with the cDNA from 1 µg RNA using the SYBR green PCR master mix (Qiagen, Hilden, Germany) in a Rotor Gene 6000 (Corbett Research, Morthlake, New South Wales, Australia). Relative expression levels were calculated using the comparative $\Delta\Delta C_t$ method and internal GAPDH for normalization.

## *Indirect immunofluorescence assay*

Indirect immunofluorescence staining using an antibody against Ki67 (Abcam, Cambridge, UK) was performed on frozen tissue sections as described previously (Willhauck *et al.*, 2007).

## *Immunohistochemical analysis of NIS protein expression*

Immunohistochemical staining of frozen tissue sections derived from HepG2 xenografts after adenovirus-mediated gene delivery was performed as described previously (Spitzweg *et al.*, 2007). For histological examination parallel slides were also routinely stained with hematoxylin and eosin.

## *Western blot analysis*

Membrane proteins were prepared from virus infected HepG2 xenografts as described previously (Castro *et al.*, 1999) and subjected to electrophoresis on a 4 - 12% Bis-Tris-HCl buffered polyacrylamide gel. After transfer of proteins to nitrocellulose membranes by electroblotting, membranes were preincubated in 2% low fat dried milk in TBS-T (20 mM Tris, 137 mM NaCl, and 0.1% Tween 20). Western blot analysis was performed using a mouse monoclonal antibody directed against amino acid residues 468-643 of human NIS (kindly provided by John C. Morris, Mayo Clinic, Rochester, MN, USA) (dilution 1:3000) as described previously (Spitzweg *et al.*, 1999c).

## *Radionuclide therapy study in vivo*

Following a 10-day L-T4 pretreatment as described above, 4 groups of mice (each n=6) were established. Each mouse received 55.5 MBq ^{131}I or [188]Re as a single i.p. injection 4 days after intratumoral injection of Ad5-AFP-NIS ($3 \times 10^9$ PFU) or Ad5-control virus ($3 \times 10^9$ PFU), respectively. In addition, two further groups of mice were treated with saline

instead of radionuclides after injection of either Ad5-AFP-NIS (n=6) or Ad5-control virus (n=6). Tumor size was measured before and twice a week after treatment for up to seven weeks using a caliper. Tumor volume was estimated using the equation: tumor volume = length x width x height x 0.52.

Mice were sacrificed before the end of the 7-week observation period, when tumors started to necrotize, in case of weight loss of more than 10% or impairment of drinking and eating behavior.

### *Statistical methods*

All *in vitro* experiments were carried out in triplicates. Results are represented as means +/- SD of triplicates. Statistical significance was tested using Student´s t-test.

# Results

## *Iodide uptake studies in vitro*

Transduction conditions using Ad5-AFP-NIS were optimized in HepG2 cells by measurement of perchlorate-sensitive iodide uptake activity (data not shown). At a dose of 60 MOI we achieved highest transduction efficiency at low cytotoxicity, which was used for all subsequent *in vitro* experiments. The perchlorate-sensitive iodide uptake activity was measured at various time points after Ad5-AFP-NIS infection (data not shown). Maximum iodide uptake activity was observed 4 days following infection, when cells showed a 102-fold increase in perchlorate-sensitive $^{125}$I accumulation as compared to cells infected with the control virus (Ad5-control) (Fig. 1A). Tumor specificity of Ad5-AFP-NIS was confirmed by infection of control cancer cell lines (LNCaP, 1205 Lu) not expressing AFP showing lack of perchlorate-sensitive iodide uptake activity (Fig. 1A).
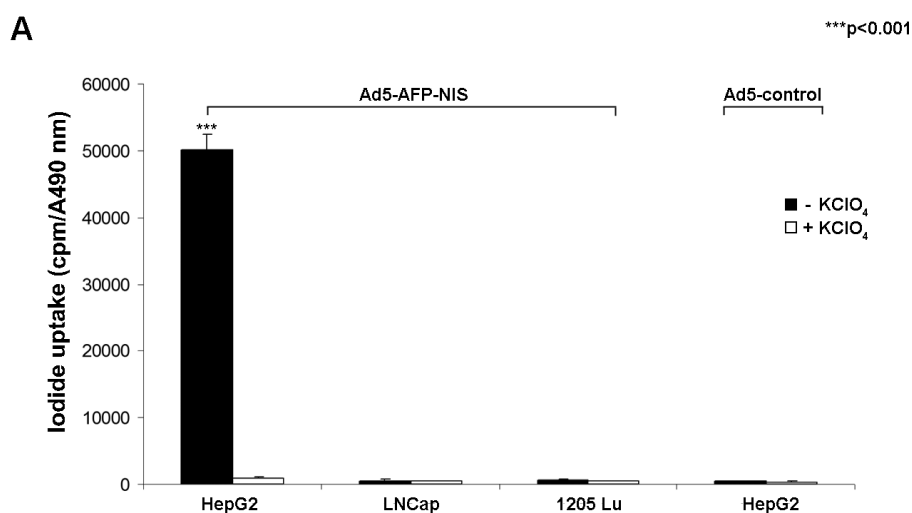


**Fig. 1:** $^{125}$I uptake was measured in HepG2 cells following infection with either Ad5-AFP-NIS or Ad5-control. LNCaP and 1205 Lu served as controls. HepG2 cells infected with Ad5-AFP-NIS showed a 102-fold increase in perchlorate-sensitive $^{125}$I accumulation. In contrast, no iodide uptake above background level was observed in HepG2 cells transfected with an Ad5-control virus or control cells transfected with Ad5-AFP-NIS (***$p < 0.001$).

## *In vitro clonogenic assay using $^{131}$I*

An *in vitro* clonogenic assay was performed to determine the therapeutic efficacy of increasing doses (7.4 MBq (0.2 mCi), 14.8 MBq (0.4 mCi), 29.6 MBq (0.8 mCi)) of $^{131}$I in HepG2 cells after adenovirus-mediated NIS gene transfer (Fig. 1B). While up to 95% of NIS-transduced HepG2 cells were killed by exposure to $^{131}$I in a dose dependent manner, 98% of uninfected HepG2 cells survived the treatment with 29.6 MBq $^{131}$I. Since HepG2 cells infected with Ad5-AFP-NIS without radioiodine treatment (saline only) had similar

survival rates, we assume that virus infection per se had no influence on cell survival of HepG2 cells.

**B**
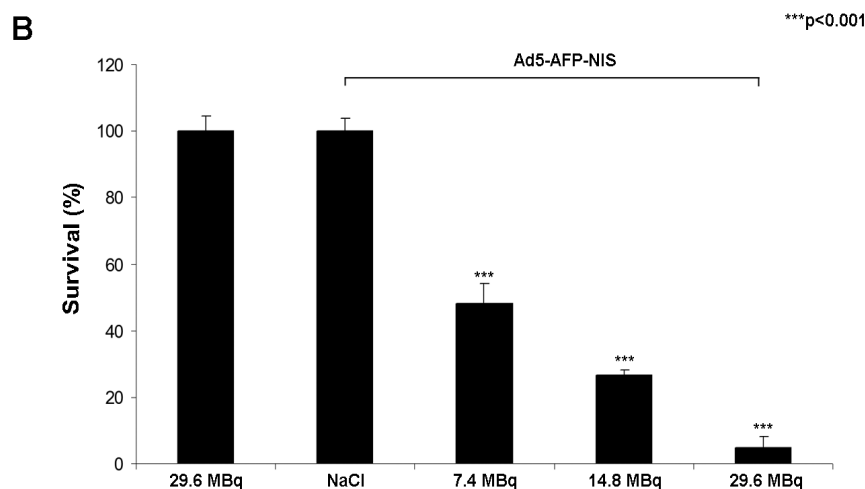


**Fig. 1:** In an *in vitro* clonogenic assay, HepG2 cells infected with Ad5-AFP-NIS were exposed for 7 h to 7.4 MBq (0.2 mCi), 14.8 MBq (0.4 mCi) or 29.6 MBq (0.8 mCi) $^{131}$I. resulting in cell killing rates of approximately 52%, 73% and 95%. Ad5-AFP-NIS-infected HepG2 cells incubated with NaCl instead of $^{131}$I as well as non-infected HepG2 cells incubated with 29.6 MBq (0.8 mCi) $^{131}$I showed almost no unselective cell death (***p<0.001). Results are expressed as means +/- SD.

### *Radionuclide uptake studies after in vivo NIS gene transfer*

Radionuclide biodistribution was monitored in tumor bearing mice 4 days after intratumoral injection of Ad5-AFP-NIS ($3 \times 10^9$ PFU) using a gamma camera. While no radionuclide accumulation was detected in tumors after infection with Ad5-control (left flank) NIS-transduced HepG2 tumors (right flank) showed a significant uptake of $^{123}$I and $^{188}$Re (Fig. 2A, B). As determined by serial scanning, 14.5% ID/g (percentage of the injected dose per gram tumor tissue) $^{123}$I and 9.2% ID/g $^{188}$Re were accumulated 2 h post injection (p.i.) in NIS-transduced xenograft tumors with effective half-lifes of 12.3 h for $^{131}$I and 13 h for $^{188}$Re. The absorbed doses to the tumor were calculated to be 318 mGy/MBq $^{131}$I as compared to 545 mGy/MBq for $^{188}$Re. In addition to tumoral uptake, significant radionuclide accumulation was observed in tissues physiologically expressing NIS, including stomach and thyroid. In this context it is important to mention that the uptake in the stomach appears to be higher than usually seen in humans, which is most probably due to higher levels of NIS protein expression in murine gastric mucosa and pooling of gastric juices due to the anesthesia for a prolonged period during imaging procedure.

In addition, tumor specificity of Ad5-AFP-NIS was confirmed by infection of control tumor xenografts (LNCaP, 1205 Lu) which did not result in tumoral iodide uptake activity (Fig. 2C, D).
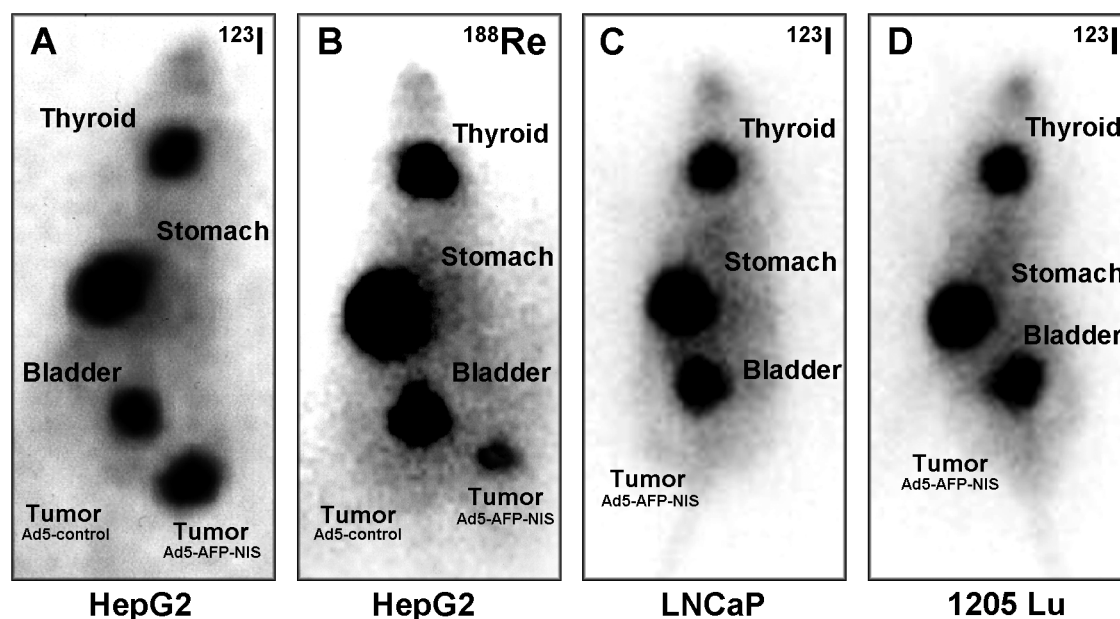
**Fig. 2:** Radionuclide uptake studies *in vivo:* [123]I (A) and [188]Re (B) scans of nude mice, bearing HepG2 xenografts located on the right and left flank, 6 h after administration of 18.5 MBq (0.5 mCi) [123]I or 111 MBq (3 mCi) [188]Re. Four days following intratumoral injection of Ad5-AFP-NIS (right) and Ad5-control (left) Ad5-AFP-NIS infected tumors trapped 14.5% ID/g [123]I (A) and 9.2% ID/g [188]Re (B), while Ad5-control infected tumors showed no radionuclide uptake (A and B). In contrast, control LNCaP xenografts (C) and 1205 Lu xenografts (D) infected with Ad5-AFP-NIS showed no tumoral iodide accumulation. Radionuclides were also accumulated physiologically in bladder, stomach and thyroid gland.

In order to further confirm tumor-specificity of the AFP promoter, we injected virus systemically via the tail vein of HCC xenograft bearing mice. Four days after systemic injection of $3 \times 10^9$ PFU Ad5-CMV-NIS high levels of iodide uptake were observed in the liver due to hepatic pooling of the adenovirus (Fig. 3B), whereas no iodide accumulation was observed in the tumor. In contrast, after administration of Ad5-AFP-NIS we did not observe significant iodide uptake in non-target organs like liver or lungs as determined by ^{123}I scintigraphy (Fig. 3A), although it is expected that most of the Ad5-AFP-NIS is also pooled in the liver after tail vein injection. Interestingly, despite significant hepatic adenovirus pooling a low level of iodide uptake could also be observed in HCC xenografts after systemic injection of Ad5-AFP-NIS underlining tumor specificity and high activity of the AFP promoter used in our study. These data were confirmed by *ex vivo* biodistribution analysis by gamma counter analysis showing that 48% ID/g were accumulated in the liver after i.v. injection of Ad5-CMV-NIS, whereas following injection of Ad5-AFP-NIS only 1% ID/g was accumulated in the liver (Fig. 3C) and 3.7% ID/g in the tumor.
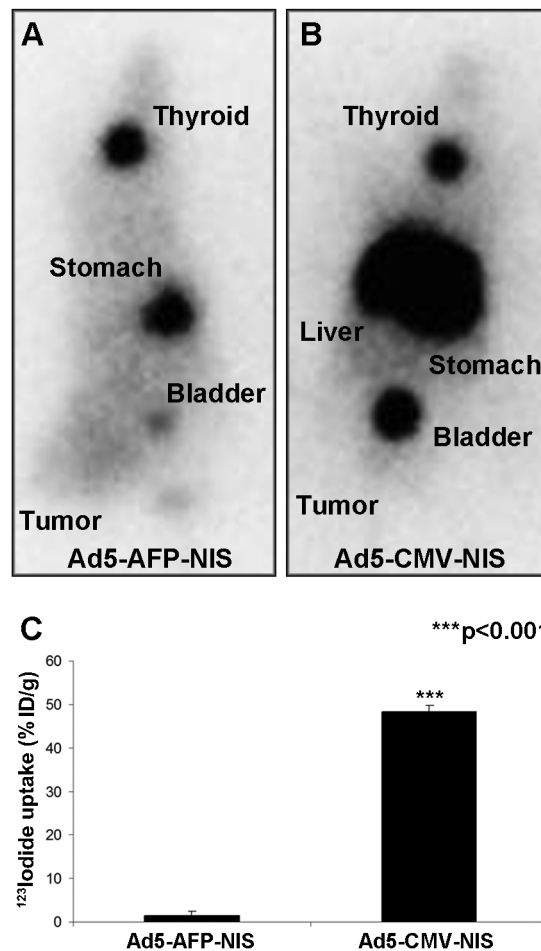
**Fig. 3:** *In vivo* imaging of $^{123}$I biodistribution in nude mice after i.p. administration of 18.5 MBq (0.5 mCi) $^{123}$I 4 days after intravenous administration of Ad5-AFP-NIS (A) or Ad5-CMV-NIS (B). Images shown were acquired 4 h after radioiodide administration. Following systemic application of Ad5-CMV-NIS high levels of iodide accumulation were observed in the liver without iodide uptake in the tumor (B). In contrast, after i.v. application of Ad5-AFP-NIS no iodide accumulation was observed in the liver or other non-target organs, while a low level of iodide uptake was observed in the tumor (3.7% ID/g) (A). Gamma counter analysis showed accumulation of 48% ID/g in the liver after i.v. injection of Ad5-CMV-NIS, whereas livers of Ad5-AFP-NIS injected mice accumulated only 1% ID/g (C). Results are expressed as means +/- SD (***p<0.001). .

## *Analysis of NIS mRNA expression in HepG2 xenografts*

In order to assess NIS mRNA expression after local adenoviral NIS gene transfer *in vivo*, mRNA of tumors was extracted and analyzed by quantitative real-time PCR (qPCR) with a pair of NIS-specific oligonucleotide primers. qPCR analysis revealed a 33-fold increase in NIS mRNA expression in HepG2 xenografts 4 days after intratumoral injection of Ad5-AFP-NIS as compared to mock-transduced tumors. Furthermore, no significant NIS mRNA expression above background level was detected in untreated tumors (Fig. 4).
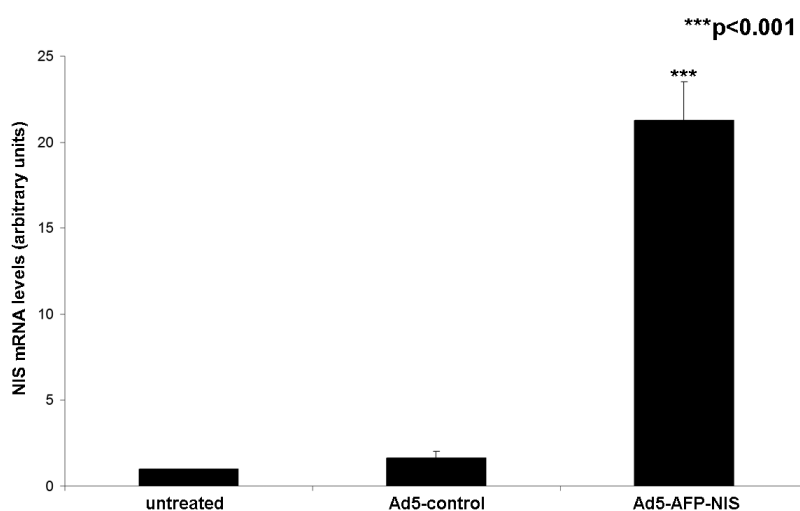


**Fig. 4:** Analysis of human NIS mRNA expression in HepG2 xenografts. A significant NIS mRNA level was observed after intratumoral injection of Ad5-AFP-NIS. In contrast, no significant NIS expression above background level was found in tumors after infection with Ad5-control or in untreated tumors (***$p<0.001$).

## *Western blot analysis*

Four days following intratumoral injection of Ad5-AFP-NIS or Ad5-control, NIS protein expression levels were determined in HepG2 cell xenografts by Western blot analysis using a mouse monoclonal antibody directed against amino-acid 468-643 of the human NIS protein. Western blotting of membrane proteins derived from Ad5-AFP-NIS-infected xenografts revealed a NIS-specific band of a molecular weight of approximately 90 kDa, which was not detected in tumors transduced with Ad5-control (Fig. 5A).
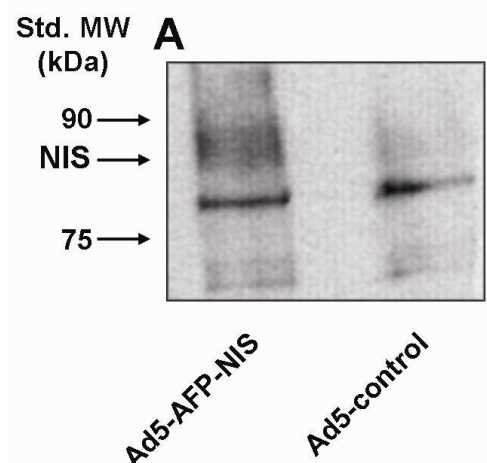
**Fig. 5:** Western blot analysis of HepG2 xenografts 4 days following infection with Ad5-AFP-NIS or Ad5-control. NIS protein was detected as a major band of approximately 90 kDa in Ad5-AFP-NIS infected HepG2 xenografts, while Ad5-control infected HepG2 xenografts did not show NIS protein expression (A).

### *Immunohistochemical analysis of NIS protein expression in HepG2 xenografts*

Immunohistochemical analysis of HepG2 xenografts using a mouse monoclonal *h*NIS-specific antibody revealed a heterogeneous staining pattern with areas of primarily membrane-associated NIS-specific immunoreactivity in tumors after intratumoral application of Ad5-AFP-NIS (Fig. 5B, white arrows). In contrast, tumors treated with Ad5-control showed no NIS-specific immunoreactivity (Fig. 5C). Parallel control slides with the primary and secondary antibodies replaced in turn by PBS and isotype-matched non immune immunoglobulin were negative (data not shown).
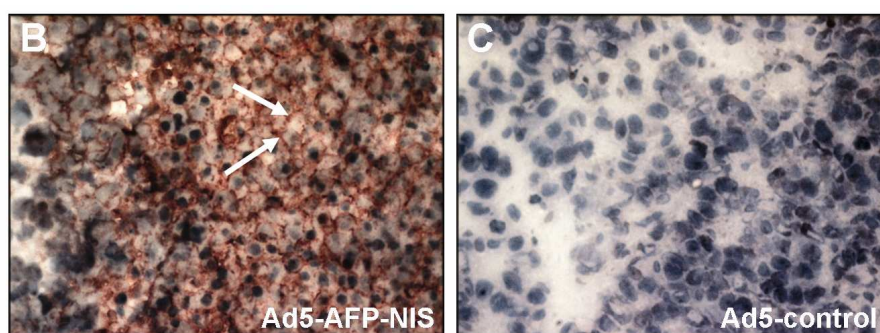


**Fig. 5:** Immunohistochemical staining of HepG2 xenografts 4 days after infection with Ad5-AFP-NIS showed heterogeneous, primarily membrane-associated NIS-specific immunoreactivity (B). In contrast, HepG2 xenografts infected with Ad5-control did not reveal NIS-specific immunoreactivity (C). Magnification: 400 x

***Radionuclide therapy study in vivo***

After 2 - 3 weeks of tumor growth (average tumor diameter 3 - 5 mm) and 4 days after local virus application, 4 groups of mice (^{131}I group: Ad5-AFP-NIS (n=6), [188]Re group: Ad5-AFP-NIS (n=6) and control groups with Ad5-control and [131]I (n=6) or [188]Re (n=6)) were administered 55.5 MBq (1.5 mCi) [131]I or [188]Re per mouse by a single i.p. injection, whereas two other control groups (saline groups: Ad5-AFP-NIS (n=6) or Ad5-control (n=6)) were treated with saline instead of radionuclides. All saline treated tumors and tumors infected with the control virus continued their growth throughout the observation period (increase in tumor size: Ad5-control/[131]I: 26.9-fold; Ad5-control/[188]Re: 25.2-fold; Ad5-control/saline: 24.5-fold; Ad5-AFP-NIS/saline: 23-fold) (Fig. 6A). In contrast, NIS transduced tumors showed a significant delay in tumor growth after injection of ^{131}I or [188]Re. 3 - 5 weeks following radionuclide injection therapeutic efficacy of [188]Re seemed to be more pronounced as compared to [131]I. However, differences were mild without reaching statistical significance. While all of the mice in the control groups had to be killed within the first 5 weeks after onset of the experiments due to excessive tumor growth, 85% of mice treated with ^{131}I or [188]Re after local *in vivo* NIS gene transfer survived approx. 7 - 8 weeks (Fig. 6B). None of the mice showed adverse effects after virus or radionuclide administration.
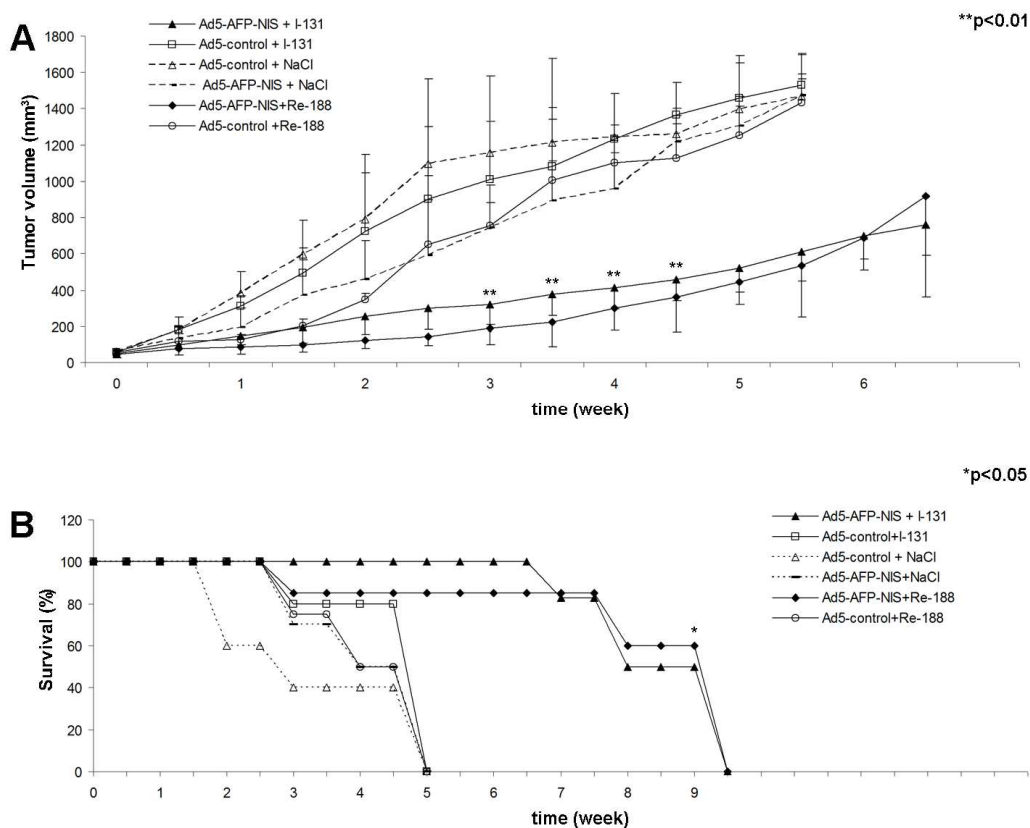
**Fig. 6:** Radionuclide therapy studies *in vivo*. Growth of Ad5-AFP-NIS infected HepG2 xenografts (solid symbols) and Ad5-control infected HepG2 xenografts (open symbols) in nude mice following injection of 55.5 MBq (1.5 mCi) $^{131}$I, $^{188}$Re (solid lines) or saline (dashed lines). Radionuclide therapy after intratumoral injection of Ad5-AFP-NIS resulted in a significant delay of tumor growth (A, $**p<0.01$) that was associated with markedly improved survival (B, Kaplan-Meier-plot) as compared to control groups that were injected with Ad5-control followed by saline or radionuclide application ($*p<0.05$).

Histological evaluation of HepG2 xenografts showed a significant degree of necrosis (arrows) in NIS-transduced tumors 4 weeks after radionuclide treatment ($^{131}$I or $^{188}$Re) (Fig. 7A, B), while saline treated tumors exhibited only small areas of necrosis (arrows) (Fig. 7C).
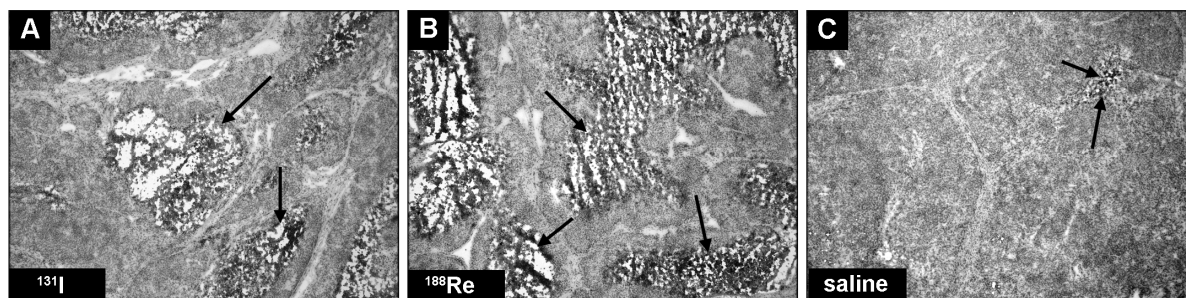


**Fig. 7**: Histological evaluation of of HepG2 tumors showed a significant degree of necrosis after NIS-mediated $^{131}$I (A) or $^{188}$Re-therapy (B). In contrast, NIS-transduced tumors followed by saline injection showed no significant necrosis (C). Magnification: 400 x

## Discussion

Gene therapy for HCC represents a new technology that, more than any currently available therapy, takes direct advantage of our new understanding of tumor carcinogenesis at the molecular level. A variety of gene therapy strategies have been examined for HCC in the recent years, such as immunomodulatory gene therapy including cytokine gene transfer, cytoreductive gene therapy using the herpes simplex virus thymidine kinase/ganciclovir system and the cytosine deaminase/5-fluorocytosine system, antiangiogenic gene therapy, corrective gene therapy aiming at restoration of p53 expression as well as oncolytic viral therapy (Sangro *et al.*, 2005). However, none of these therapeutic approaches has reached the clinical area yet.

As one of the oldest and most successful targets of molecular imaging and therapy, cloning and characterization of NIS has provided us with a powerful new therapy gene, that allowed the development of a promising cytoreductive gene therapy strategy based on NIS gene transfer in extrathyroidal tumors followed by targeted radionuclide therapy (Smanik *et al.*, 1996; Smanik *et al.*, 1997; Dai *et al.*, 1996; Hingorani *et al.*, 2010a). In its dual role as reporter and therapy gene NIS allows direct, non-invasive imaging of functional NIS expression by ^{123}I-scintigraphy and [124]I-PET-imaging as well as exact dosimetric calculations before proceeding to therapeutic application of ^{131}I or alternative radionuclides (Spitzweg and Morris, 2002b; Dingli *et al.*, 2003b; Hingorani *et al.*, 2010a).

As one of the first groups to explore the efficacy of NIS gene therapy in extrathyroidal tumors we chose prostate cancer as initial tumor model and used the PSA and probasin promoters to transcriptionally target functional NIS expression to prostate cancer cells, that resulted in a highly significant therapeutic effect after application of [131]I *in vitro* and *in vivo* (Spitzweg *et al.*, 1999; Spitzweg *et al.*, 2000b; Kakinuma *et al.*, 2003). In further studies we were able to confirm these data by the successful application of other tumor-specific promoters, such as the carcinoembryonic antigen (CEA) promoter and the calcitonin promoter, to induce tumor-specific iodide accumulation in colon and medullary thyroid cancer cells, respectively (Cengic *et al.*, 2005; Scholz *et al.*, 2005; Spitzweg *et al.*, 2007). Moreover, based on our promising preliminary work and the proof-of-principle of tumor-specific NIS gene therapy in prostate cancer, a first phase I clinical trial was approved after extensive toxicity and efficacy studies in rats and large animal models at the Mayo Clinic for radioiodine therapy of locally recurrent prostate cancer after local adenoviral NIS gene transfer (Dwyer *et al.*, 2005b).

In addition, in the prostate cancer model we have convincingly demonstrated that the application of the alternative radionuclides $^{188}$Re and $^{211}$At, which are also transported by NIS, is capable of significantly enhancing therapeutic efficacy of NIS-mediated radionuclide therapy (Willhauck *et al.*, 2007; Willhauck *et al.*, 2008a). While the high energy alpha emitter $^{211}$At with a maximal path length of only 70 µm was more potent in smaller tumors as compared to $^{131}$I, therapeutic efficacy of $^{188}$Re (maximal path length of up to 10.4 mm) was superior in larger tumors (Willhauck *et al.*, 2007; Willhauck *et al.*, 2008a).

In liver cancer Chen *et al.* reported that stop of tumor growth could be achieved *in vivo* in a subcutanous HCC rat model after $^{131}$I application following retroviral NIS gene transfer under control of the albumin promoter (Chen *et al.*, 2006). However, application of the albumin promoter implies the problem of possible substantial toxicity to normal hepatocytes, which, in our opinion, significantly impairs the feasibility of this approach. We have therefore chosen to apply the tumor-specific AFP promoter to transcriptionally target NIS expression selectively to liver cancer cells thereby minimizing toxicity in normal liver cells and other organs (Willhauck *et al.*, 2008b). AFP is a 70 kilo-dalton protein that is exclusively expressed in the yolk sac and liver of mammals during embryonic development and after birth only reexpressed in neoplastic transformation or injury to the liver as well as in teratocarcinomas. Due to its tumor-specific regulation, AFP is widely used as highly specific tumor marker for HCC and teratocarcinomas and the AFP promoter therefore represents an ideal means for HCC-specific transcriptional targeting of therapeutic genes (Ido *et al.*, 2001; Lu *et al.*, 2003).

As a next crucial step towards clinical application of the NIS gene therapy approach in liver cancer patients, in the current study we performed *in vivo* NIS gene transfer into HCC xenograft tumors using a replication-deficient human adenovirus carrying the human NIS gene linked to the AFP promoter (Ad5-AFP-NIS) and examined radionuclide accumulation and therapeutic efficacy of $^{131}$I and $^{188}$Re.

We decided to use a recombinant adenovirus serotype 5 vector for our experiments since it was demonstrated that these vectors are highly efficient for *in vivo* gene transfer upon intratumoral administration due to high titers they can produce and their ability to infect non-dividing cells (Zhang *et al.*, 1999). In addition, using adenoviral vectors efficient *in vivo* gene transfer has been demonstrated in numerous tissue types, including glioma (Lang *et al.*, 2003), bladder carcinoma (Pagliaro *et al.*, 2003), ovarian cancer (Wolf *et al.*, 2004) and liver tissue (Faivre *et al.*, 2004; Herve *et al.*, 2008) tested either alone or in combination with chemotherapy or radiotherapy. It is known that adenoviral gene transfer is

dependent on several critical steps, including virus attachment to the cellular coxsackievirus-adenovirus receptor (CAR), internalization via endocytosis, endosome escape and transport of virion DNA to the cell nucleus (Svensson and Persson, 1984). Expression of CAR was shown to be a crucial prerequisite for successful adenovirus cell entry (Bergelson et al., 1997). In this context it was shown that hepatic tissue, especially hepatocellular carcinoma cells including HepG2 cells, highly express CAR (Nakamura et al., 2003). In addition, in liver cancer the possibility of regional virus application via the hepatic artery maximizes regional toxicity with minimal systemic toxicity, still allowing to reach disseminated HCC tumors throughout the liver. Even after systemic application most of the adenovirus is passively pooled in the liver. With the tool of transcriptional targeting by application of the AFP promoter NIS expression can be actively targeted to tumor cells thereby avoiding toxicity to normal hepatocytes.

In the current study, after in vitro characterization of Ad5-AFP-NIS in human HCC cells, HepG2 tumors injected with Ad5-AFP-NIS were demonstrated to accumulate 14.5% ID/g of the total radioiodine administered with an average effective half-life of 12.3 h. In comparison, NIS expressing tumors accumulated approximately 9.2% ID/g $^{188}$Re, with an effective half-life of 13 h. These data are consistent with previous biodistribution studies in different tumor models showing higher amounts of accumulated iodide than $^{188}$Re in NIS expressing tumors suggesting a higher affinity of NIS for iodide than for $^{188}$Re (Kang et al., 2004; Dadachova et al., 2005; Willhauck et al., 2007). In our study, a tumor absorbed dose of 545 mGy / MBq $^{188}$Re was calculated, which was 1.7 times higher than for $^{131}$I (318 mGy / MBq). In contrast, Dadachova et al. showed a radiation dose 4.5 times higher for $^{188}$Re than for $^{131}$I in NIS expressing mammary adenocarcinomas in MMTV-NeuT mice (Dadachova et al., 2005). Similarly in one of our earlier studies in NIS-expressing prostate cancer xenografts, the tumor absorbed dose was increased 4.5-fold after application of $^{188}$Re as compared to $^{131}$I (Willhauck et al., 2007). This difference might be due to a more inhomogeneous NIS expression pattern and therefore heterogeneous radionuclide accumulation after adenoviral in vivo NIS gene transfer as compared to stably or endogenously NIS expressing tumor models in the former studies.

To further confirm tumor-specificity of the AFP promoter construct we administered Ad5-AFP-NIS systemically via the tail vein, which did not result in any iodide uptake in the liver or other non-target organs demonstrating selectivity and safety of this construct, despite the significant adenovirus pooling in the liver as demonstrated by i.v. application of the unspecific Ad5-CMV-NIS, that resulted in high levels of hepatic iodide uptake.

Interestingly, even after systemic tail vein injection of Ad5-AFP-NIS and pooling of most of the virus in the liver, enough virus particles reached the peripheral HCC xenografts to induce a low level of iodide uptake of approx. 4% ID/g, demonstrating high tumor specificity and promoter activity of our adenoviral vector. These data confirm that transcriptional tumor targeting by application of the AFP promoter allows to restrict NIS expression to tumor cells to avoid toxicity to normal hepatocytes suggesting a safe gene transfer method even in the case of virus leakage or after systemic application.

Tumoral NIS expression was further confirmed by real-time qPCR, Western blot analysis as well as NIS-specific immunostaining, which was primarily membrane-associated and showed a heterogeneous pattern throughout the tumor.

Our comparative $^{131}$I and $^{188}$Re therapy experiments after *in vivo* NIS gene transfer in HepG2 xenografts were performed with a single injection of 55.5 MBq (1.5 mCi) $^{131}$I or $^{188}$Re. Using each of the radionuclides tumor growth of NIS-transduced HepG2 xenografts was significantly delayed which was associated with markedly improved survival. The therapeutic effect of the NIS-mediated radionuclide therapy was less pominent in the current study as compared to earlier studies in other tumor models showing tumor volume reductions of up to 80 - 90% (Spitzweg *et al.*, 2000b; Spitzweg *et al.*, 2001a; Dingli *et al.*, 2003a; Faivre *et al.*, 2004; Dwyer *et al.*, 2006a; Dwyer *et al.*, 2006b; Willhauck *et al.*, 2007; Willhauck *et al.*, 2008a). This might be due to the extraordinarily high proliferation rate of HepG2 tumors that showed a Ki67 index of approximately 70% in contrast to 35% in the LNCaP tumors used in our earlier studies (Spitzweg *et al.*, 2000b; Spitzweg *et al.*, 2001a; Willhauck *et al.*, 2007; Willhauck *et al.*, 2008a). Given the fact that tumors with such a high proliferation index are usually treated with systemic cytotoxic chemotherapy, such as etoposid and cisplatin, and do not respond well to radiation therapy, the observed level of tumor growth delay in contrast to the explosive growth of control tumors can be interpreted as highly significant therapy effect. Further, histological examination of NIS-transduced HepG2 cell tumors revealed a significant degree of necrosis after radionuclide therapy with $^{131}$I or $^{188}$Re, which was not seen after application of saline suggesting significant therapeutic efficacy. These data also demonstrate that measurement of tumor size alone is not sufficient for proper analysis of therapeutic efficacy of molecularly targeted therapies including NIS-mediated radionuclide therapy. It will therefore be important to analyze antiproliferative and antiangiogenic effects by *ex vivo* immunohistochemical analysis as well as *in vivo* imaging modalities which is currently being studied.

Our data are consistent with previously published studies showing significant therapeutic efficacy of NIS-mediated radioiodide therapy in HCC. Faivre et al., who applied an adenovirus carrying the rat NIS gene under control of the unspecific CMV promoter intratumorally or via the portal vein demonstrated strong tumor growth inhibition up to complete tumor regression after application of $^{131}$I in a HCC rat model (Faivre et al., 2004). In a more recent study, Herve et al. applied a recombinant adenovirus carrying the NIS gene under control of the tumor-specific hepatocarcinoma-intestine-pancreas promoter intratumorally or via the hepatic artery showing growth inhibition of orthotopic liver tumors after application of $^{131}$I (Herve et al., 2008).

In our study the growth retardation of NIS transduced HepG2 xenografts was slightly more pronounced after administration of $^{188}$Re than after injection of $^{131}$I, however, differences were mild without reaching statistical significance. In contrast, in our previous study in stably NIS expressing prostate cancer xenotransplants the application of $^{188}$Re resulted in a significantly improved tumor volume reduction of 85% as compared to 73% after injection of $^{131}$I when treating larger tumors (Willhauck et al., 2007). The difference in therapeutic efficacy of $^{188}$Re and $^{131}$I as seen in the prostate cancer model were attenuated in the hepatoma model used in the current study which is consistent with the dosimetry data. While the tumor absorbed dose in the current study was only increased approx. 1.7-fold after application of $^{188}$Re, the dose delivered to the tumor in the prostate cancer model was 4.5-fold higher compared to that by $^{131}$I as already outlined above. In addition, due to the aggressive growth behaviour of the HepG2 cells adenoviral NIS gene transfer had to be carried out approximately 2 - 3 weeks following tumor cell implantation, when tumors had reached a size of only 3 - 5 mm in diameter, therefore the tumors were smaller than those used in the prostate cancer study. The beta particles emitted by $^{188}$Re are characterized by a longer path length with a maximum range of 10.4 mm as compared to $^{131}$I (maximum path length of up to 2.4 mm) resulting in a more pronounced crossfire effect which is attenuated in small tumors due to energy deposition beyond the tumor borders.

In conclusion, a therapeutic effect of $^{131}$I and $^{188}$Re has been demonstrated in HepG2 cell xenografts after tumor-specific, adenovirus-mediated in vivo NIS gene transfer, opening new perspectives for HCC therapy. Provided that further studies aiming at systemic and regional in vivo gene delivery in orthotopic multifocal HCC models will confirm therapeutic efficacy of AFP promoter-targeted NIS gene therapy, these data clearly demonstrate the potential of NIS as a novel therapeutic gene allowing targeted radionuclide therapy of HCC.

## Acknowledgments

## Author Disclosure Statement

No competing financial interest exists.

# 3. Chapter 2

**Targeted radioiodine therapy of neuroblastoma tumors following systemic non-viral delivery of the sodium iodide symporter (NIS) gene**

# Statement of Translational Relevance

Based on the effective administration of radioiodine in the management of thyroid cancer, cloning of the sodium iodide symporter (NIS) has paved the way for the development of a novel gene therapy strategy based on targeted NIS expression in cancer cells followed by therapeutic application of $^{131}$I. Our pioneer studies have convincingly demonstrated the oncology communities the enormous potential of NIS as a novel reporter and therapy gene and allowed the approval of a first phase I clinical trial for radioiodine therapy of prostate cancer after local adenoviral NIS gene transfer. The next crucial step towards clinical application in metastatic cancer, has to be the evaluation of gene transfer methods that own the potential to achieve sufficient tumor-selective transgene expression levels after systemic application.

The present report is the first preclinical study convincingly demonstrating the high potential of polycations based on polypropylenimine dendrimers for tumor-specific delivery of the NIS gene after systemic application resulting in a significant therapeutic effect of $^{131}$I in a neuroblastoma mouse model. This translational study therefore opens the exciting prospect of NIS-targeted radionuclide imaging and therapy of metastatic cancer using polyplex-mediated systemic NIS gene delivery.

# Abstract

Purpose: We have recently reported significant therapeutic efficacy of radioiodine therapy in various tumor mouse models following transcriptionally targeted sodium iodide symporter (NIS) gene transfer. These studies demonstrated the high potential of NIS as a novel diagnostic and therapeutic gene for the treatment of extrathyroidal tumors. As a next crucial step towards clinical application of NIS-mediated radionuclide therapy we aim at systemic delivery of the NIS gene to target extrathyroidal tumors even in the metastatic stage.

Experimental Design: Therefore, in the current study, we used synthetic polymeric vectors based on pseudodendritic oligoamines with high intrinsic tumor affitnity (G2-HD-OEI) to target a NIS-expressing plasmid (CMV-NIS-pcDNA3) to neuroblastoma (Neuro2A) cells.

Results: Incubation with NIS-containing polyplexes (G2-HD-OEI/NIS) resulted in a 51-fold increase in perchlorate-sensitive iodide uptake activity in Neuro2A cells *in vitro*. Using $^{123}$I scintigraphy and *ex vivo* gamma counting Neuro2A tumors in syngeneic A/J mice were demonstrated to accumulate 8-13 % ID/g $^{123}$I with a biological half-life of 13 h, resulting in a tumor absorbed dose of 247 mGy/MBq $^{131}$I after intravenous application of G2-HD-OEI/NIS. Non-target organs, including liver, lung, kidneys and spleen revealed no significant iodide uptake. Moreover, 2 cycles of systemic NIS gene transfer followed by $^{131}$I application (55.5 MBq) resulted in a significant delay in tumor growth associated with markedly improved survival.

Conclusions: In conclusion, our data clearly demonstrate the high potential of novel pseudodendritic polymers for tumor-specific NIS gene delivery after systemic application opening the prospect of targeted NIS-mediated radionuclide therapy of non-thyroidal tumors even in metastatic disease.

## Introduction

The exact mechanism by which iodide is actively transported across the basolateral membrane of thyroid follicular cells has been clarified by cloning and characterization of the sodium iodide symporter (NIS) 13 years ago (Dai *et al.*, 1996; Smanik *et al.*, 1996; Smanik *et al.*, 1997). NIS, an intrinsic transmembrane glycoprotein with 13 putative transmembrane domains, is responsible for the ability of the thyroid gland to concentrate iodide, the first and rate-limiting step in the process of thyroid hormonogenesis (De *et al.*, 2000; Spitzweg *et al.*, 2000a). Moreover, due to its expression in follicular cell-derived thyroid cancer cells, NIS provides the molecular basis for the diagnostic and therapeutic application of radioiodine, which has been successfully used for more than 60 years in the treatment of thyroid cancer patients and therefore represents the most effective form of systemic anticancer radiotherapy available to the clinician today (Spitzweg *et al.*, 2001c). Since its cloning in 1996 NIS has been identified and characterized as a novel promising target gene for the treatment of extrathyroidal tumors following selective NIS gene transfer into tumor cells which allows diagnostic and therapeutic application of radioiodine and alternative radionuclides, such as $^{188}$Re and $^{211}$At (Spitzweg *et al.*, 2001c; Spitzweg and Morris, 2002b; Willhauck *et al.*, 2007; Willhauck *et al.*, 2008a). We have proven the feasibility of extrathyroidal radioiodine therapy after induction of iodide uptake by *ex vivo* stable NIS transfection or local adenoviral NIS gene transfer using tissue-specific promoters, such as the prostate specific antigen (PSA) promoter, alpha fetoprotein (AFP) promoter, carcinoembryonic antigen (CEA) promoter and the calcitonin promoter to specifically target NIS expression to prostate, liver, colon and medullary thyroid cancer cells, respectively (Spitzweg *et al.*, 1999c; Spitzweg *et al.*, 2000b; Spitzweg *et al.*, 2001a; Kakinuma *et al.*, 2003; Cengic *et al.*, 2005; Scholz *et al.*, 2005; Spitzweg *et al.*, 2007; Willhauck *et al.*, 2008b). Further, cloning of NIS has provided us not only with a powerful therapeutic gene, but also with one of the most promising reporter genes available today, that allows direct, non-invasive imaging of functional NIS expression by $^{123}$I-scintigraphy and $^{124}$I-PET-imaging, as well as exact dosimetric calculations before proceeding to therapeutic application of $^{131}$I (Spitzweg and Morris, 2002b; Dingli *et al.*, 2003b). Therefore, in its role as reporter gene NIS provides a direct way to monitor the *in vivo* distribution of viral and non-viral vectors, as well as biodistribution, level and duration of transgene expression – all critical elements in the design of clinical gene therapy trials (Spitzweg and Morris, 2002b; Dingli *et al.*, 2003b).

As logical consequence of our pioneer studies in the NIS gene therapy field, the next crucial step towards clinical application of the promising NIS gene therapy concept, has to be the evaluation of gene transfer methods that own the potential to achieve sufficient tumor-selective transgene expression levels not only after local or regional but also after systemic application to be able to reach tumor metastases.

Viral vectors are the most commonly used gene transfer systems employed in clinical trials due to their high potency in gene transfer (Everts and Van Der Poel, 2005). However, the limitations associated with viral vectors including induction of immune and inflammatory responses, limited transgene loading size, potential toxicity and tumorigenicity as well as high production costs have encouraged researchers to focus on alternative gene transfer vehicles.

Delivering genes to target organs with synthetic vectors is a vital alternative to virus-based methods. For systemic delivery polycationic molecules are used to condense DNA into sub-micrometer particles termed polyplexes, which are efficiently internalized into cells, while DNA is protected from nucleases. Several polycations, like polyethylenimine (PEI), bear an intrinsic endosomolytic mechanism, which allows the transition of the polyplex from the endosome to the cytoplasm (Meyer and Wagner, 2006). Non-viral vectors can be easily synthesized and convince especially by their absent immunogenicity and enhanced biocompatibility. The "golden standard" of PEI-based gene carriers is LPEI, the linear form of polyethylenimine, with a molecular weight of 22 kDa, also known as the commercially available JetPEI®. The major drawback of LPEI is its significant toxicity after systemic application due to acute and long-term toxic effects (Chollet *et al.*, 2002). Therefore, several biodegradable polymers were developed for gene transfer (Forrest *et al.*, 2003; Kloeckner *et al.*, 2006a) aiming to reduce the toxicity profile while maintaining high transduction efficiency comparable to the standard synthetic gene vectors. We have recently developed a series of biodegradable carriers based on low molecular weight polycations crosslinked either via ester or disulfide bonds (Kloeckner *et al.*, 2006b; Russ *et al.*, 2008a; Russ *et al.*, 2008), demonstrating very promising toxicity profiles and similar or even superior transfection efficiency in comparison with LPEI (Russ *et al.*, 2008). Continuing this work, a novel class of branchend polycations was synthesized based on oligoethylenimine (OEI)-grafted polypropylenimine dendrimers (G2-HD-OEI) (Russ *et al.*, 2008a). Low toxicity in association with high transfection efficiency was observed in different tumor cell lines *in vitro* using these polymers. Moreover, polyplexes formed by these biodegradable polymers prevented aggregation with erythrocytes and toxic side effects

after systemic administration *in vivo*. Transgene expression was almost exclusively detected intratumorally in tumor bearing mice, whereas with polyplexes based on linear PEI transgene expression in lung was more than 100 times higher than in the tumor (Russ and Wagner, 2007; Russ *et al.*, 2008a; Russ *et al.*, 2008). Apparently, polyplexes based on branched polycations exhibit a high intrinsic tumor affinity, significantly improving tumor-specific targeting of transgene expression, one of the major hurdles of gene therapy. In this context, Dufes *et al.* showed that systemic injection of polypropylenimine dendrimer nanoparticles containing a TNFα expression plasmid regulated by telomerase gene promoter leads to tumor-specific transgene expression, resulting in tumor regression and improved survival in various tumor models (Dufes *et al.*, 2005).

In the current study, we applied the above described OEI-grafted polypropylenimine dendrimers (G2-HD-OEI) as novel biodegradable and highly efficient non-viral gene delivery vehicles for systemic NIS gene transfer in a syngeneic neuroblastoma mouse model. Based on its dual function as reporter and therapy gene, NIS was used for non-invasive imaging of vector biodistribution by ^{123}I-scintigraphy followed by assessment of the therapy response after application of [131]I.

# Materials and Methods

*Cell culture*

The murine neuroblastoma (Neuro2A) cell line (ATCC-CCL-131) was cultured in DMEM (1g/L glucose) supplemented with 10% fetal bovine serum (v/v) (PAA; Colbe, Germany) and 1% penicillin /streptomycin. Cells were maintained at 37°C and 5% $CO_2$ in an incubator with 95% humidity. The cell culture medium was replaced every second day and cells were passaged at 85% confluency.

*Plasmids and polycation*

The expression vector CMV-NIS-pcDNA3 (pCMV-NIS) containing the full-length NIS cDNA coupled to the CMV promoter was kindly provided by Dr. S. M. Jhiang, Ohio State Univesity, Columbus, OH, USA. As control, NIS cDNA was removed using *EcoRI* and re-ligated into the same expression vector in antisense direction (pCMV-antisense/NIS). G2-HD-OEI was synthesized as described previously (Russ *et al.*, 2008a) and used as a 5 mg/ml stock solution.

*Polyplex formation*

Plasmid DNA was condensed with polymers at indicated conjugate/plasmid (c/p) - ratios (w/w) in HEPES buffered glucose (HBG: 20 mM HEPES, 5% glucose (w/v), pH 7.4) as described (Russ, 2008) and incubated at room temperature for 20 min. prior to use. Final DNA concentration of polyplexes for *in vitro* studies was 4 µg/ml, for *in vivo* studies 200 µg/ml.

*Transient transfection*

For *in vitro* transfection experiments, Neuro2A cells were grown to 60-80% confluency. Cells were incubated for 4 h with polyplexes in the absence of serum and antibiotics followed by incubation with growth medium for 24 h. Transfection efficiency was evaluated by measurement of iodide uptake activity as described below.

*$^{125}I$ uptake assay*

Following transfections, iodide uptake of Neuro2A cells was determined at steady-state conditions as described by Weiss *et al.* (Weiss *et al.*, 1984). Results were normalized

to cell survival measured by cell viability assay (see below) and expressed as cpm/A 490 nm.

### *Cell viability assay*

Cell viability was measured using the commercially available MTS-assay (Promega Corp., Mannheim, Germany) according to the manufacturer´s recommendations as described previously (Unterholzner *et al.*, 2006).

### *Establishment of Neuro2A tumors*

Neuro2A tumors were established in syngeneic male A/J mice (Harlan Winkelmann, Borchen, Germany) by subcutaneous injection of $1 \times 10^6$ Neuro2A cells suspended in 100 µl PBS into the flank region. Animals were maintained under specific pathogen-free conditions with access to mouse chow and water *ad libitum*. The experimental protocol was approved by the regional governmental commission for animals (Regierung von Oberbayern).

### *NIS gene transfer and radioiodine biodistribution studies in vivo*

Experiments started when tumors had reached a tumor size of 8-10 mm after a 10-day pretreatment with L-T4 (intraperitoneal (i.p.) injection of 2 µg L-T4/day (Henning, Sanofi-Aventis, Germany) diluted in 100 µl PBS) to suppress thyroidal iodine uptake. For systemic *in vivo* gene transfer polyplexes (c/p 2) were applied via the tail vein at a DNA dose of 2.5 mg/kg (i.e. for a 20 g mouse 250 µl polyplex in HBG at 200 µg/ml DNA); either NIS containing polyplexes (G2-HD-OEI/NIS) or polyplexes with the control vector (G2-HD-OEI/antisense-NIS). Two groups of mice were established and treated as follows: (1) i.v. injection of G2-HD-OEI/NIS (n=24); (2) i.v. injection of G2-HD-OEI/antisense-NIS (control vector) (n=9). As an additional control, in a subset of mice treated with G2-HD-OEI/NIS (n=9) the specific NIS-inhibitor sodium-perchlorate ($NaClO_4$ 2 mg/per mouse) was injected i.p. 30 min. prior to $^{123}I$ administration. 24 h after polyplex application, mice were injected i.p. with 18.5 MBq (0.5 mCi) $^{123}I$ and iodide biodistribution was assessed using a gamma camera equipped with UXHR collimator (Ecam, Siemens, Germany) as described previously (Willhauck *et al.*, 2007; Willhauck *et al.*, 2008a). Regions of interest were quantified and expressed as a fraction of the total amount of applied radionuclide per gram tumor tissue. The retention time within the tumor was determined by serial scanning

after radionuclide injection, and dosimetric calculations were performed according to the concept of MIRD, with the dosis factor of RADAR-group (www.doseinfo-radar.com).

*Analysis of radioiodine biodistribution ex vivo*

For *ex vivo* biodistribution studies, mice were injected with G2-HD-OEI/NIS (n=24) or G2-HD-OEI/antisense-NIS (n=9) as described above followed by i.p. injection of 18.5 MBq [123]I 24 h later. A subset of NIS-transduced mice (n=9) was treated with sodium-perchlorate prior to ^{123}I administration as an additional control. Two, 6 and 12 h after ^{123}I injection, mice were sacrificed and organs of interest were dissected, weighed and radioiodide uptake was measured in a gamma counter (5 NIS-transduced animals per time point (G2-HD-OEI/NIS) and 3 mice of each control). Results were reported as percentage of injected dose per organ (% ID/organ).

*Analysis of NIS mRNA expression using quantitative real-time PCR*

Total RNA was isolated from Neuro2A tumors or other tissues using the RNeasy Mini Kit (Qiagen, Hilden, Germany) according to the manufacturer's recommendations. Single stranded oligo (dT)-primer cDNA was generated using Superscript III Reverse Transcriptase (Invitrogen). Following primers were used: hNIS (5`-TGCGGGACTTTGCAGTACATT-3´) and (5`-TGCAGATAATTCCGGTGGACA-3´), GAPDH: (5`-GAGAAGGCTGGGGCTCATTT-3´) and (5`-CAGTGGGGACACGGAAGG-3`). Quantitative real-time PCR (qPCR) was performed with the cDNA from 1µg RNA using the SYBR green PCR master mix (Quiagen) in a Rotor Gene 6000 (Corbett Research, Morthlake, New South Wales, Australia). Relative expression levels were calculated using the comparative $\Delta\Delta C_t$ method and internal GAPDH for normalization.

*Immunohistochemical analysis of NIS protein expression*

Immunohistochemical staining of frozen tissue sections derived from Neuro2A tumors after systemic gene delivery was performed as described previously (Spitzweg *et al.*, 2007).

*Radioiodine therapy study in vivo*

Following a 10-day L-T4 pretreatment as described above, two groups of mice were established receiving 55.5 MBq ^{131}I as a single i.p. injection 24 h after systemic application

of G2-HD-OEI/NIS (n=6) or G2-HD-OEI/antisense-NIS (n=6), respectively. As control, two further groups of mice were treated with saline instead of $^{131}$I after injection of either G2-HD-OEI/NIS (n=6) or G2-HD-OEI/antisense-NIS (n=6). A further control group was injected with saline only (n=6). The treatment consisting of systemic polyplex application followed by $^{131}$I or saline application after 24 h was repeated once on day three and four, respectively. Tumor sizes were measured before treatment and daily thereafter for up to four weeks. Tumor volume was estimated using the equation: tumor volume = length x width x height x 0.52. Experiments were repeated twice, tumor volumes are expressed as means of 12 mice per group.

### *Indirect immunofluorescence assay*

Indirect immunofluorescence was performed on frozen sections as described previously (Willhauck *et al.*, 2007).

### *Statistical methods*

All *in vitro* experiments were carried out in triplicates. Results are represented as mean +/- SD of triplicates. Statistical significance was tested using Student´s t test.

# Results

## *Iodide uptake studies in vitro*

Transfection conditions using G2-HD-OEI/NIS were optimized in Neuro2A cells by measurement of perchlorate-sensitive iodide uptake activity 24 h following polyplex application (data not shown). We found an optimal c/p ratio of 2, which resulted in highest transfection efficiency at low cytotoxicity. This ratio was used in all subsequent experiments. 24 h after transfection with G2-HD-OEI/NIS, Neuro2A cells showed a 51-fold increase in $^{125}$I accumulation as compared to cells incubated with empty G2-HD-OEI (Fig. 1). Furthermore, no perchlorate-sensitive iodide uptake above background level was observed in cells transfected with the control vector G2-HD-OEI/antisense-NIS. Polyplex-mediated NIS gene transfer did not alter cell viability as measured by MTS-assay (Fig. 1).
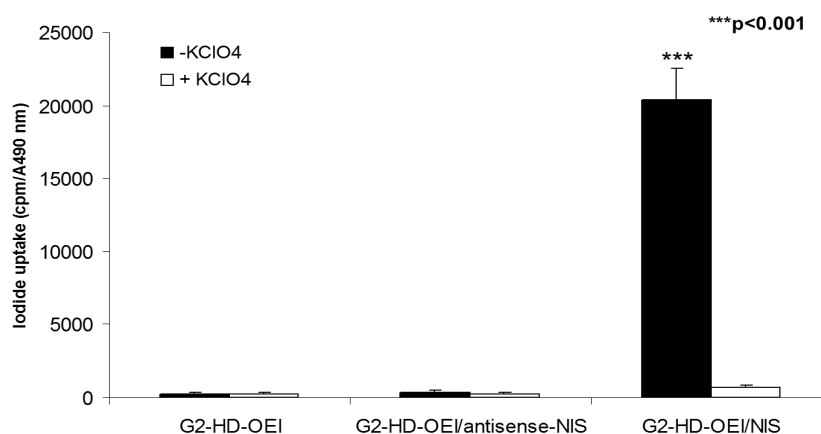


**Fig. 1:** Iodide uptake was measured in Neuro2A cells following *in vitro* transfection with G2-HD-OEI/NIS, control vector G2-HD-OEI/antisense-NIS, or with G2-HD-OEI alone. Neuro2A cells transfected with G2-HD-OEI/NIS showed a 51-fold increase in perchlorate-sensitive $^{125}$I accumulation. In contrast, no perchlorate-sensitive iodide uptake above background level was observed in cells transfected with control vector or without DNA (***p <0.001).

## *In vivo radioiodine biodistribution studies*

To investigate the iodide uptake activity in Neuro2A tumors after systemic *in vivo* NIS gene transfer, $^{123}$I distribution was monitored in tumor bearing mice 24 h after G2-HD-OEI/DNA administration by gamma camera imaging. While no iodide accumulation was detected in tumors after application of G2-HD-OEI/antisense-NIS (Fig. 2C), significant iodide uptake was observed in 85% (13 out of 15) of Neuro2A tumors following systemic injection of G2-HD-OEI/NIS, in addition to physiological iodide accumulation in thyroid, stomach and bladder (Fig. 2A). As determined by serial scanning, approximately 8-13%

ID/g $^{123}$I was accumulated in NIS-transduced tumors with a biological half-life of 13 h. Considering a tumor mass of 1 g, an effective half-life of 12 h for $^{131}$I and a tumor absorbed dose of 247 ± 94 mGy/MBq $^{131}$I were calculated (Fig. 2D). To confirm that tumoral iodide uptake was indeed NIS-mediated, a subset of G2-HD-OEI/NIS injected mice (n=9) received sodium-perchlorate 30 min prior to $^{123}$I administration. In all experiments a single injection of 2 mg sodium-perchlorate completely blocked tumoral iodide accumulation in addition to abolished physiological iodide uptake in stomach and thyroid gland (Fig. 2B). Moreover, no significant iodide uptake was observed in non-target organs, including lung, liver, kidney or spleen which confirms tumor-specificity of nanoparticle-mediated NIS gene delivery.
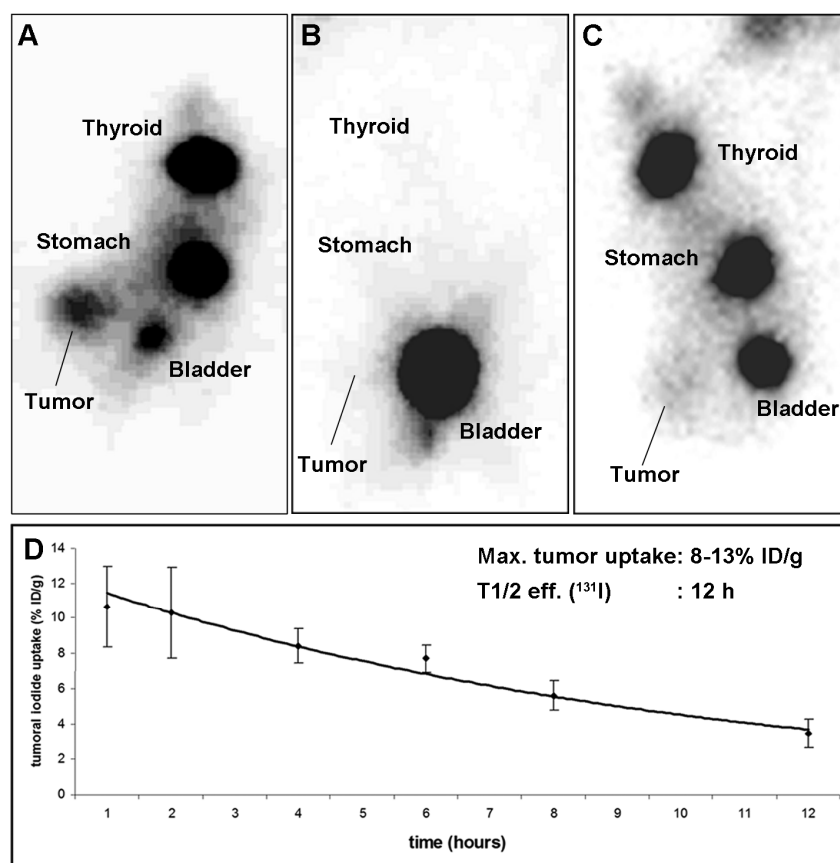


**Fig. 2:** $^{123}$I gamma camera imaging of mice harbouring Neuro2A tumors 4 h following i.p. injection of 18.5 MBq $^{123}$I after G2-HD-OEI-mediated NIS gene delivery. While mice treated with control vectors (G2-HD-OEI/antisense-NIS) showed no tumoral iodide uptake (C), treatment with G2-HD-OEI/NIS induced significant tumor-specific iodide accumulation in Neuro2A tumors with accumulation of 8-13% ID/g $^{123}$I (A), which was completely abolished upon pretreatment with NaClO$_4$ (B). Iodide was also accumulated physiologically in thyroid, stomach and bladder (A, C).
Time course of $^{123}$I accumulation in Neuro2A tumors after systemic polyplex-mediated NIS gene delivery followed by injection of 18.5 MBq $^{123}$I as determined by serial scanning (D). Maximum tumoral radioiodine uptake was 8-13% ID/g tumor with an average effective $T_{1/2}$ of 12 h for $^{131}$I (D).

*Ex vivo radioiodine biodistribution studies*

  *Ex vivo* biodistribution analysis confirmed significant iodide uptake in tumors following systemic NIS gene transfer (Fig. 3). While NIS-transduced Neuro2A tumors accumulated 6-8% ID/organ $^{123}$I 2 hours after radioiodine injection, mock-transduced tumors showed no significant iodide uptake. In both groups the thyroid gland and the stomach accumulated approx. 40% and 39% ID/organ (data not shown). Noteworthy, the average tumor weight in this experiment was approximately 0.7 g. Further, a single perchlorate injection prior to radioiodine application significantly blocked iodide uptake in NIS-transduced tumors and in physiologically NIS-expressing tissues, including thyroid and stomach, throughout the observation period up to 12 h. In addition, no significant iodide uptake above background levels was observed in non-target organs, including lung, liver, kidney or spleen confirming tumor-specific NIS gene delivery (see also Fig. 2A).
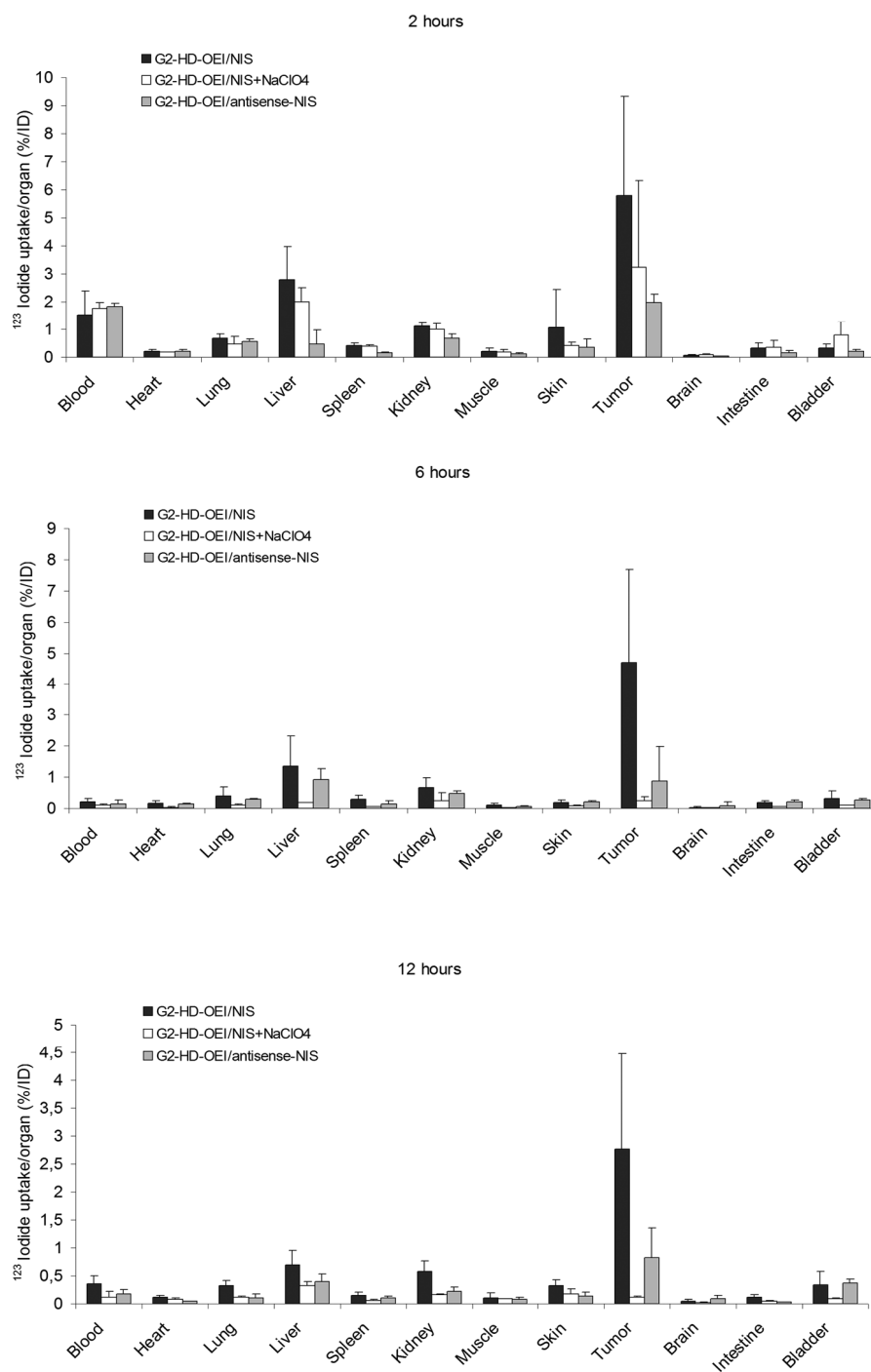
**Fig. 3:** Evaluation of iodide biodistribution *ex vivo* 2, 6 and 12 hours following injection of 18.5 MBq [123]I. While tumors in NIS-transduced mice showed high perchlorate-sensitive iodide uptake activity (up to 6-8% ID/organ), non-target organs revealed no significant iodide accumulation. No iodide accumulation was measured after injection of control vector. Results were reported as percent of injected dose per organ ± SD.

## Analysis of NIS mRNA expression by quantitative real-time PCR analysis

In order to assess NIS mRNA expression after systemic NIS gene transfer, mRNA of various tissues was extracted and analyzed by quantitative real-time PCR (qPCR) with a pair of NIS-specific oligonucleotide primers 24 h after NIS gene transfer. Only a low background level of NIS mRNA expression was detected in untreated tumors or tumors after application of G2-HD-OEI/antisense-NIS. In contrast, a significant level of NIS gene expression was induced in Neuro2A tumors after systemic injection of G2-HD-OEI/NIS (Fig. 4A). As expected, administration of the competitive NIS inhibitor sodium-perchlorate had no influence on NIS mRNA expression in NIS transduced tumors. Furthermore, no significant NIS mRNA expression above background level was detected in non-target organs, like liver and lung after systemic application of G2-HD-OEI/NIS or G2-HD-OEI/antisense-NIS (Fig. 4A).
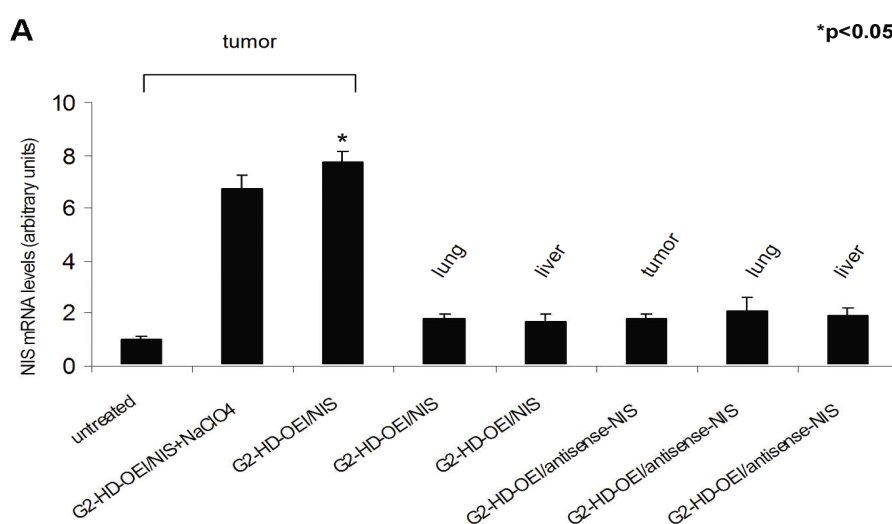


**Fig. 4:** Analysis of human NIS mRNA expression in Neuro2A tumors and non-target organs by qPCR. A significant level of NIS mRNA expression was induced in Neuro2A tumors after systemic NIS gene transfer with or without sodium-perchlorate pretreatment. Only a low background level of NIS mRNA expression was detected in untreated tumors, which was set as 1 arbitrary unit. Moreover, no significant NIS expression above background level was found in tumors after application of G2-HD-OEI/antisense-NIS or non-target organs, like liver and lung. Results were reported as NIS/GAPDH ratios.

## Analysis of NIS protein expression in Neuro2A tumors

Immunohistochemical analysis of Neuro2A tumors using a mouse monoclonal NIS-specific antibody revealed a heterogeneous staining pattern with clusters of primarily membrane-associated NIS-specific immunoreactivity in tumors after systemic application of G2-HD-OEI/NIS (Fig. 4B, left, white arrows). In contrast, tumors treated with G2-HD-OEI/antisense-NIS (Fig. 4B, right) or untreated tumors showed no NIS-specific

immunoreactivity. Parallel control slides with the primary and secondary antibodies replaced in turn by PBS and isotype-matched non immune immunoglobulin were negative (data not shown).

**B**
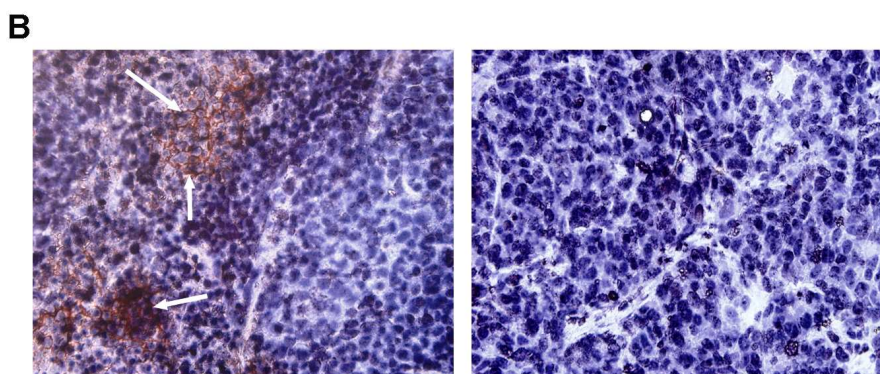


**Fig. 4:** Immunohistochemical staining of Neuro2A tumors 24 h after G2-HD-OEI/NIS application showed clusters of primarily membrane-associated NIS-specific immunoreactivity (left). In contrast, Neuro2A tumors treated with the control plasmid (G2-HD-OEI/antisense-NIS) did not reveal NIS-specific immunoreactivity (right). Magnification: 320x

## *Radioiodine therapy studies after in vivo NIS gene transfer*

24 h after systemic administration of G2-HD-OEI/NIS or G2-HD-OEI/antisense-NIS polyplexes, a therapeutic dose of 55.5 MBq (1.5 mCi) $^{131}$I or saline was injected i. p. This cycle consisting of systemic NIS gene transfer followed by radioiodine or saline administration was repeated once on day 3 and 4 (Fig. 5A). As an additional control, tumor growth of mice injected with saline only was assessed (n=6).

Mice treated with G2-HD-OEI/NIS or G2-HD-OEI/antisense-NIS followed by application of saline and mice treated with G2-HD-OEI/antisense-NIS followed by application of $^{131}$I as well as saline treated mice showed an exponential tumor growth. In contrast, NIS-transduced (G2-HD-OEI/NIS) and $^{131}$I-treated tumors showed a significant delay in tumor growth (Fig. 5A). While all mice in the control groups had to be killed within two weeks after the onset of the experiments due to excessive tumor growth, 70 % of the mice treated with $^{131}$I after injection of G2-HD-OEI/NIS survived approx. four weeks (Fig. 5B). Importantly, none of these mice showed major adverse effects of radionuclide or polyplex treatment in terms of lethargy or respiratory failure. However, a minor body weight loss of 3-5% was observed in mice after systemic administration of polyplexes.
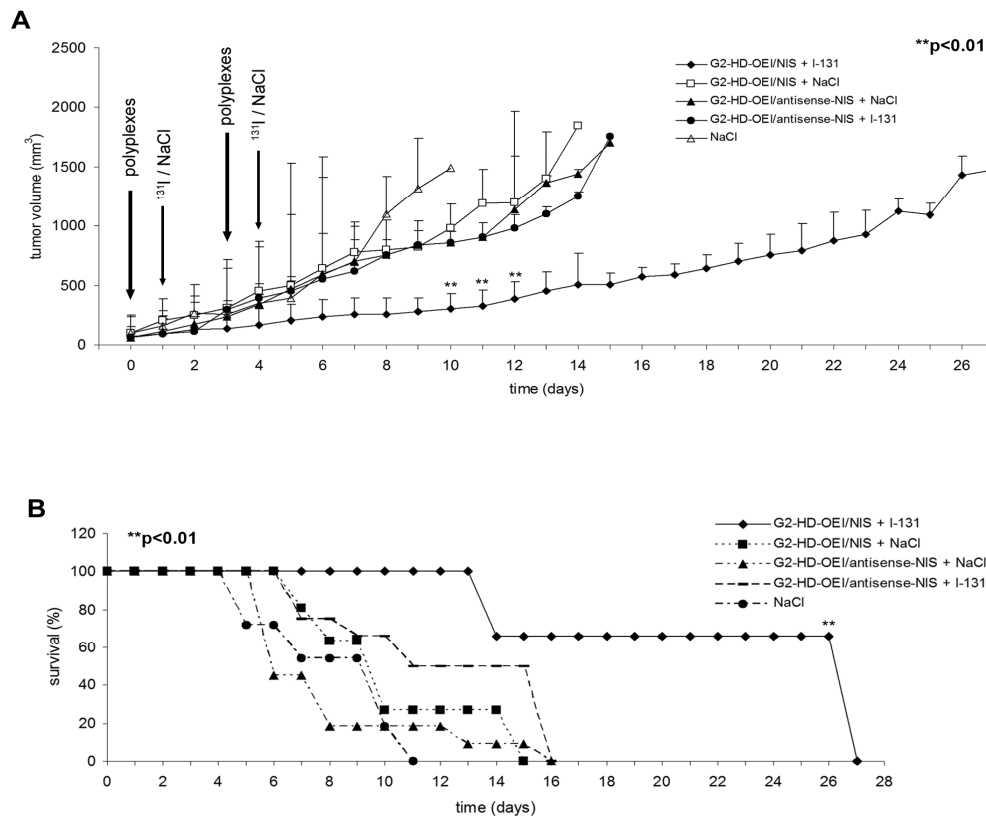
**Fig 5:** Radioiodine treatment of Neuro2A tumors after systemic polyplex-mediated NIS gene transfer *in vivo*. 24 h after i. v. polyplex injection (big arrow), 55.5 MBq $^{131}$I was injected i.p. (small arrow). This treatment cycle was repeated once on day 3 and 4. $^{131}$I therapy after systemic G2-HD-OEI/NIS application resulted in a significant delay in tumor growth (A, **p<0.01) which was associated with markedly improved survival (B, Kaplan-Meier-plot (**p<0.01)) as compared to the control groups that were injected with saline only, with G2-HD-OEI/NIS followed by saline application, or with G2-HD-OEI/antisense-NIS followed by saline or $^{131}$I application.

### *Immunofluorescence analysis*

Three to four weeks after treatment, mice were sacrificed, tumors were dissected and processed for immunofluorescence analysis. Immunofluorescence analysis using a Ki67-specific antibody (green) and an antibody against CD31 (red, labeling blood vessels) showed striking differences between NIS-transduced (Fig. 6A) and mock-transduced $^{131}$I-treated tumors (Fig. 6B). As compared to mock-transduced tumors (G2-HD-OEI/antisense-NIS), NIS-transduced tumors (G2-HD-OEI/NIS) exhibited a significantly lower intratumoral blood vessel density and proliferation index after $^{131}$I therapy.

**Fig. 6:** Immunofluorescence analysis using a Ki67-specific antibody (green) and an antibody against CD31 (red, labelling blood vessels) showed significantly decreased proliferation and blood vessel density in NIS-transduced tumors (A) following ^{131}I treatment as compared to mock-transduced tumors (B). Slides were counterstained with DAPI nuclear stain. Magnification 100x

## Discussion

As one of the oldest and most successful targets of molecular imaging and therapy, cloning and characterization of NIS has provided us with a powerful new reporter and therapy gene, that allowed the development of a promising cytoreductive gene therapy strategy based on NIS gene transfer in extrathyroidal tumors followed by targeted radionuclide therapy (Spitzweg *et al.*, 2001c). Many of the characteristics of NIS, which have been confirmed by our work to date, suggest that it represents an ideal therapy gene due to several advantages. NIS as a normal human gene and protein implies that its expression in cancer cells is unlikely to be toxic or to elicit a significant immune response that could limit its efficacy. In addition, NIS gene therapy is associated with a substantial bystander effect based on the crossfire effect of the beta-emitter $^{131}$I with a path length of up to 2.4 mm. A bystander effect is desirable for any kind of gene therapy strategy, because it reduces the level of transduction efficiency required for a therapeutic response (Dingli *et al.*, 2003b). In its dual role as reporter and therapy gene NIS allows direct, non-invasive imaging of functional NIS expression by $^{123}$I-scintigraphy and $^{124}$I-PET-imaging, as well as exact dosimetric calculations before proceeding to therapeutic application of $^{131}$I (Spitzweg and Morris, 2002b; Dingli *et al.*, 2003b). Moreover, NIS is already being used clinically as molecular basis of $^{131}$I therapy, an already approved anticancer therapy in thyroid cancer with a well-understood therapeutic window and safety profile (Spitzweg *et al.*, 2001c).

The capacity of the NIS gene to induce radioiodine accumulation in non-thyroidal tumors has been investigated in a variety of tumor models by several groups including our own (Spitzweg *et al.*, 1999c; Spitzweg *et al.*, 2000b; Spitzweg *et al.*, 2001a; Dohan *et al.*, 2003; Kakinuma *et al.*, 2003; Cengic *et al.*, 2005; Scholz *et al.*, 2005; Spitzweg *et al.*, 2007; Willhauck *et al.*, 2007; Willhauck *et al.*, 2008a; Willhauck *et al.*, 2008b). In our initial studies in the prostate cancer model we used the prostate-specific antigen (PSA) promoter to achieve prostate-specific iodide accumulation, which resulted in a significant therapeutic effect after application of $^{131}$I, and alternative radionuclides such as $^{188}$Re and $^{211}$At even in the absence of iodide organification (Spitzweg *et al.*, 1999c; Spitzweg *et al.*, 2000b; Spitzweg *et al.*, 2003; Scholz *et al.*, 2004; Willhauck *et al.*, 2007; Willhauck *et al.*, 2008a). Taken together, our pioneer work in the prostate cancer model and consecutive work in other tumor models, such as medullary thyroid, colon and hepatocellular cancer (Cengic *et al.*, 2005; Scholz *et al.*, 2005; Spitzweg *et al.*, 2007; Willhauck *et al.*, 2008b) has convincingly demonstrated the enormous potential of NIS as novel reporter and therapy

gene. Based on our promising preliminary work and the proof-of-principle of tumor-specific NIS gene therapy in prostate cancer including extensive toxicity studies, a first phase I clinical trial was approved at the Mayo Clinic for radioiodine therapy of locally recurrent prostate cancer after local adenoviral NIS gene transfer (Dwyer *et al.*, 2005b). One of the major hurdles on the way to efficient and safe application of the NIS gene therapy concept in the clinical setting, in particular in metastatic disease, is optimal tumor-specific targeting in the presence of low toxicity and high transduction efficiency of gene delivery vectors, with the ultimate goal of systemic vector application. Only a limited number of studies have investigated systemic NIS gene delivery approaches with the aim of NIS-targeted radionuclide therapy of metastatic disease. An oncolytic measles virus encoding human NIS was applied systemically in a multiple myeloma mouse model and allowed to enhance the oncolytic potency of the virus after $^{131}$I application (Dingli *et al.*, 2004). In a more recent study, an oncolytic vesicular stomatitis virus was designed to express NIS to be able to monitor virus replication by $^{123}$I scintigraphic imaging in addition to stimulation of the oncolytic potency by the combination with $^{131}$I therapy, which was successfully investigated in a multiple myeloma mouse model after systemic vesicular stomatitis virus application (Goel *et al.*, 2007).

In the current study we have utilized a non-viral gene delivery system for tumor-targeted NIS gene transfer in the neuroblastoma mouse model Neuro2A. The syngeneic Neuro2A mouse model develops well vascularized tumors with leaky vasculature thereby allowing intratumoral accumulation of polyplexes with subsequent diffusion from the blood vessel into the tumor tissue (Smrekar *et al.*, 2003). Similar effects were observed with hepatoma models like the human xenografts HepG2 and HuH7, while other xenograft models such as the A549 lung carcinoma model were less susceptible to polyplex-mediated gene delivery (Smrekar *et al.*, 2003). Branched polycations based on oligoethylenimine (OEI)-grafted polypropylenimine dendrimers (G2-HD-OEI) have recently been characterized as biodegradable synthetic gene delivery vectors with high *in vivo* transduction efficiency and remarkable intrinsic tumor affinity in the presence of low toxicity (Russ *et al.*, 2008a). G2-HD-OEI complexed with the human NIS cDNA under the control of the unspecific CMV promoter revealed high transfection efficiency *in vitro* resulting in a 51-fold increase in iodide uptake activity in Neuro2A cells at an optimal polymer to plasmid w/w ratio of 2 that provided highest transfection efficiency at low cytotoxicity. Following systemic application of NIS-conjugated G2-HD-OEI via the tail vein *in vivo*, 85% of Neuro2A tumors in a syngeneic mouse model showed tumor-specific

[123]I accumulation with approximately 8-13 % ID/g, a biological half-life of 13 h and a calculated effective half-life of 12 h for [131]I. In contrast, mice pretreated with the competitive NIS-inhibitor sodium-perchlorate or mice injected with control vectors showed no tumoral iodide uptake, confirming that the observed radioiodine accumulation in the tumors was mediated by functional NIS expression. These data are consistent with a recently published study by Chisholm *et al.,* demonstrating tumor-specific targeting of NIS in various xenograft tumor mouse models by nano-SPECT/computer tomography imaging of radioiodine biodistribution using polypropylenimine dendrimers for systemic NIS gene delivery (Chisholm *et al.*, 2009).

In addition, in our study *in vivo* [123]I scintigraphic imaging studies were confirmed by *ex vivo* biodistribution experiments revealing significant tumoral radioiodine accumulation, while no iodide uptake was measured in non target organs, like lung, liver, spleen or kidneys. Tumoral NIS expression was further confirmed by real time q-PCR as well as NIS-specific immunoreactivity, which was primarily membrane-associated and occured in clusters. The patchy staining pattern nicely correlates with experiments using PEI-based polyplexes carrying the beta-galactosidase reporter gene, in which a heterogeneous and patchy distribution of transgene activity in transduced tumors was observed (Kircheis *et al.*, 2001b). These data are also consistent with previously reported studies using luciferase as reporter gene for the evaluation of transduction efficiency and tumor specificity of various oligoethylenimine acrylate ester-based pseudodendrimers including G2-HD-OEI. After systemic polyplex application high luciferase activity was found selectively in tumor tissue, while no significant expression was detected in non-target organs concomitant with absent or low toxicity (Russ *et al.*, 2008a; Russ *et al.*, 2008). In contrast, when standard LPEI were used as gene delivery vectors, high luciferase activity was observed in the lung and acute or long-term toxic effects were observed (Goula *et al.*, 1998; Chollet *et al.*, 2002; Russ *et al.*, 2008). In our study, even after repeated injection of G2-HD-OEI followed by administration of ^{131}I no major side effects occured. Data from previous studies suggest that polyplexes formed with branched structures like G2-HD-OEI do not show pronounced aggregation with erythrocytes that usually results in high transgene expression in the first vascular bed encountered, namely the lung. Consequently such polymers are able to deliver the nucleic acid payload toward the tumor site, most probably due to passive tumor targeting, that occurs due to the imperfect and leaky tumor vasculature combined with an inadequate lymphatic drainage (Maeda, 2001).

In our mouse studies $^{123}$I uptake of 40 % ID was detected in the thyroid gland and 39 % ID in the stomach 2h after $^{123}$I injection, resulting from endogenous NIS expression in thyroid and stomach, which has been described by several groups including our own (Spitzweg and Morris, 2002b). However, in the current study, $^{123}$I uptake in the stomach was significantly higher than that expected in humans, which may be the result of increased NIS expression in the murine gastric mucosa and may also be caused by pooling of gastric juices as mice were anaesthetized for prolonged period for serial imaging. In addition, due to exquisite regulation of thyroidal NIS expression by TSH, $^{123}$I accumulation in the thyroid gland can effectively be down regulated by thyroid hormone treatment as shown in humans (Wapnir *et al.*, 2004).

Most importantly, systemic polyplex-mediated NIS gene transfer resulted in tumor-specific iodide uptake activity in Neuro2A tumor bearing mice which was sufficiently high for a significant therapeutic effect of $^{131}$I. After two cycles of systemic polyplex application followed by $^{131}$I injection tumor-bearing mice showed a significant delay of tumor growth associated with a significantly prolonged survival. In addition, immunofluorescence analysis showed markedly reduced proliferation associated with decreased blood vessels density inside and surrounding the tumor after systemic polyplex-mediated NIS gene transfer followed by $^{131}$I application, suggesting radiation-induced tumor stroma cell damage in addition to tumor cell death. The crossfire effect of $^{131}$I with a maximum path length of up to 2.4 mm might be responsible for stromal cell damage leading to reduced angiogenesis and secretion of growth-stimulatory factors, thereby enhancing therapeutic efficacy.

Following polyplex-mediated systemic NIS gene delivery, therapeutic efficacy of NIS-targeted radionuclide therapy could be further stimulated by application of alternative radionuclides, such as the beta-emitter $^{188}$Re or the alpha-emitter $^{211}$At. Both are known to be also transported by NIS, but offer the possibility of higher energy deposition in a shorter time period due to their higher energy and shorter half-lifes. This has convincingly been demonstrated by several groups, including our own studies in the prostate cancer model described above (Dadachova *et al.*, 2002; Petrich *et al.*, 2006). In view of the patchy and heterogeneous expression pattern of NIS protein expression after polyplex-mediated systemic NIS gene transfer, $^{188}$Re might be a promising alternative radionuclide due to the longer path length of the beta particles (mean range 3.1 mm, maximum range 10.4 mm) and therefore superior crossfire effect, which will be addressed in future studies.

Moreover, tumor-specific targeting could be enhanced by coupling of tumor-targeting ligands, such as the serum glycoprotein transferrin (Tf) or epidermal growth factor

(EGF) (Kircheis *et al.*, 2001a; De Bruin *et al.*, 2007), and further optimized by application of tumor-specific promoters as shown in our earlier work (Spitzweg *et al.*, 1999c; Spitzweg *et al.*, 2000b; Kakinuma *et al.*, 2003; Cengic *et al.*, 2005; Scholz *et al.*, 2005; Spitzweg *et al.*, 2007; Willhauck *et al.*, 2008b).

In conclusion, our data clearly demonstrate the high potential of branched polycations based on oligoethylenimine (OEI)-grafted polypropylenimine dendrimers for tumor-specific delivery of the NIS gene after systemic application. Based on the role of NIS as a potent and well characterized reporter gene allowing non-invasive imaging of functional NIS expression by $^{123}$I-scintigraphy and $^{124}$I-PET imaging, this study allowed detailed characterization of *in vivo* biodistribution of polyplex-mediated functional NIS expression by gamma camera imaging, which is an essential prerequisite for exact planning and monitoring of clinical gene therapy trials with the aim of individualization of the NIS gene therapy concept in the clinical setting. Tumor-specific iodide accumulation was further demonstrated to be sufficiently high for a significant delay of tumor growth associated with increased survival in syngeneic mice bearing neuroblastoma tumors after two cycles of NIS-polyplex application followed by $^{131}$I therapy. This study therefore opens the exciting prospect of NIS-targeted radionuclide therapy of metastatic cancer using polyplexes based on biodegradable polymers for systemic NIS gene delivery.

# Acknowledgments

# 4.  Chapter 3

**Image-guided tumor-selective radioiodine therapy of liver cancer following systemic non-viral delivery of the sodium iodide symporter gene**

# Abstract

We evaluated the therapeutic concept of tumor-selective radioiodine therapy following systemic nonviral delivery of the sodium iodide symporter (NIS) gene in a clinically important tumor model of human hepatocellular cancer (HCC). Incubation with synthetic gene delivery vectors (polyplexes), in which a NIS expressing plasmid was condensed with pseudodendritic oligoamines (G2-HD-OEI polymer), resulted in a 44-fold increase of perchlorate-sensitive iodide uptake in HCC cells *in vitro* as compared to mock-transduced cells. Polyplexes were injected via the tail vein in a HCC xenograft mouse model followed by analysis of radioiodine distribution after i.p. injection of $^{123}$I using γ-camera or SPECT-CT imaging. After systemic NIS gene delivery HCC tumors accumulated 6 - 11% ID/g $^{123}$I with an effective half-life of 10 h for $^{131}$I resulting in a tumor absorbed dose of 281 mGy/MBq, while tumors transduced with control vectors showed no iodide uptake. After 2 cycles of polymer application followed by $^{131}$I application, a significant delay in tumor growth was observed associated with markedly improved survival.

These results clearly demonstrate that systemic NIS gene transfer using novel biodegradable non-viral gene carriers is capable of inducing tumor-targeted radioiodine uptake in a liver cancer model, which therefore represents a promising innovative strategy for NIS-mediated radioiodine therapy of advanced HCC.

# Introduction

Hepatocellular carcinoma (HCC) is the fifth most common cancer worldwide and third most common cause of cancer mortality (Shariff *et al.*, 2009). Due to limited response to conventional chemo- or radiotherapy, surgery, including partial hepatectomy or liver transplantation, is currently the only potentially curative therapy available for patients with resectable disease. Despite a variety of alternative therapeutic options, including locally ablative therapies, such as radiofrequency thermal ablation and chemoembolization, the prognosis for advanced HCC has remained poor. Thus, in addition to novel strategies for early diagnosis, new therapeutic strategies have to be explored, such as multikinase inhibitors, immunotherapy, as well as gene therapy (Gerolami *et al.*, 2003).

In order to investigate an innovative, alternative therapeutic approach, in an earlier study we examined the feasibility of ^{131}I therapy of HCC following stable transfection with the sodium iodide symporter (NIS) using a mouse alpha-fetoprotein (AFP) promoter construct to target NIS expression to HCC cells (Willhauck *et al.*, 2008b). NIS is a transmemebrane glycoprotein that mediates the uptake of iodide into thyroid follicular cells (Dai *et al.*, 1996; Smanik *et al.*, 1996). The presence of NIS at the basolateral membrane of thyroid follicular cells has been exploited for many years for diagnostic imaging purposes as well as for ablative therapy of differentiated thyroid cancer using radioactive iodide (^{131}I). This non-invasive therapy has proven to be a safe and effective treatment for thyroid cancer, even in advanced metastatic disease (Van Nostrand and Wartofsky, 2007). In order to extend the use of NIS-mediated radioiodine therapy to other types of cancer, we have proven the feasibility of extrathyroidal radioiodine therapy after induction of iodide uptake by *ex vivo* NIS transfection or local adenoviral *in vivo* NIS gene transfer using tissue-specific promoters, such as the prostate-specific antigen (PSA) promoter, the carcinoembryonic antigen (CEA) promoter and the calcitonin promoter to specifically target NIS expression to prostate, colon and medullary thyroid cancer, respectively (Spitzweg *et al.*, 1999c; Spitzweg *et al.*, 2000b; Spitzweg *et al.*, 2001a; Cengic *et al.*, 2005; Scholz *et al.*, 2005; Spitzweg *et al.*, 2007; Willhauck *et al.*, 2007; Willhauck *et al.*, 2008a). In the liver cancer model we applied the AFP promoter for HCC-specific delivery of the NIS gene and demonstrated tumor-specific iodide uptake activity that allowed a therapeutic effect of ^{131}I in a HCC xenograft mouse model (Willhauck *et al.*, 2008b).

After the proof of principle of the NIS gene therapy concept in liver cancer in our study outlined above and by other investigators after retroviral or local/regional adenoviral

NIS gene delivery (Faivre *et al.*, 2004; Chen *et al.*, 2006; Herve *et al.*, 2008), the next crucial step towards clinical application has to be the evaluation of gene delivery vehicles that allow tumor-selective transgene expression in the presence of a sufficiently high transduction efficiency after systemic application to be able to reach disseminated tumor manifestations. In the evaluation of systemic application of gene delivery vectors, the dual function of NIS as therapy and reporter gene provides the advantage of detailed characterization and direct monitoring of *in vivo* vector biodistribution as well as localization, level and duration of transgene expression, which have been recognized as critical elements in the design of clinical gene therapy trials (Spitzweg and Morris, 2002b; Dingli *et al.*, 2003b; Baril *et al.*, 2010). Several research groups, including our own have demonstrated the potential of NIS as reporter gene in various applications, showing that *in vivo* imaging of radioiodine accumulation by $^{123}$I- or $^{99m}$Tc-scintigraphy as well as $^{123}$I-SPECT-CT fusion or $^{124}$I-PET imaging correlates well with the results of *ex vivo* gamma counter measurements as well as NIS mRNA and protein analysis. In addition, SPECT-CT imaging using $^{123}$I provides significant advantages for exact localization and quantitative analysis of NIS-mediated radioiodine accumulation due to enhanced resolution and sensitivity (Spitzweg *et al.*, 1999c; Spitzweg *et al.*, 2000b; Spitzweg *et al.*, 2001a; Dingli *et al.*, 2003b; Groot-Wassink *et al.*, 2004; Dwyer *et al.*, 2005a; Blechacz *et al.*, 2006; Carlson *et al.*, 2006; Goel *et al.*, 2007; Merron *et al.*, 2007; Spitzweg *et al.*, 2007; Willhauck *et al.*, 2007; Willhauck *et al.*, 2008a; Willhauck *et al.*, 2008b; Willhauck *et al.*, 2008c; Carlson *et al.*, 2009; Klutz *et al.*, 2009; Baril *et al.*, 2010; Li *et al.*, 2010; Penheiter *et al.*, 2010; Trujillo *et al.*, 2010; Watanabe *et al.*, 2010).

With the aim of systemic delivery of therapeutic genes, we have developed a series of biodegradable synthetic vectors based on low molecular weight polycations crosslinked either *via* ester or disulfide bonds (Kloeckner *et al.*, 2006b; Russ *et al.*, 2008a; Russ *et al.*, 2008), demonstrating very promising toxicity profiles and similar or even superior transfection efficiency in comparison with LPEI (linear polyethylenimine), the golden standard of PEI-based gene carriers (Russ *et al.*, 2008). In a recent study, we have demonstrated the high potential of synthetic, biodegradable polymeric vectors based on pseudodendritic oligoethylenimine (OEI)-grafted polypropylenimine dendrimers (G2-HD-OEI) with high intrinsic tumor affinity for tumor-specific delivery of the NIS gene. After intravenous application of NIS-conjugated polyplexes in a syngeneic neuroblastoma mouse model NIS-mediated radioiodine accumulation was mainly restricted to the tumor and

sufficiently high for a significant delay of tumor growth associated with improved survival (Klutz *et al.*, 2009).

Here we apply this concept of NIS gene delivery with biodegradable OEI-grafted polypropylenimine dendrimers in a human HCC xenograft mouse model. Based on its dual function as reporter and therapy gene, NIS was used for non-invasive imaging of vector biodistribution by $^{123}$I-scintigraphy and $^{123}$I-single photon emission computed tomography-computed tomography (SPECT-CT) imaging followed by assessment of the therapy response after application of $^{131}$I.

# Materials and Methods

*Cell culture*

The human hepatoma cell line (HuH7, JCRB 0403) was cultured in DMEM/F12 medium (Invitrogen Life Technologies Inc., Karlsruhe, Germany) supplemented with 10% fetal bovine serum (v/v) (PAA; Colbe, Germany), 5% L-glutamine (Invitrogen Life Technologies Inc.) and 1% penicillin/streptomycin. Cells were maintained at 37°C and 5% $CO_2$ in an incubator with 95% humidity. The cell culture medium was replaced every other day and cells were passaged at 85% confluency.

*Plasmids and polymers*

The expression vector CMV-NIS-pcDNA3 (pCMV-NIS) containing the full-length NIS cDNA coupled to the CMV promoter was kindly provided by Dr. S. M. Jhiang, Ohio State Univesity, Columbus, OH, USA. As a control, NIS cDNA was removed using *EcoRI* and re-ligated into the same expression vector in antisense direction (pCMV-antisense-NIS).

G2-HD-OEI was synthesized as described previously (Russ *et al.*, 2008a) and used as a 5 mg/ml stock solution.

*Polyplex formation*

Plasmid DNA was condensed with polymers at indicated conjugate/plasmid (c/p) - ratios (w/w) in HEPES buffered glucose (HBG: 20 mM HEPES, 5% glucose (w/v), pH 7.4) and incubated at room temperature for 20 min. prior to use as described previously (Russ, 2008). Final DNA concentrations of polyplexes for *in vitro* studies were 4 µg/ml, for *in vivo* studies 200 µg/ml.

*Transient transfection*

For *in vitro* transfection experiments, HuH7 cells were grown to 60 - 80% confluency. Cells were incubated for 4 h with polyplexes in the absence of serum and antibiotics followed by incubation with growth medium for 24 h. Transfection efficiency was evaluated by measurement of iodide uptake activity as described below.

### *$^{125}$I uptake assay*

Following transfections, iodide uptake of HuH7 cells was determined at steady-state conditions as described previously (Spitzweg *et al.*, 1999c). Results were normalized to cell survival measured by cell viability assay (see below) and expressed as cpm/A490 nm.

### *Cell viability assay*

Cell viability was measured using the commercially available MTS-assay (Promega Corp., Mannheim, Germany) according to the manufacturer´s recommendations as described previously (Willhauck *et al.*, 2007).

### *Establishment of HuH7 xenografts*

HuH7 xenografts were established in female CD-1 nu/nu mice (Charles River, Sulzfeld, Germany) by subcutaneous injection of $5 \times 10^6$ HuH7 cells suspended in 100 µl PBS into the flank region. Animals were maintained under specific pathogen-free conditions with access to mouse chow and water *ad libitum*. The experimental protocol was approved by the regional governmental commission for animals (Regierung von Oberbayern).

### *NIS gene transfer and radiodine biodistribution studies in vivo*

Experiments started when tumors had reached a tumor size of 8 - 10 mm and after a 10-day pretreatment with L-T4 (l-thyroxine, Henning, Sanofi-Aventis, Frankfurt, Germany) (5 mg/l) in their drinking water to maximize radioiodine uptake in the tumor and reduce iodide uptake by the thyroid gland. For systemic *in vivo* gene transfer polyplexes (c/p 2) were applied via the tail vein at a DNA dose of 2.5 mg/kg (i.e. for a 20 g mouse 250 µl polyplex in HBG at 200 µg/ml DNA), either NIS containing polyplexes (G2-HD-OEI/NIS) or polyplexes with the control vector (G2-HD-OEI/antisense-NIS). Two groups of mice were established and treated as follows: (1) i.v. injection of G2-HD-OEI/NIS (n=24); (2) i.v. injection of G2-HD-OEI/antisense-NIS (control vector) (n=9). As an additional control, in mice treated with G2-HD-OEI/NIS (n=9) the specific NIS-inhibitor sodium-perchlorate (NaClO$_4$, 2 mg/per mouse) was injected i.p. 30 min. prior to $^{123}$I administration. 24 h after polyplex application, mice were injected i.p. with 18.5 MBq (0.5 mCi) $^{123}$I, and radioiodine biodistribution was monitored by serial imaging on a gamma camera (Ecam, Siemens, Germany) equipped with a UXHR (Ultra Extra High Resolution) collimator ($^{123}$I) as described previously (Willhauck *et al.*, 2007). Regions of interest were quantified and expressed as a fraction of the total amount of applied radioiodine per gram tumor tissue. The

retention time within the tumor was determined by serial scanning after radioiodine injection, and dosimetric calculations were performed according to the concept of MIRD, with the dosis factor of RADAR-group (www.doseinfo-radar.com).

*SPECT-CT imaging*

For SPECT-CT imaging the same groups of mice were prepared as outlined above and 24 h after polyplex application. Mice were injected i.p. with 50 MBq (1. 35 mCi) $^{123}$I, followed by monitoring of radioiodine biodistribution by serial imaging (1, 3, 5 h after $^{123}$I application) on a NanoSPECT/CT (Mediso Ltd., Hungary), CT scans were taken covering the same FOV as the SPECT scans. Total scan time was between 30 and 40 minutes, with 48 projections and a scan time of 20 seconds per projection in the case of the SPECT scans.

The SPECT component of the NanoSPECT/CT uses 4 detector heads, each comprising a NaI(TI) crystal with a size of 262 mm x 255 mm x 6.35 mm. It gives an axial field of view of 20 mm and, with the medium-resolution aperture/collimator (9 pinholes per head) that was used in this study, has a spatial resolution of about 1.2 mm. The CT component employs a continuously operating miniature micro focus x-ray tube with a maximum anode current of less than 0.2 mA. The detector has an active area of 98.6 mm x 49.2 mm and consists of 1024 x 2048 pixels. It provides an axial field of view of 45 mm and a maximum spatial resolution of 48 microns.

*Analysis of radioiodine biodistribution ex vivo*

For *ex vivo* biodistribution studies, mice were injected with G2-HD-OEI/NIS (n = 24) or G2-HD-OEI/antisense-NIS (n = 9) as described above followed by i.p. injection of 18.5 MBq $^{123}$I 24 h later. A subgroup of NIS-transduced mice (n = 9) was treated with sodium-perchlorate prior to $^{123}$I administration as an additional control. Two, 6 and 12 h after $^{123}$I injection, mice were sacrificed and tumors as well as organs of interest were dissected, weighed and radioiodine uptake was measured using a gamma counter (5 NIS-transduced animals per time point (G2-HD-OEI/NIS) and 3 mice of each control). Results were reported as percentage of injected dose per organ (% ID/organ).

*Analysis of NIS mRNA expression using quantitative real-time PCR*

Total RNA was isolated from HuH7 tumors or other tissues using the RNAeasy Mini Kit (Qiagen, Hilden, Germany) according to the manufacturer`s recommendations and

quantitative real-time PCR (qPCR) was performed as described previously (Klutz *et al.*, 2009).

### *Immunohistochemical analysis of NIS protein expression*

Immunohistochemical staining of frozen tissue sections derived from HuH7 tumors after systemic NIS gene delivery was performed using a mouse monoclonal antibody directed against amino acid residues 468-643 of human NIS (kindly provided by John C. Morris, Mayo Clinic, Rochester, MN, USA) as described previously (Spitzweg *et al.*, 2007).

### *Radioiodine therapy study in vivo*

Following a 10-day L-T4 pretreatment as described above, two groups of mice were established receiving 55.5 MBq $^{131}$I as a single i.p. injection 24 h after systemic application of G2-HD-OEI/NIS (n = 6) or G2-HD-OEI/antisense-NIS (n = 6), respectively. As control, two further groups of mice were treated with saline instead of $^{131}$I after injection of either G2-HD-OEI/NIS (n = 6) or G2-HD-OEI/antisense-NIS (n = 6). An additional control group was treated with saline only (n = 6). The treatment consisting of systemic polyplex application followed by $^{131}$I or saline application after 24 h was repeated once on days seven and eight. Tumor sizes were measured before treatment and daily thereafter for up to 30 days. Tumor volume was estimated using the equation: tumor volume = length x width x height x 0.52.

### *Indirect immunofluorescence assay*

Indirect immunofluorescence staining was performed on frozen tissues using an antibody against human Ki67 (Abcam, Cambridge, UK) and an antibody against mouse CD31 (BD, Pharmingen, New Jersey, USA) as described previously (Willhauck *et al.*, 2007).

### *Statistical methods*

All *in vitro* experiments were carried out in triplicates. Results are represented as mean +/- SD of triplicates. Statistical significance was tested using Student´s t test.

# Results

## *Iodide uptake studies in vitro*

Transfection conditions using G2-HD-OEI/NIS were optimized in HuH7 cells by measurement of perchlorate-sensitive iodide uptake activity 24 h following polyplex application (data not shown). We found an optimal c/p ratio of 2, which resulted in highest transfection efficiency at low cytotoxicity. This ratio was used in all subsequent experiments. 24 h after transfection with G2-HD-OEI/NIS, HuH7 cells showed a 44-fold increase in ^{125}I accumulation as compared to cells incubated with empty G2-HD-OEI (Fig. 1). Furthermore, no perchlorate-sensitive iodide uptake above background levels was observed in cells transfected with the control vector G2-HD-OEI/antisense-NIS. Polyplex-mediated NIS gene transfer did not alter cell viability as measured by MTS-assay (Fig. 1).
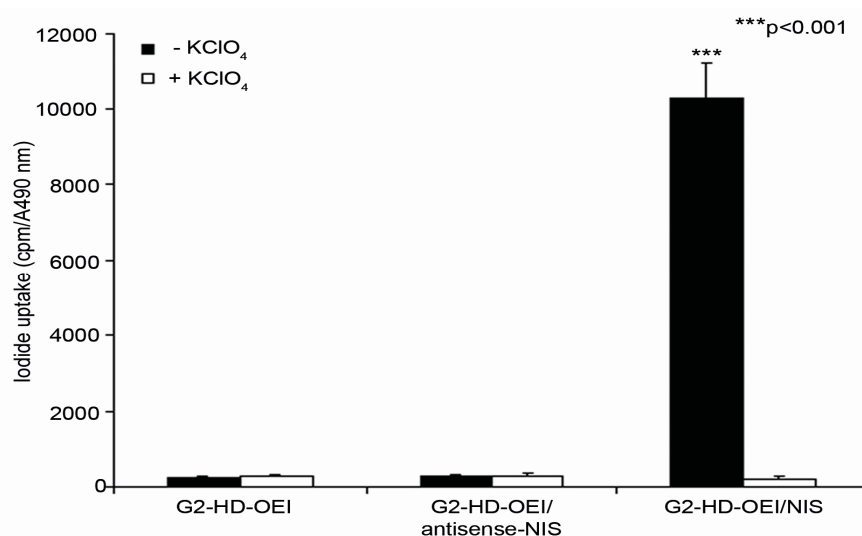


**Fig. 1:** Iodide uptake was measured in HuH7 cells following *in vitro* transfection with G2-HD-OEI/NIS, control vector G2-HD-OEI/antisense-NIS, or with G2-HD-OEI alone. HuH7 cells transfected with G2-HD-OEI/NIS showed a 44-fold increase in perchlorate-sensitive ^{125}I accumulation. In contrast, no perchlorate-sensitive iodide uptake above background level was observed in cells transfected with control vector or without DNA (***p <0.001).

## *In vivo radioiodine biodistribution studies*

To investigate the iodide uptake activity in HuH7 xenografts after systemic *in vivo* NIS gene transfer, ^{123}I distribution was monitored in tumor bearing mice 24 h after G2-HD-OEI/DNA administration by gamma camera imaging. While no radioiodine accumulation was detected in tumors after application of G2-HD-OEI/antisense-NIS (Fig. 2C), significant radioiodine uptake was observed in 80% (12 out of 15) of HuH7 tumors following systemic injection of G2-HD-OEI/NIS (Fig. 2A), in addition to physiological radioiodine

accumulation in thyroid, stomach and bladder (Fig. 2A, C). As determined by serial scanning, 6 - 11% ID/g $^{123}$I (percentage of the injected dose per gram tumor tissue) was accumulated in NIS-transduced xenograft tumors with a biological half-life of 11 h. Considering a tumor mass of 1 g and an effective half-life of 10 h for $^{131}$I, a tumor-absorbed dose of 281 mGy/MBq $^{131}$I was calculated (Fig. 2D). To confirm that tumoral radioiodine uptake was indeed NIS-mediated, a subset of G2-HD-OEI/NIS injected mice (n = 9) received sodium-perchlorate 30 min prior to radioiodine administration. In all experiments a single injection of 2 mg sodium-perchlorate completely blocked tumoral radioiodine accumulation in addition to abolished physiological iodide uptake in stomach and thyroid gland (Fig. 2B). Moreover, no significant radioiodine uptake was observed in non-target organs, including lungs, liver, kidney or spleen, which confirms tumor-specificity of nanoparticle-mediated NIS gene delivery.
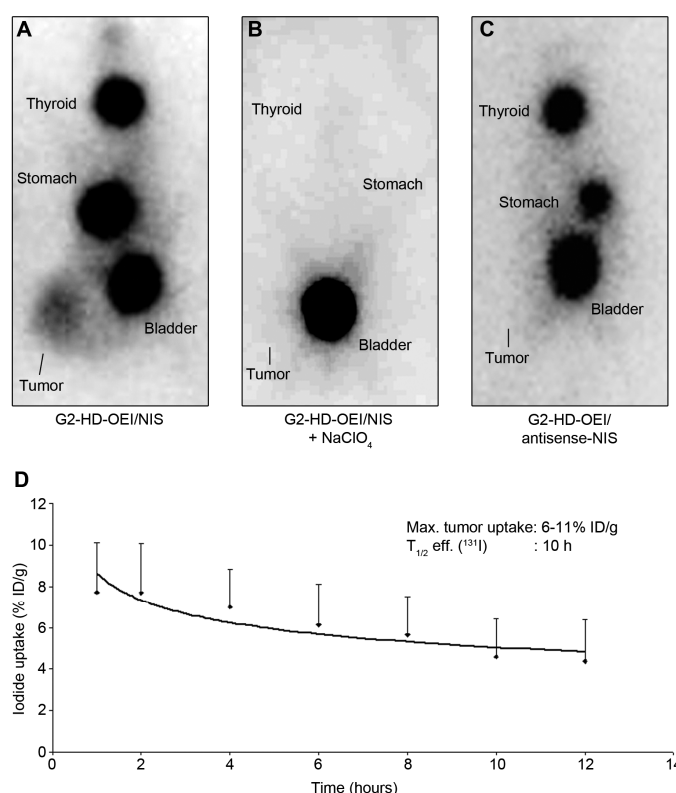


**Fig. 2:** $^{123}$I scans of nude mice harbouring HuH7 tumors 4 h following i.p. injection of 18.5 MBq $^{123}$I after G2-HD-OEI-mediated NIS gene delivery (A). While mice treated with control vectors (G2-HD-OEI/antisense-NIS) showed no tumoral radioiodine uptake (C), treatment with G2-HD-OEI/NIS induced significant tumor-specific iodide accumulation in HuH7 tumors with accumulation of 6 - 11% ID/g $^{123}$I (A), which was completely abolished upon pretreatment with NaClO$_4$ (B). Radioiodine was also accumulated physiologically in thyroid, stomach and bladder (A, C).
Time course of $^{123}$I accumulation in HuH7 tumors after systemic polyplex-mediated NIS gene delivery followed by injection of 18.5 MBq $^{123}$I as determined by serial scanning using $^{123}$I-scintigraphy (D). Maximum tumoral radioiodine uptake was 6 - 11% ID/g for $^{123}$I with an average effective T$_{1/2}$ of 10 h for $^{131}$I.

In a subset of mice, radioiodine biodistribution was also monitored using $^{123}$I SPECT-CT imaging after i.p. injection of 50 MBq $^{123}$I (Fig. 3). Tumor-selective iodide accumulation was confirmed following systemic G2-HD-OEI/NIS application (Fig. 3A, B). SPECT-CT imaging allowed a more detailed three-dimensional analysis of tumoral iodide accumulation revealing inhomogeneous iodide accumulation appearing as clusters of iodide uptake throughout the tumor. A maximum tumoral iodide uptake of approximately 7% ID/g was measured in mice after systemic application of G2-HD-OEI/NIS, as compared to the control groups injected with the control polyplexes G2-HD-OEI/antisense-NIS (2.5% ID/g) or after application of sodium-perchlorate (3.2% ID/g) (Fig. 3C).

In addition to tumoral iodide uptake, significant radioiodine accumulation was observed in tissues physiologically expressing NIS, including stomach and thyroid. In this context it is important to mention that the uptake in the stomach appears to be higher than usually seen in humans, which is most probably due to higher levels of NIS protein expression in murine gastric mucosa and pooling of gastric juices due to the anesthesia for a prolonged period during imaging procedure. In addition, due to exquisite regulation of thyroidal NIS expression by TSH, $^{123}$I accumulation in the thyroid gland can effectively be downregulated in patients by thyroid hormone pretreatment (Wapnir *et al.*, 2004).
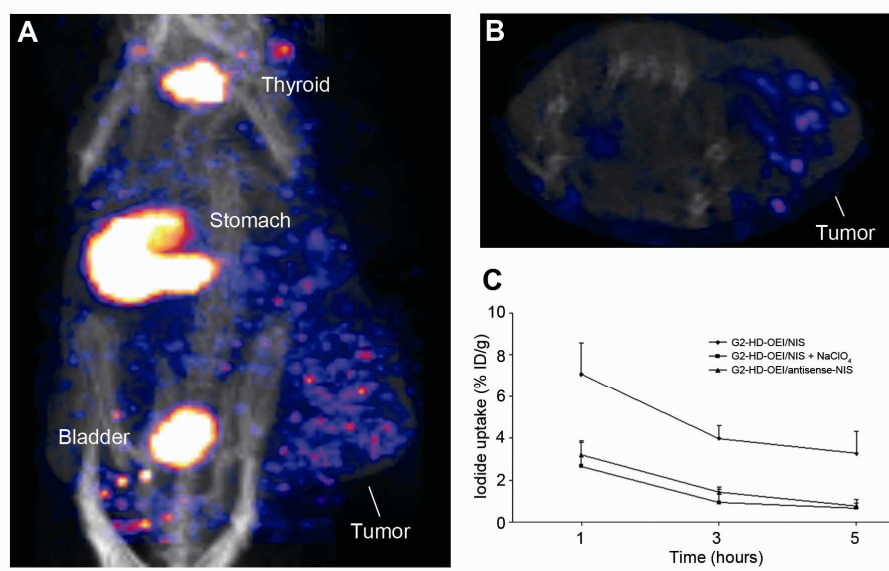


**Fig. 3:** $^{123}$I SPECT/CT scan of tumor bearing nude mice after systemic NIS gene transfer 5 h following i.p. injection of 50 MBq $^{123}$I. Planar (A) and transversal (B) slides indicate tumor specific iodide accumulation. Time course of tumoral iodide accumulation 1, 3 and 5 h p.i. as determined by SPECT-CT scans (C). A maximum radioiodine uptake of 7% ID/g tumor was measured.

***Ex vivo radioiodine biodistribution studies***

*Ex vivo* biodistribution analysis confirmed significant iodide uptake in tumors following systemic NIS gene transfer (Fig. 4A-C). While NIS-transduced HuH7 tumors accumulated 6.6% ID/organ [123]I 2 hours after radioiodine injection, mock-transduced tumors showed no significant radioiodine uptake. In both groups the thyroid gland and the stomach accumulated approx. 41% and 38% ID/organ (data not shown). Noteworthy, the average tumor weight in this experiment was approximately 0.9 g. Further, a single perchlorate injection prior to radioiodine application significantly blocked iodide uptake in NIS-transduced tumors and in physiologically NIS-expressing tissues, including thyroid and stomach, throughout the observation period up to 12 h. In addition, no significant radioiodine uptake above background levels was observed in non-target organs, including lung, liver, kidney or spleen confirming tumor-specificity of G2-HD-OEI (see also Fig. 2A, 3A).
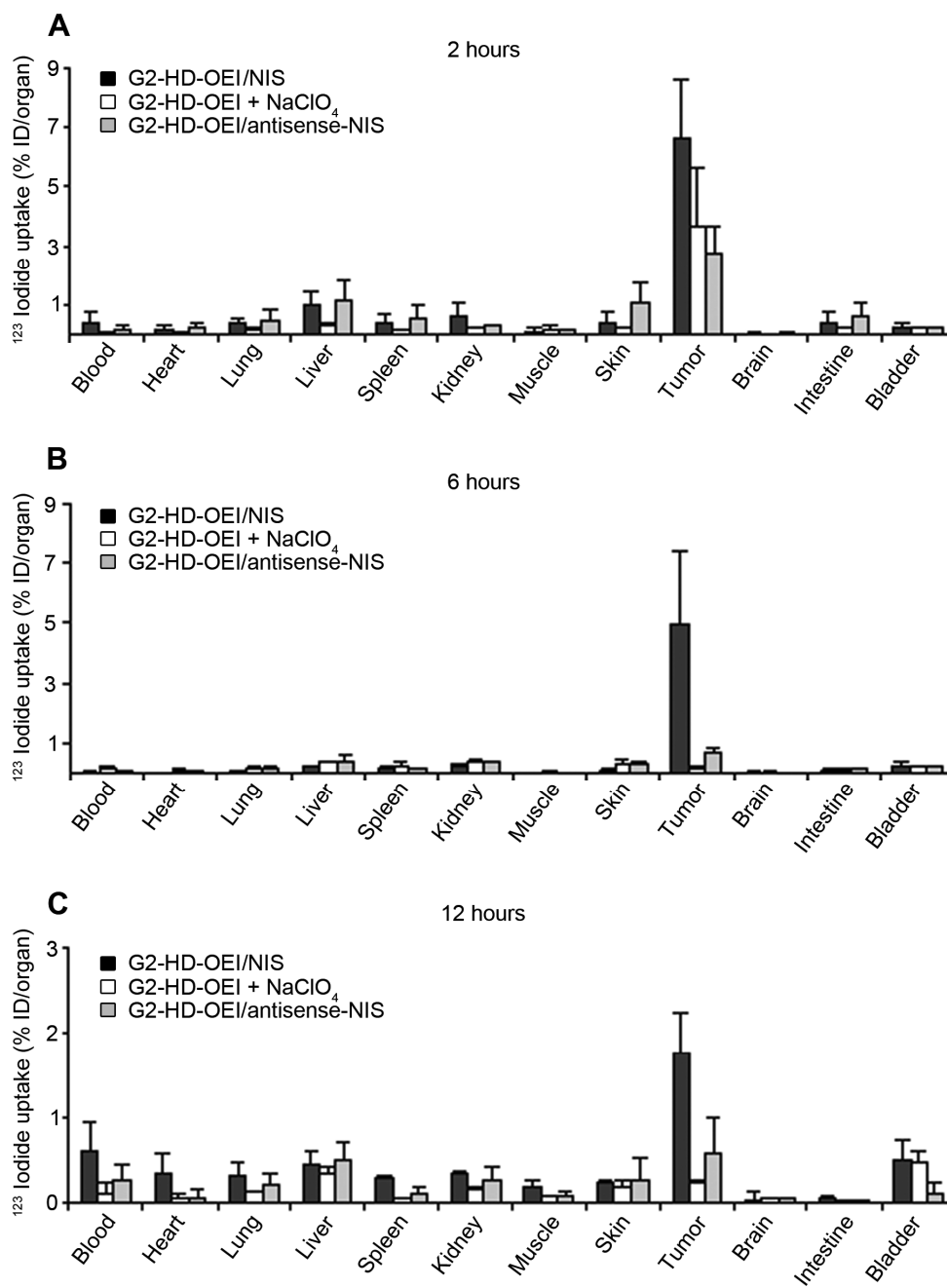
**Fig. 4:** Evaluation of iodide biodistribution *ex vivo* 2, 6 and 12 hours following injection of 18.5 MBq [123]I. While tumors in NIS-transduced mice showed high perchlorate-sensitive iodide uptake activity (up to 4.7–8.5% ID/organ), non-target organs revealed no significant radioiodine accumulation. No radioiodine accumulation was measured after injection of control vectors. Results were reported as percent of injected dose per organ ± SD.

### Analysis of NIS mRNA expression by quantitative real-time PCR analysis

In order to assess NIS mRNA expression after systemic NIS gene transfer, mRNA of various tissues was extracted and analyzed by quantitative real-time PCR (qPCR) with a pair of NIS-specific oligonucleotide primers 24 h after NIS gene transfer (Fig. 5A). Only a low background level of NIS mRNA expression was detected in untreated tumors or tumors after application of G2-HD-OEI/antisense-NIS. In contrast, a significant level of NIS gene expression was induced in HuH7 tumors after systemic injection of G2-HD-OEI/NIS. As expected, administration of the competitive NIS inhibitor sodium-perchlorate had no influence on NIS mRNA expression in NIS-transduced tumors. Furthermore, no significant NIS mRNA expression above background levels was detected in non-target organs, like liver and lung after systemic application of G2-HD-OEI/NIS or G2-HD-OEI/antisense-NIS.
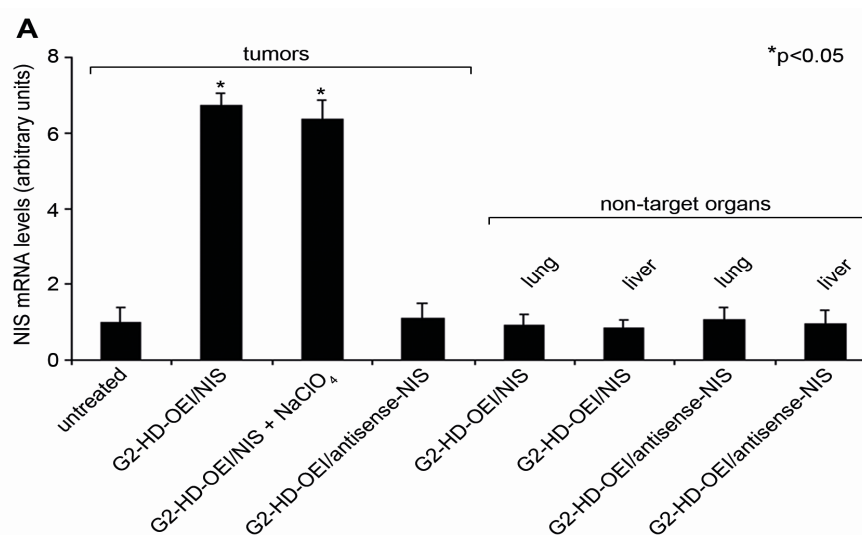


**Fig. 5:** Analysis of human NIS mRNA expression in HuH7 tumors and non-target organs by qPCR. A significant level of NIS mRNA expression was induced in HuH7 tumors after systemic NIS gene transfer with or without sodium-perchlorate pretreatment. Only a low background level of NIS mRNA expression was detected in untreated tumors, which was set as 1 arbitrary unit. Moreover, no significant NIS expression above background level was found in tumors after application of G2-HD-OEI/antisense-NIS, or in non-target organs, like liver and lung. Results were reported as NIS/GAPDH ratios.

### Analysis of NIS protein expression in HuH7 xenografts

Immunohistochemical analysis of HuH7 tumors using a mouse monoclonal NIS-specific antibody revealed a heterogeneous staining pattern with clusters of primarily membrane-associated NIS-specific immunoreactivity in tumors after systemic application of G2-HD-OEI/NIS (Fig. 5B, arrows). In contrast, tumors treated with G2-HD-OEI/antisense-NIS (Fig. 5C) or untreated tumors (not shown) showed no NIS-specific immunoreactivity. Parallel control slides with the primary and secondary antibodies replaced in turn by PBS and isotype-matched non immune immunoglobulin were negative (data not shown).
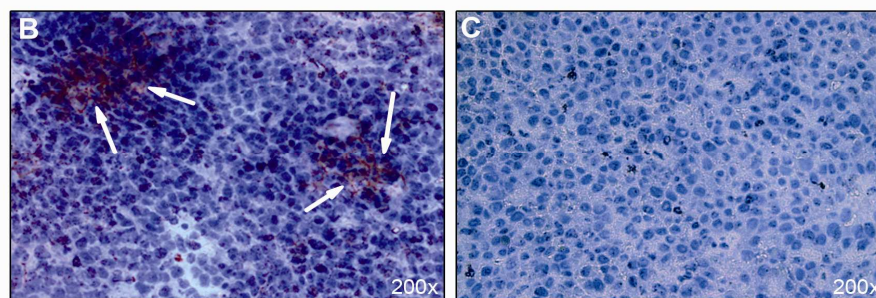
**Fig. 5:** Immunohistochemical staining of HuH7 tumors 24 h after G2-HD-OEI/NIS application showed clusters of primarily membrane-associated NIS-specific immunoreactivity (B, arrows). In contrast, HuH7 tumors treated with the control plasmid (G2-HD-OEI/antisense-arrows) did not reveal NIS-specific immunoreactivity (C). Magnification: 200x .

### *Radioiodine therapy studies after in vivo NIS gene transfer*

24 h after systemic administration of G2-HD-OEI/NIS or G2-HD-OEI/antisense-NIS polyplexes, a therapeutic dose of 55.5 MBq (1.5 mCi) $^{131}$I was injected i.p. As control saline was injected instead of radioiodine. This cycle consisting of systemic NIS gene transfer followed by radioiodine or saline administration was repeated once on days 7/8 (Fig. 6A). As an additional control, tumor growth of mice injected with saline only was assessed.

Mice treated with G2-HD-OEI/NIS or G2-HD-OEI/antisense-NIS followed by application of saline and mice treated with G2-HD-OEI/antisense-NIS followed by application of $^{131}$I as well as saline treated mice showed an exponential tumor growth. In contrast, NIS-transduced (G2-HD-OEI/NIS) and $^{131}$I-treated tumors showed a significant delay in tumor growth (Fig. 6A). While all mice in the control groups had to be killed within two weeks after the onset of the experiments due to excessive tumor growth, 100% of the mice treated with $^{131}$I after injection of G2-HD-OEI/NIS survived approx. three weeks and 50% survived up to four weeks (Fig. 6B). Importantly, none of these mice showed major adverse effects of radionuclide or polyplex treatment in terms of lethargy or respiratory failure. However, a minor body weight loss of 3 - 5 % was observed in mice after systemic administration of polyplexes.
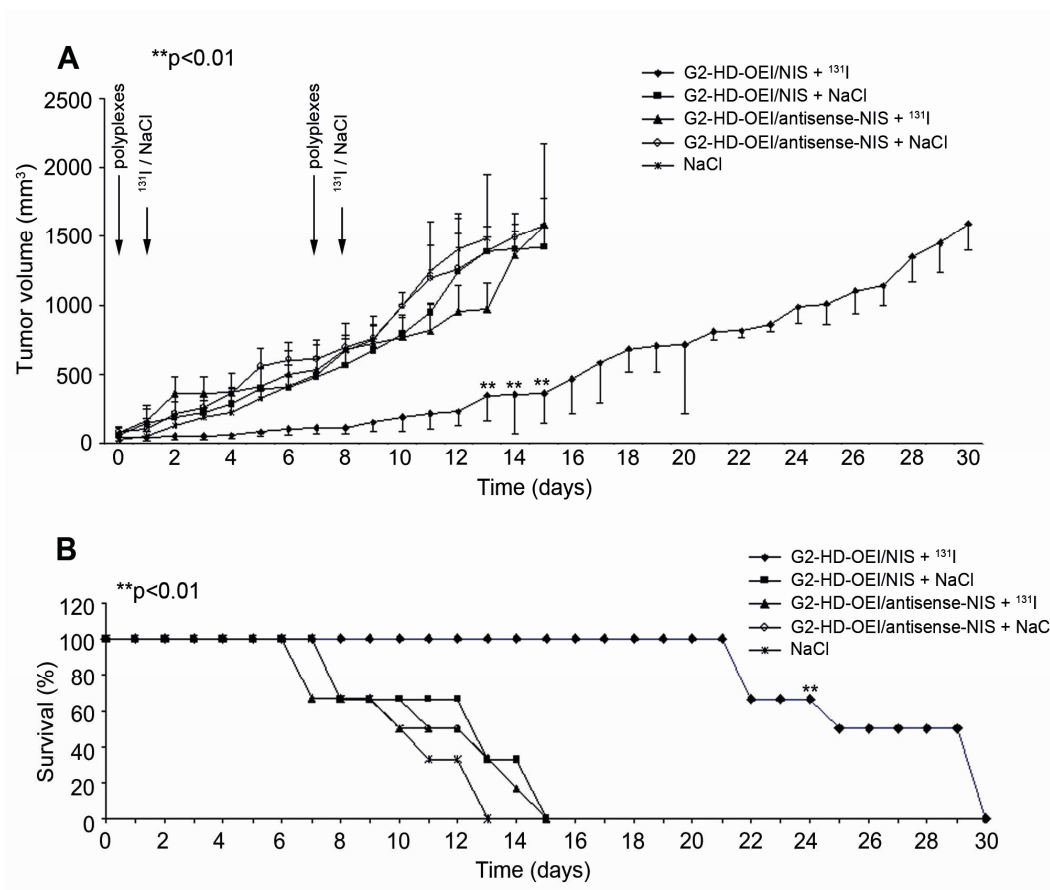
**Fig. 6:** Radioiodine treatment of HuH7 tumors after systemic polyplex-mediated NIS gene transfer *in vivo*. 24 h after i. v. polyplex injection (big arrow), 55.5 MBq $^{131}$I, or saline was injected i.p. (small arrow). This treatment cycle was repeated once on days 7 and 8. $^{131}$I therapy after systemic G2-HD-OEI/NIS application resulted in a significant delay in tumor growth (A, **p<0.01) which was associated with markedly improved survival (B, Kaplan-Meier-plot (**p<0.01)) as compared to the control groups that were injected with saline only, with G2-HD-OEI/NIS followed by saline application, or with G2-HD-OEI/antisense-NIS followed by saline or $^{131}$I.

### *Immunofluorescence analysis*

Three to four weeks after treatment, mice were sacrificed, tumors were dissected and processed for immunofluorescence analysis. Immunofluorescence analysis using a Ki67-specific antibody (green) and an antibody against CD31 (red, labeling blood vessels) showed striking differences between NIS-transduced (Fig. 7A) and mock-transduced $^{131}$I-treated tumors (Fig. 7B). As compared to mock-transduced tumors (G2-HD-OEI/antisense-NIS), NIS-transduced tumors (G2-HD-OEI/NIS) exhibited a significantly lower intratumoral blood vessel density and proliferation index after $^{131}$I therapy.
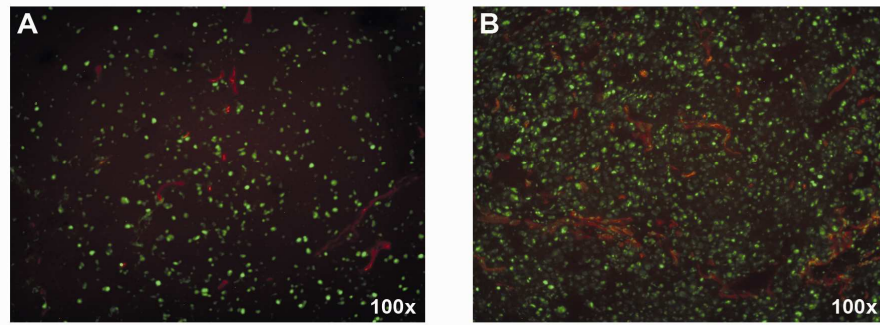
**Fig. 7:** Immunofluorescence analysis using a Ki67-specific antibody (green) and an antibody against CD31 (red, labelling blood vessels) showed significantly decreased proliferation and blood vessel density in NIS-transduced tumors (A) following ^{131}I treatment as compared to mock-transduced tumors (B). Slides were counterstained with DAPI nuclear stain. Magnification 100x

# Discussion

In the present study we investigated the efficacy of synthetic nanoparticle vectors (G2-HD-OEI) to achieve tumor-selective NIS-mediated radioiodine accumulation in a HCC mouse model. After confirmation of high transduction efficiency *in vitro*, i.v. application of NIS-conjugated G2-HD-OEI in nude mice carrying HCC xenografts was demonstrated to result in tumor-selective radioiodine accumulation, which was high enough for a significant therapeutic effect after application of [131]I.

Thyroid cancer, even in advanced metastatic disease, can be effectively treated by radioiodine therapy, due to thyroidal expression of NIS (Dai *et al.*, 1996; Smanik *et al.*, 1996; Spitzweg and Morris, 2002a). NIS expressing thyroid cancer metastases can be detected and treated by administration of radioiodine, while avoiding adverse effects of ionising radiation to other organs, which do not express NIS and thus do not concentrate radioiodine. NIS therefore represents one of the oldest and most successful targets for molecular imaging and targeted radionuclide therapy. Cloning and characterization of the NIS gene has therefore allowed the development of the NIS gene therapy concept based on NIS gene transfer into nonthyroidal tumor cells, followed by diagnostic and therapeutic application of radioiodine (Dai *et al.*, 1996; Smanik *et al.*, 1996; Hingorani *et al.*, 2010a).

One of the major challenges on the way to efficient application of the NIS gene therapy concept in the clinical setting of metastatic cancer is optimal tumor targeting in the presence of low toxicity and sufficiently high transduction efficiency after systemic administration of gene delivery vectors. Only a limited number of studies have investigated systemic NIS gene delivery approaches with the aim of NIS-targeted radionuclide therapy of metastatic disease using an oncolytic measles virus or vesicular stomatitis virus encoding human NIS in multiple myeloma mouse models (Dingli *et al.*, 2004; Goel *et al.*, 2007; Liu *et al.*, 2010). In a recent study we have utilized a promising non-viral gene delivery system for tumor-targeted NIS gene transfer in the syngeneic Neuro2A neuroblastoma mouse model. Branched polycations based on OEI-grafted polypropylenimine dendrimers (G2-HD-OEI) have recently been characterized as biodegradable synthetic gene delivery vectors with high *in vivo* transduction efficiency and remarkable intrinsic tumor affinity in the presence of low toxicity (Russ *et al.*, 2008a). Following systemic application of NIS-conjugated G2-HD-OEI via the tail vein, 85% of Neuro2A tumors showed tumor-specific ^{123}I accumulation which resulted in a significant delay of tumor growth after two cycles of systemic polyplex application followed by ^{131}I injection (Klutz *et al.*, 2009).

In the present study we applied this therapeutic concept in another distinct tumor model, and used G2-HD-OEI for systemic NIS gene delivery in a human HCC xenograft model. G2-HD-OEI complexed with the human NIS cDNA under the control of the unspecific CMV promoter revealed high transfection efficiency *in vitro* resulting in a 44-fold increase in iodide uptake activity in HuH7 cells at an optimal polymer to plasmid w/w ratio of 2 that provided highest transfection efficiency at low cytotoxicity. Following systemic application of NIS-conjugated G2-HD-OEI via the tail vein *in vivo*, 80% of HuH7 tumors showed tumor-specific iodide accumulation as determined by ^{123}I-scintigraphic gamma camera imaging with accumulation of approximately 6 - 11% ID/g and an effective half-life of 10 h for [131]I. In contrast, mice pretreated with the competitive NIS-inhibitor sodium-perchlorate or mice injected with control vectors showed no tumoral iodide uptake, confirming that the observed radioiodine accumulation in the tumors was mediated by functional NIS expression. In addition to ^{123}I-gamma camera imaging we have used small animal whole body SPECT-CT imaging in a subset of animals using ^{123}I as a radiotracer. Despite the widespread availability of ^{123}I-scintigraphy, SPECT imaging is attractive for tracking the delivery of the NIS gene due to its higher sensitivity and enhanced resolution. The cross-sectional fusion imaging techniques such as SPECT-CT provide a useful means to improve three-dimensional spatial resolution and separate the overlapping regions of radioiodine uptake *in vivo*, thereby allowing a more robust biodistribution analysis. In our study ^{123}I SPECT-CT imaging allowed a more detailed 3D analysis of NIS-mediated radioiodine accumulation, which appeared inhomogenous in clusters of iodide uptake throughout the tumor. The examination of all projections of the SPECT-CT images failed to detect any other NIS gene transfer-related signals, suggesting that systemic NIS gene transfer using G2-HD-OEI is highly tumor-specific. In addition, our data are consistent with several studies demonstrating the sensitivity of micro-SPECT-CT for imaging and quantitation of NIS-mediated radionuclide uptake (Marsee *et al.*, 2004; Carlson *et al.*, 2006; Merron *et al.*, 2007; Carlson *et al.*, 2009; Chisholm *et al.*, 2009; Peerlinck *et al.*, 2009; Penheiter *et al.*, 2010).

Moreover, ^{123}I-scintigraphic and SPECT-CT imaging studies were confirmed by *ex vivo* biodistribution experiments revealing significant tumoral radioiodine accumulation, while no iodide uptake was measured in non-target organs, like lung, liver, spleen or kidneys. Tumor-specific NIS expression was further confirmed by real time q-PCR as well as NIS-specific immunoreactivity, which was primarily membrane-associated with an inhomogenous, patchy staining pattern, and therefore nicely correlates with the clusters of

iodide accumulation detected with the ^{123}I-SPECT-CT imaging. Due to the limited polyplex spread in the tumor resulting in the inhomogenous transgene expression, non-viral gene delivery is ideally combined with therapy genes that are able to provide a bystander effect. The path-length of up to 2.4 mm of the beta-particles emitted by ^{131}I causes a significant crossfire effect after NIS gene transfer resulting in a bystander effect, which makes NIS an ideal candidate gene for synthetic vector-based systemic cancer gene therapy (Dingli *et al.*, 2003b).

One explanation for the remarkable tumor-selectivity of these synthetic vectors based on pseudodendritic oligoamines used in this study is the so-called "enhanced permeability and retention" (EPR)-effect: due to large endothelial fenestrations in tumor vasculature combined with poor lymphatic drainage circulating macromolecules can preferentially accumulate in solid tumors (Matsumura and Maeda, 1986; Iyer *et al.*, 2006). We (Smrekar *et al.*, 2003; Schwerdt *et al.*, 2008) and others (Dufes *et al.*, 2005) also observed an intrinsic affinity of well-vascularized tumors for polycations, as their removal from tumor tissue is prevented due to their affinity to tumor cells and tumor matrix. Very recently, we demonstrated that polyplex organ distribution and transgene expression does not necessarily correlate (Navarro *et al.*, 2010). Although considerable amounts of polyplexes can be entrapped in non-target organs like lung and liver, expression is limited to tumor tissue. This can be explained by additional selectivity being achieved by the mitotic activity of tumor cells that is advantageous for polyplex-mediated transgene expression (Brunner *et al.*, 2000).

Most importantly, systemic polyplex-mediated NIS gene transfer resulted in tumor-specific radioiodine uptake activity in HuH7 tumor-bearing mice which was sufficiently high for a significant therapeutic effect of [131]I. After two cycles of systemic polyplex application followed by ^{131}I injection tumor-bearing mice showed a significant delay of tumor growth associated with a markedly prolonged survival. In addition, immunofluorescence analysis showed a significantly reduced proliferation and blood vessel density after systemic polyplex-mediated NIS gene transfer followed by ^{131}I application, suggesting radiation-induced tumor stroma cell damage in addition to tumor cell death.

These data correlate well with the data aquired in the syngeneic neuroblastoma mouse model (Klutz *et al.*, 2009), demonstrating that the application of these synthetic nanoparticles based on OEI-grafted pseudodendritic oligoamines for systemic NIS gene delivery is not restricted to a specific tumor model, but is suitable for all cancers with well-vascularized tumors.

In conclusion, our data clearly demonstrate the high potential of branched polycations based on oligoethylenimine (OEI)-grafted polypropylenimine dendrimers for tumor-specific delivery of the NIS gene after systemic application in well-vascularized tumors, such as liver cancer. Using NIS as reporter gene, this study allowed detailed characterization of *in vivo* biodistribution of polyplex-mediated functional NIS expression by $^{123}$I-scintigraphic gamma camera and $^{123}$I-SPECT-CT imaging, which is an essential prerequisite for exact and safe planning and monitoring of clinical gene therapy trials with the aim of individualization of the NIS gene therapy concept in the clinical setting. Tumor-specific radioiodine accumulation was further demonstrated to be sufficiently high for a significant therapeutic effect in a HCC xenograft mouse model after two cycles of NIS-polyplex application followed by $^{131}$I therapy. This study therefore opens the exciting prospect of NIS-targeted radioiodine therapy of disseminated HCC using polyplexes based on biodegradable polymers for systemic NIS gene delivery.

## Acknowledgments

# 5. Chapter 4

**Epidermal growth factor receptor-targeted radioiodine therapy of hepatocellular cancer following systemic non-viral delivery of the sodium iodide symporter gene**

## Statement of Translational Relevance

Cloning of the sodium iodide symporter (NIS) – the molecular basis of radioiodine therapy in thyroid cancer - has paved the way for the development of a novel gene therapy strategy based on targeted NIS expression in cancer cells followed by application of $^{131}$I. Our pioneer studies have convincingly shown the enormous potential of NIS as a novel reporter and therapy gene, and allowed the approval of a first phase I clinical trial for radioiodine therapy of prostate cancer after local adenoviral NIS gene transfer. The next crucial step towards clinical application in metastatic cancer has to be the evaluation of gene transfer methods that have the potential to achieve sufficient tumor-selective transgene expression levels after systemic application.

The present report convincingly demonstrates the high potential of novel nanoparticle vectors based on linear polyethylenimine (LPEI), shielded by attachment of polyethylene glycol (PEG), and coupled with the synthetic peptide GE11 as an epidermal growth factor receptor (EGFR)-specific ligand for tumor-specific delivery of the NIS gene. Systemic application of NIS polyplexes resulted in a significant therapeutic effect of $^{131}$I in a human hepatocellular carcinoma mouse model. This translational study therefore opens the exciting perspective of NIS-targeted radionuclide therapy of metastatic cancer using EGFR-targeted polyplexes for systemic NIS gene delivery

# Abstract

Purpose: We recently demonstrated significant tumor-selective iodide uptake and therapeutic efficacy of radioiodine in neuroblastoma tumors after systemic non-viral polyplex-mediated NIS gene delivery.

Experimental Design: In the current study, we used novel nanoparticle vectors (polyplexes) based on linear polyethylenimine (LPEI), polyethylene glycol (PEG), and the synthetic peptide GE11 as an epidermal growth factor receptor (EGFR)-specific ligand to target a NIS-expressing plasmid to EGFR overexpressing human hepatocellular carcinoma (HuH7).

Results: Incubation of HuH7 cells with EGFR-targeted LPEI-PEG-GE11/NIS polyplexes resulted in a 22-fold increase in iodide uptake activity *in vitro*. Using $^{123}$I-scintigraphy and *ex vivo* γ-counting, HuH7 tumors in nude mice accumulated 6.5 - 9% ID/g $^{123}$I with an effective half-life of approx. 6 h, resulting in a tumor absorbed dose of 47 mGy/MBq $^{131}$I after i.v. application of LPEI-PEG-GE11/NIS, while injection of control vectors did not result in tumoral iodide accumulation. No significant iodide uptake was observed in organs like liver, lungs and kidneys. After application of the EGFR-specific antibody cetuximab 24 h prior to administration of LPEI-PEG-GE11/NIS, tumoral iodide uptake and NIS mRNA expression were markedly reduced confirming the specificity of EGFR-targeted polyplexes. After 3 or 4 cycles of polyplex/$^{131}$I application, a significant delay in tumor growth was observed associated with prolonged survival.

Conclusion: These results clearly demonstrate that systemic NIS gene transfer using synthetic nanoparticle vectors coupled with an EGFR-targeting ligand is capable of inducing tumor-specific iodide uptake, which represents a promising innovative strategy for systemic NIS gene therapy in metastatic cancers.

## Introduction

The growing understanding of the biology of the sodium iodide symporter (NIS) since its cloning in 1996 has paved the way for the development of a novel cytoreductive gene therapy strategy using NIS as powerful therapy and reporter gene (Dai *et al.*, 1996; Smanik *et al.*, 1996; Hingorani *et al.*, 2010a). NIS, an intrinsic transmembrane glycoprotein with 13 putative transmembrane domains, is responsible for the ability of the thyroid gland to concentrate iodide, the first and rate-limiting step in the process of thyroid hormonogenesis (Spitzweg and Morris, 2002b). Moreover, due to its expression in follicular cell-derived thyroid cancer cells, NIS provides the molecular basis for the diagnostic and therapeutic application of radioiodine, which has been successfully used for more than 70 years in the treatment of thyroid cancer patients representing the most effective form of systemic anticancer radiotherapy available to the clinician today (Spitzweg *et al.*, 2001c).

After extensive preclinical evaluation in several tumor models by various groups including our own, NIS has been characterized as a promising target gene for the treatment of non-thyroid cancers following selective NIS gene transfer into tumor cells which allows therapeutic application of radioiodine and alternative radionuclides, such as $^{188}$Re and $^{211}$At (Spitzweg and Morris, 2002b; Willhauck *et al.*, 2007; Willhauck *et al.*, 2008a; Hingorani *et al.*, 2010a). In our initial studies in the prostate cancer model we used the prostate-specific antigen (PSA) promoter to achieve prostate-specific iodide accumulation, which resulted in a significant therapeutic effect after application of $^{131}$I and alternative radionuclides such as $^{188}$Re and $^{211}$At even in the absence of iodide organification (Spitzweg *et al.*, 2000b; Spitzweg *et al.*, 2001a; Willhauck *et al.*, 2007; Willhauck *et al.*, 2008a). Further, cloning of NIS has also provided us with one of the most promising reporter genes available today, that allows direct, non-invasive imaging of functional NIS expression by $^{123}$I-scintigraphy and $^{124}$I-PET-imaging, as well as exact dosimetric calculations before proceeding to therapeutic application of $^{131}$I. Therefore, in its role as reporter gene NIS provides a direct way to monitor the *in vivo* distribution of viral and non-viral vectors, as well as biodistribution, level and duration of transgene expression – all critical elements in the design of clinical gene therapy trials (Spitzweg *et al.*, 1999c; Spitzweg *et al.*, 2001a; Spitzweg and Morris, 2002b; Dingli *et al.*, 2003b; Groot-Wassink *et al.*, 2004; Goel *et al.*, 2007; Merron *et al.*, 2007; Spitzweg *et al.*, 2007; Willhauck *et al.*, 2007; Willhauck *et al.*, 2008b; Willhauck *et al.*, 2008c; Carlson *et al.*, 2009; Klutz *et al.*, 2009; Peerlinck *et al.*, 2009; Baril *et al.*, 2010; Li *et al.*, 2010; Trujillo *et al.*, 2010; Watanabe *et al.*, 2010).

As logical consequence of our pioneer studies in the NIS gene therapy field, the next crucial step towards clinical application of the promising NIS gene therapy concept, has to be the evaluation of gene transfer methods that own the potential to achieve sufficient tumor-selective transgene expression levels not only after local or regional but also after systemic application to be able to reach tumor metastases.

Delivering genes to target organs with synthetic vectors is a vital alternative to virus-based methods. For systemic delivery polycationic molecules are used to condense DNA into sub-micrometer particles termed polyplexes, which are efficiently internalized into cells, while DNA is protected from nucleases. Several polycations, like polyethylenimine (PEI), bear an intrinsic endosomolytic mechanism, which allows the transition of the polyplex from the endosome to the cytoplasm (Meyer and Wagner, 2006). Non-viral vectors can be easily synthesized and convince especially by their absent immunogenicity and enhanced biocompatibility.

We have recently developed a novel class of branched polycations based on oligoethylenimine (OEI)-grafted polypropylenimine dendrimers (G2-HD-OEI) (Russ *et al.*, 2008a), which showed high intrinsic tumor affinity in the presence of low toxicity and high transfection efficiency (Russ *et al.*, 2008a; Russ *et al.*, 2008). In a syngeneic neuroblastoma (Neuro2A) mouse model we have used these synthetic polymeric vectors to target NIS expression to neuroblastoma tumors. After i.v. application of NIS containing polyplexes (G2-HD-OEI/NIS) Neuro2A tumors were shown to accumulate 8 - 13% ID/g ^{123}I by scintigraphy and *ex vivo* gamma counting, resulting in a tumor absorbed dose of 247 mGy/MBq [131]I. No iodide uptake was observed in non-target organs and two cycles of polyplex application followed by [131]I (55.5 MBq) administration resulted in a significant delay in tumor growth associated with markedly improved survival (Klutz *et al.*, 2009). Polyplexes formed with branched structures like G2-HD-OEI are able to deliver the nucleic acid payload primarily toward the tumor site due to passive tumor targeting based on the imperfect and leaky tumor vasculature combined with inadequate lymphatic drainage (Maeda, 2001).

With the aim of optimizing tumor selectivity active ligand-mediated tumor targeting by the application of receptor-specific ligands can be used. The epidermal growth factor receptor (EGFR) is upregulated in a broad range of epithelial tumors, such as liver cancer, and has therefore been evaluated as a target structure for gene delivery vectors (De Bruin *et al.*, 2007). Epidermal growth factor (EGF), the natural ligand of the EGFR, has strong growth promoting properties by activation of the receptor tyrosine kinase via

phosphorylation and thereby represents a strong tumor promoting agent. Therefore, a synthetic ligand with high receptor affinity which does not activate the receptor tyrosine kinase is required to function as a plausible ligand to target gene delivery vectors to EGFR-expressing tumor cells. In this context, Li *et al*. discovered a new EGFR ligand by phage display library analysis called GE11 (Sequence: CYHWYGYFPQNVI) which showed high affinity towards EGFR with no significant activation potential at the receptor tyrosine kinase (Li *et al.*, 2005).

In the current study, we therefore used novel synthetic nanoparticle vectors based on linear polyethylenimine (LPEI), shielded by attachment of polyethylene glycol (PEG) and coupled with the synthetic EGFR-specific peptide GE11 for targeting the NIS gene to human hepatocellular carcinoma (HCC) cells. Based on its dual function as reporter and therapy gene, NIS was used for non-invasive imaging of vector biodistribution by $^{123}$I-scintigraphy followed by assessment of the therapy response after application of $^{131}$I.

# Materials and Methods

## *Cell culture*

The human hepatoma cell line (HuH7, JCRB 0403) was cultured in DMEM/F12 medium (Invitrogen Life Technologies Inc., Karlsruhe, Germany) supplemented with 10% fetal bovine serum (v/v) (PAA, Colbe, Germany), 5% L-glutamine (Invitrogen Life Technologies Inc.) and 1% penicillin/streptomycin. Cells were maintained at 37°C and 5% $CO_2$ in an incubator with 95% humidity. Cell culture medium was replaced every second day and cells were passaged at 85% confluency.

## *Plasmid and polymer synthesis*

The NIS cDNA has been synthesized by GENEART (Regensburg, Germany) codon-optimized for gene expression in human tissue and cloned into the plasmid pCpG-hCMV-Luc with a backbone completely devoid of potentially immune stimulatory CpG dinucleotides (Navarro *et al.*, 2010). NIS transcription is driven by the human elongation factor-1 alpha promoter in combination with the human cytomegalovirus enhancer element. The LucSh transgene was replaced by NIS cDNA using restriction enzymes NheI and BglII (NIS plasmid). NIS cDNA, digested with NheI and BglII, was cloned into the NheI and BglII restriction sites of pMOD-ZGFP (InvivoGen, San Diego, CA, USA). The resulting pMOD-NIS was digested with AvrII and BamHI and re-ligated into the NheI and BglII restriction sites of pCpG-hCMV-Luc generating a control vector featuring NIS in antisense direction (antisense-NIS plasmid).

LPEI and LPEI-based conjugates were synthesized in analogous fashion as recently described (Schaffert *et al.*, 2010) and will be described in detail elsewhere (Schaefer *et al*, manuscript in preparation). In brief, LPEI-PEG-GE11 and LPEI-PEG-Cys were synthesized by coupling heterobifunctional (poly)ethylene glycol (NHS-PEG-OPSS, 2 kDa, Rapp Polymere GmbH, Tübingen, Germany) via N-hydroxy succiniminyl ester onto amine groups in LPEI and were subsequently purified by cation exchange chromatography. GE11 peptide (CYHWYGYFPQNVI, >95 % purity, synthesized by solid phase peptide (Biosynthan GmbH, Berlin, Germany) was coupled to the terminal OPSS group (orthopyridyl disulfide) and purified again by size exclusion chromatography (Superdex 75, GE Healthcare Europe GmbH, Freiburg, Germany). LPEI-PEG-Cys was similarly synthesized only using cysteine instead of GE11 peptide. The resulting conjugates were dialyzed against HBS (20 mM

HEPES pH 7.4, 150 mM NaCl) and stored frozen at -80°C as 1 - 5 mg/ml stock solutions until further use.

### *Polyplex formation*

Plasmid DNA was condensed with polymers at indicated conjugate/plasmid (c/p) - ratios (w/w) in HEPES buffered glucose (HBG: 20 mM HEPES, 5% glucose (w/v), pH 7.4) as described previously (Russ *et al.*, 2008a) and incubated at room temperature for 20 min. prior to use. Final DNA concentration of polyplexes for *in vitro* studies was 2 µg/ml, for *in vivo* studies 200 µg/ml.

### *Transient transfection*

For *in vitro* transfection experiments, HuH7 cells were grown to 60 - 80% confluency. Cells were incubated for 4 h with polyplexes in the absence of serum and antibiotics followed by incubation with growth medium for 24 h. Transfection efficiency was evaluated by measurement of iodide uptake activity as described below.

### $^{125}$*Iodide uptake assay*

Following transfections, iodide uptake of HuH7 cells was determined at steady-state conditions as described previously (Spitzweg *et al.*, 1999c). Results were normalized to cell survival measured by cell viability assay (see below) and expressed as cpm/A490 nm.

### *Cell viability assay*

Cell viability was measured using the commercially available MTS-assay (Promega Corp., Mannheim, Germany) according to the manufacturer´s recommendations as described previously (Willhauck *et al.*, 2007).

### *Establishment of HuH7 xenografts*

HuH7 xenografts were established in female CD-1 nu/nu mice (Charles River, Sulzfeld, Germany) by subcutaneous injection of 5 x $10^6$ HuH7 cells suspended in 100 µl PBS into the flank region. Animals were maintained under specific pathogen-free conditions

with access to mouse chow and water *ad libitum*. The experimental protocol was approved by the regional governmental commission for animals (Regierung von Oberbayern).

*NIS gene transfer and radioiodine studies in vivo*

Experiments started when tumors had reached a tumor size of 8 - 10 mm after a 10-day pretreatment with L-T4 (intraperitoneal (i.p.) injection of 2 µg L-T4/day (Henning, Sanofi-Aventis, Germany) diluted in 100 µl PBS) to suppress thyroidal iodine uptake. For systemic *in vivo* NIS gene transfer polyplexes (c/p 0.8) were applied intravenously (i.v.) via the tail vein at a DNA dose of 2.5 mg/kg (50 µg DNA in 250 µl HBG); either NIS containing polyplexes (LPEI-PEG-GE11/NIS) or control polyplexes (LPEI-PEG-GE11/antisense-NIS, LPEI-PEG-Cys/NIS and LPEI/NIS). Four groups of mice were established and treated i.v. as follows: (1) LPEI-PEG-GE11/NIS (n=15); (2) LPEI-PEG-GE11/antisense-NIS (n=9), (3) LPEI-PEG-Cys/NIS (n=9), (4) LPEI/NIS (n=9). As an additional control, mice treated with LPEI-PEG-GE11/NIS received (n=9) the competitive NIS-inhibitor sodium-perchlorate (NaClO$_4$ 2 mg/per mouse) 30 min. prior to ^{123}I administration as a single i.p application. For competitive inhibition studies the EGFR-specific monoclonal antibody cetuximab (Erbitux®, Merck, Darmstadt, Germany) was injected i.p. (0.25 mg/per mouse) 24 h prior to the LPEI-PEG-GE11/NIS application (n=4). 24 h after polyplex application, mice were injected i.p. with 18.5 MBq (0.5 mCi) [123]I and iodide biodistribution was assessed using a gamma camera equipped with UXHR collimator (Ecam, Siemens, Germany) as described previously (Willhauck *et al.*, 2007). Regions of interest were quantified and expressed as a fraction of the total amount of applied radioiodine per gram tumor tissue. The retention time within the tumor was determined by serial scanning after radionuclide injection and dosimetric calculations were performed according to the concept of MIRD with the dosis factor of RADAR-group (www.doseinfo-radar.com).

*Analysis of radioiodine biodistribution ex vivo*

For *ex vivo* analysis of ^{123}I biodistribution, mice were injected with LPEI-PEG-GE11/NIS (n=10) or LPEI-PEG-GE11/antisense-NIS (n=6), LPEI-PEG-Cys/NIS (n=6) or LPEI/NIS (n=6) as described above followed by i.p. injection of 18.5 MBq [123]I 24 h later. In addition LPEI-PEG-GE11/NIS-transduced mice (n=6) were treated with sodium-perchlorate prior to ^{123}I administration as an additional control. Four and 12 h after ^{123}I injection, mice

were sacrificed and indicated organs were dissected, weighed and radioiodide uptake was measured in a gamma counter (5 NIS-transduced animals per time point (LPEI-PEG-GE11/NIS) and 3 mice of each control). Results were reported as percentage of injected dose per organ (% ID/organ).

### *Analysis of NIS mRNA expression using quantitative real-time PCR*

Total RNA was isolated from HuH7 tumors or other tissues using the RNeasy Mini Kit (Qiagen, Hilden, Germany) according to the manufacturer's recommendations. Single stranded oligo (dT)-primer cDNA was generated using Superscript III Reverse Transcriptase (Invitrogen). Following primers were used: hNIS: (5`-ACACCTTCTGGACCTTCGTG-3´) and (5`-GTCGCAGTCGGTGTAGAACA-3´), GAPDH: (5`-GAGAAGGCTGGGGCTCATTT-3´) and (5`-CAGTGGGGACACGGAAGG-3´). Quantitative real-time PCR (qPCR) was performed with the cDNA from 1μg RNA using the SYBR green PCR master mix (Quiagen) in a Rotor Gene 6000 (Corbett Research, Morthlake, New South Wales, Australia). Relative expression levels were calculated using the comparative $\Delta\Delta C_t$ method and internal GAPDH for normalization.

### *Immunohistochemical analysis of NIS protein expression*

Immunohistochemical staining of frozen tissue sections derived from HuH7 tumors after systemic gene delivery was performed using a mouse monoclonal antibody directed against amino acid residues 468-643 of human NIS (kindly provided by John C. Morris, Mayo Clinic, Rochester, MN, USA) as described previously (Spitzweg *et al.*, 2007).

### *Radioiodine therapy study in vivo*

Following a 10-day L-T4 pretreatment, mice received 55.5 MBq ^{131}I as a single i.p. injection 24 h after systemic application of LPEI-PEG-GE11/NIS (n=16) or LPEI-PEG-GE11/antisense-NIS (n=6). As a control, mice were treated with saline instead of ^{131}I after injection of LPEI-PEG-GE11/NIS (n=16) or LPEI-PEG-GE11/antisense-NIS (n=6) or saline instead of polyplexes (n=6). Polyplex application was followed after 24 h by ^{131}I or saline application in three cycles (days 0/1, 3/4, 7/8). In additional experiments mice were treated with 4 cycles of LPEI-PEG-GE11 followed by radioiodine (n=8) or saline (n=8) application on days 0/1, 3/4, 7/8 and 14/15. Tumor sizes were measured before treatment and daily

thereafter for up to five weeks and tumor volume estimated using the equation: tumor volume = length x width x height x 0.52.

### *Indirect immunofluorescence assay*

Indirect immunofluorescence staining was performed on frozen tissues using an antibody against human Ki67 (Abcam, Cambridge, UK) and an antibody against mouse CD31 (BD, Pharmingen, New Jersey, USA) as described previously (Willhauck *et al.*, 2007).

### *Statistical methods*

All *in vitro* experiments were carried out in triplicates. Results are represented as mean +/- SD of triplicates. Statistical significance was tested using Student´s t test.

# Results

## *EGFR-targeted NIS gene transfer in vitro*

Transfection conditions using LPEI-PEG-GE11/NIS were optimized in HuH7 cells by measurement of perchlorate-sensitive iodide uptake activity 24 h following application of polyplexes (data not shown). We found an optimal c/p ratio of 0.8 resulting in highest transfection efficiency at lowest cytotoxicity. This ratio was used in all subsequent experiments. 24 h after transfection with LPEI-PEG-GE11/NIS, HuH7 cells showed a 22-fold increase in $^{125}$I accumulation as compared to cells incubated with LPEI-PEG-GE11/antisense-NIS (Fig. 1). Transfection with untargeted LPEI-PEG-Cys/NIS polyplexes led to significantly lower iodide uptake activity in HuH7 cells (Fig.1). Furthermore, no perchlorate-sensitive iodide uptake above background level was observed in cells transfected with the empty vector LPEI-PEG-GE11. Polyplex-mediated NIS gene transfer did not alter cell viability as measured by MTS-assay (Fig. 1).
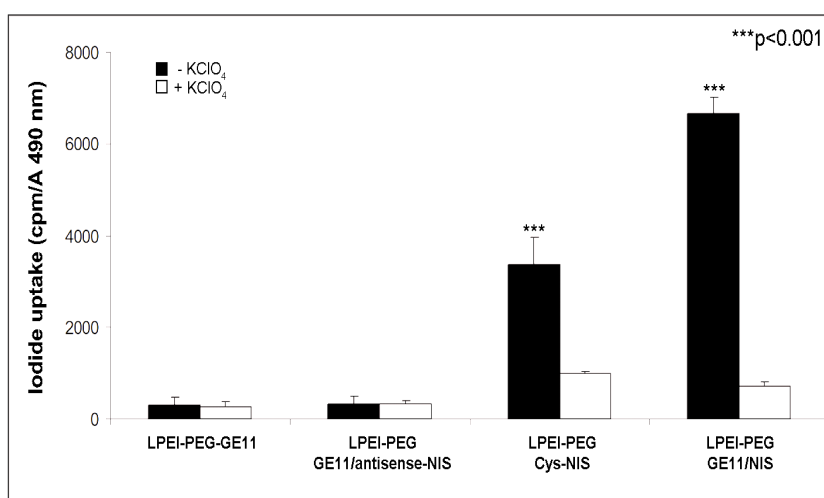


**Fig. 1:** Iodide uptake was measured in HuH7 cells following *in vitro* transfection with LPEI-PEG-GE11/NIS, control polyplexes LPEI-PEG-Cys/NIS, LPEI-PEG-GE11/antisense-NIS, or with LPEI-PEG-GE11 alone. Cells transfected with LPEI-PEG-GE11/NIS showed a 22-fold increase in perchlorate-sensitive $^{125}$I accumulation. After transfection with LPEI-PEG-Cys/NIS the iodide uptake was decreased to approx. 50%. In contrast, no perchlorate-sensitive iodide uptake above background level was observed in cells transfected with LPEI-PEG-GE11/antisense-NIS or without DNA (***p <0.001).

*Induction of iodide accumulation after systemic EGFR-targeted NIS gene transfer in vivo*

To investigate the iodide uptake activity in HuH7 tumors after systemic *in vivo* NIS gene transfer, $^{123}$I distribution was monitored in tumor bearing mice 24 h after administration of polyplexes (Fig. 2). High levels of iodide uptake were observed in 80% (12 out of 15) of HuH7 tumors following systemic injection of LPEI-PEG-GE11/NIS (Fig. 2A), whereas no significant iodide uptake was observed in non-target organs, including lungs and liver confirming tumor-specificity of LPEI-PEG-GE11-mediated NIS gene delivery. No iodide accumulation was detected in tumors after application of LPEI-PEG-GE11/antisense-NIS and LPEI/NIS (Fig. 2C, E), and weak tumoral iodide accumulation was observed after application of LPEI-PEG-Cys/NIS (Fig. 2D). To confirm that tumoral iodide uptake was indeed NIS-mediated, LPEI-PEG-GE11/NIS-injected mice received sodium-perchlorate 30 min prior to $^{123}$I administration (2 mg i.p.), which completely blocked tumoral iodide accumulation in addition to the physiological iodide uptake in stomach and thyroid gland (Fig. 2B). As determined by serial scanning, approximately 6.5 - 9% ID/g $^{123}$I were accumulated in NIS-transduced tumors with a biological half-life of 5 h after application of LPEI-PEG-GE11/NIS (Fig. 2G). Considering a tumor mass of 1 g and an effective half-life of 6 h for $^{131}$I, a tumor absorbed dose of 47 mGy/MBq $^{131}$I was calculated. After application of the EGFR-specific antibody cetuximab 24 h prior to administration of NIS-conjugated LPEI-PEG-GE11 tumoral iodide uptake was significantly reduced to 4% ID/g $^{123}$I (Fig. 2F).

Besides tumoral uptake, significant radioiodine accumulation was observed in tissues physiologically expressing NIS, including stomach and thyroid. In this context it is important to mention that the uptake in the stomach appears to be higher than usually seen in humans, which is most probably due to higher levels of NIS expression in murine gastric mucosa and pooling of gastric juices due to the anesthesia for a prolonged period during imaging procedure. In addition, due to exquisite regulation of thyroidal NIS expression by TSH, $^{123}$I accumulation in the thyroid gland can effectively be downregulated by thyroid hormone treatment as shown in humans (Wapnir *et al.*, 2004).
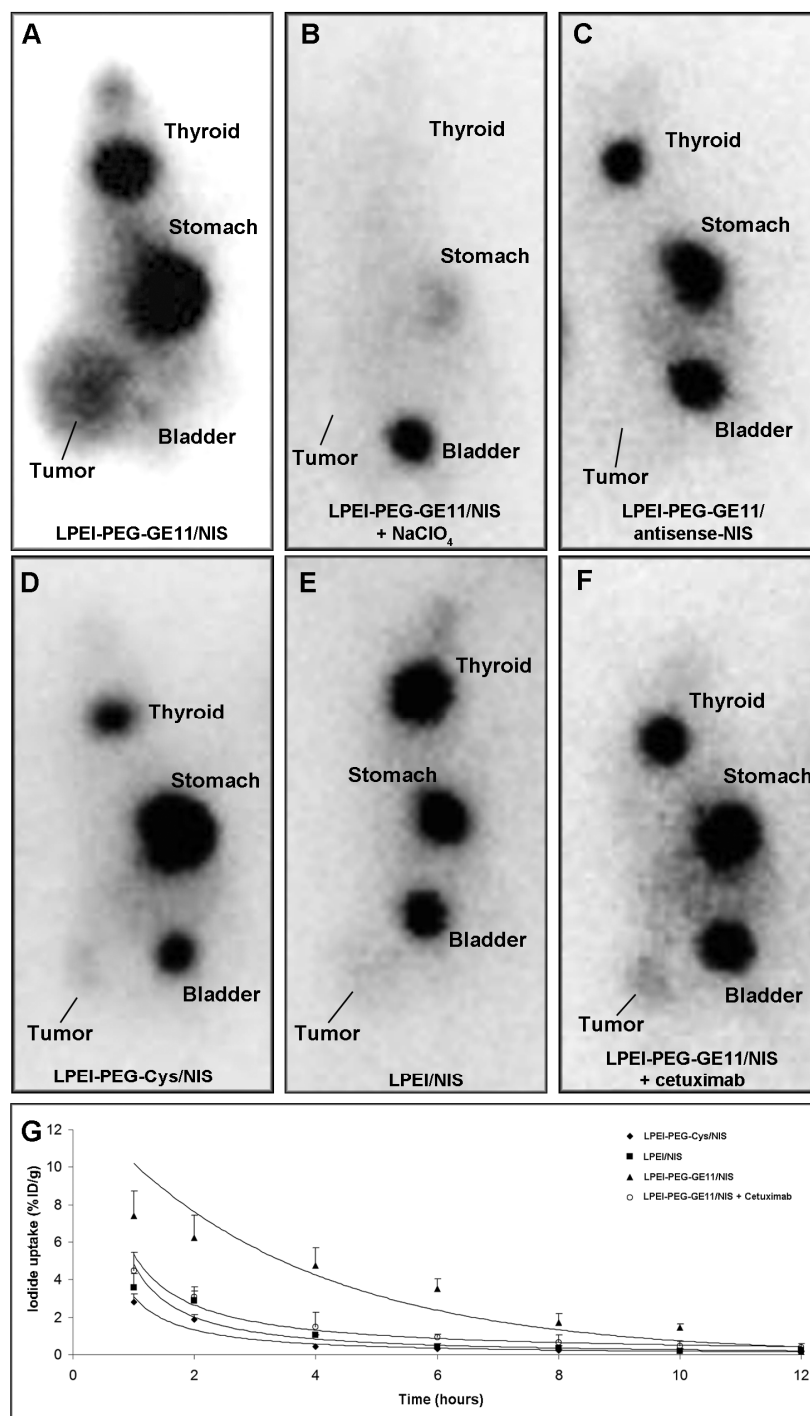
**Fig. 2:** [123]I gamma camera imaging of mice harbouring HuH7 tumors 3 h following i.p. injection of 18.5 MBq [123]I 24 h after LPEI-PEG-GE11-mediated NIS gene delivery. While mice treated with control polyplexes (LPEI-PEG-GE11/antisense-NIS, LPEI/NIS) showed no tumoral iodide uptake (C, E), treatment with LPEI-PEG-Cys/NIS led to a mild iodide uptake of 2.4% ID/g (D). Treatment with LPEI-PEG-GE11/NIS induced significant tumor-specific iodide accumulation in HuH7 tumors with accumulation of 6.5 - 9% ID/g [123]I (A), which was completely abolished upon pretreatment with NaClO$_4$ (B). Iodide was also accumulated physiologically in thyroid, stomach and bladder (A, C, D, E, F). After pretreatment with cetuximab the iodide uptake was significantly reduced to 4% ID/g (F).
Time course of ^{123}I accumulation in HuH7 tumors after systemic polyplex-mediated NIS gene delivery followed by injection of 18.5 MBq ^{123}I as determined by serial scanning. After application of LPEI-PEG-GE11/NIS the maximum tumoral radioiodine uptake was 6.5 - 9% ID/g tumor with an average effective t$_{1/2}$ of 6 h for [131]I. Following injection of control polyplexes (LPEI-PEG-Cys/NIS, LPEI/NIS) or after pretreatment with cetuximab iodide accumulation was significantly decreased (G).

### Ex vivo radioiodine biodistribution studies

*Ex vivo* biodistribution analysis confirmed induction of significant iodide uptake activity in tumors by systemic NIS gene transfer (Fig. 3). LPEI-PEG-GE11/NIS-transduced HuH7 tumors accumulated 4.3% ID/organ $^{123}$I 4 hours after radioiodine injection (Fig. 3A), whereas tumors transduced with control polyplexes (LPEI-PEG-Cys/NIS, LPEI-PEG-GE11/antisense-NIS and LPEI/NIS) showed only mild (LPEI-PEG-Cys/NIS) or no (LPEI/NIS, LPEI-PEG-GE11/antisense-NIS) iodide uptake. In all groups the thyroid gland and the stomach accumulated approx. 40% and 39% ID/organ (data not shown). Further, a single perchlorate injection prior to radioiodine application significantly blocked iodide uptake in NIS-transduced tumors and in physiologically NIS-expressing tissues, including thyroid and stomach, throughout the observation period up to 12 h (Fig. 3B). No iodide uptake above background level was observed in non-target organs, including lungs, liver, kidneys or spleen.
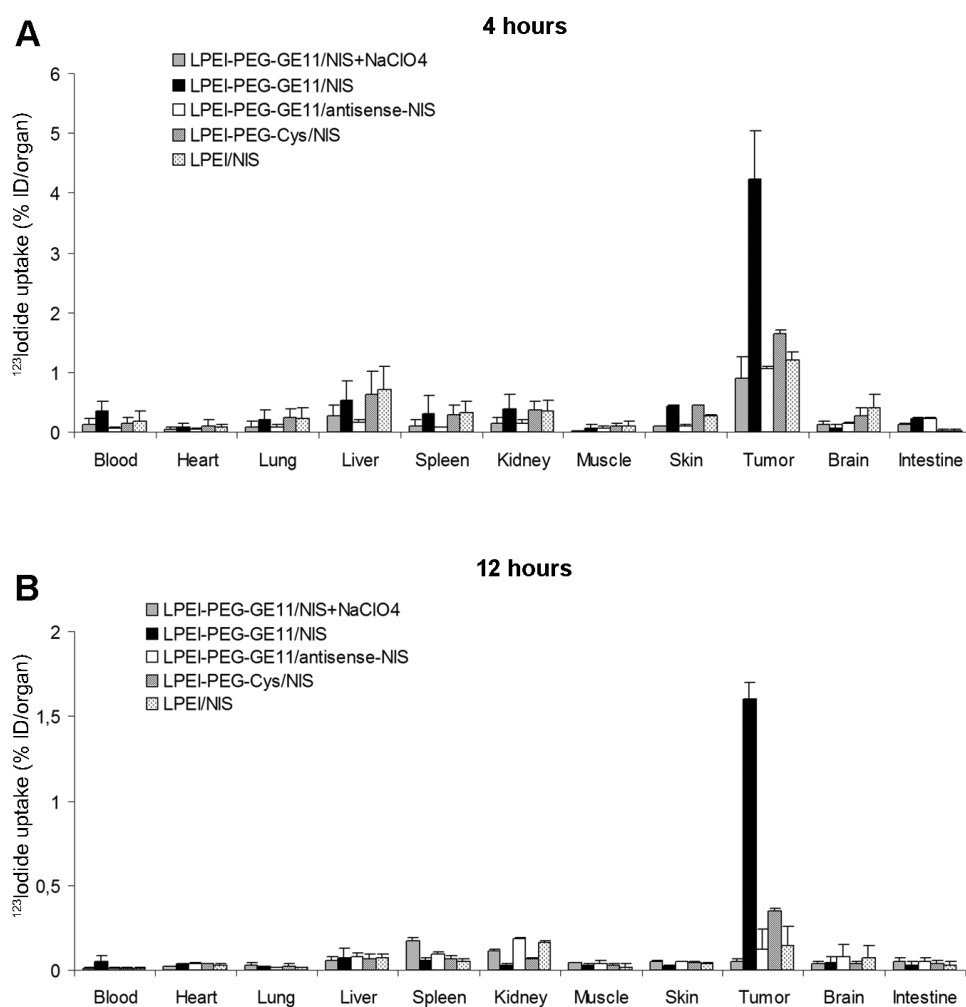
**Fig. 3:** Evaluation of iodide biodistribution *ex vivo* 4 h (A) and 12 h (B) following injection of 18.5 MBq $^{123}$I. While tumors in NIS-transduced mice showed high perchlorate-sensitive iodide uptake activity (up to 4.3% ID/organ), non-target organs revealed no significant iodide accumulation. No iodide accumulation was measured after injection of control polyplexes LPEI-PEG-GE11/antisense-NIS or LPEI/NIS, or after pretreatment with NaClO$_4$. A mild iodide uptake was observed after application of LPEI-PEG-Cys/NIS. Results were reported as percent of injected dose per organ ± SD.

### *Analysis of NIS mRNA expression by quantitative real-time PCR analysis*

In order to assess NIS mRNA levels after systemic NIS gene transfer, mRNA of various tissues was extracted and analyzed by quantitative real-time PCR (qPCR) with a pair of NIS-specific oligonucleotide primers 24 h after NIS gene transfer. Significant levels of NIS gene expression were induced in HuH7 tumors after systemic injection of LPEI-PEG-GE11/NIS (Fig. 4A), whereas only low background levels were detected after application of LPEI-PEG-GE11/antisense-NIS, LPEI-PEG-Cys/NIS and LPEI/NIS. As expected, administration of the competitive NIS inhibitor sodium-perchlorate had no influence on NIS mRNA expression in NIS-transduced tumors. After application of the EGFR-specific antibody cetuximab tumoral NIS mRNA expression was significantly reduced. Furthermore, analysis of non-target organs like lungs and liver, showed no significant NIS mRNA expression above background level (Fig. 4A). In contrast, high levels of NIS mRNA were detected in the lungs of mice receiving LPEI/NIS suggesting unspecific pulmonary accumulation of these polyplexes due to their aggregation with erythrocytes (Fig. 4A).
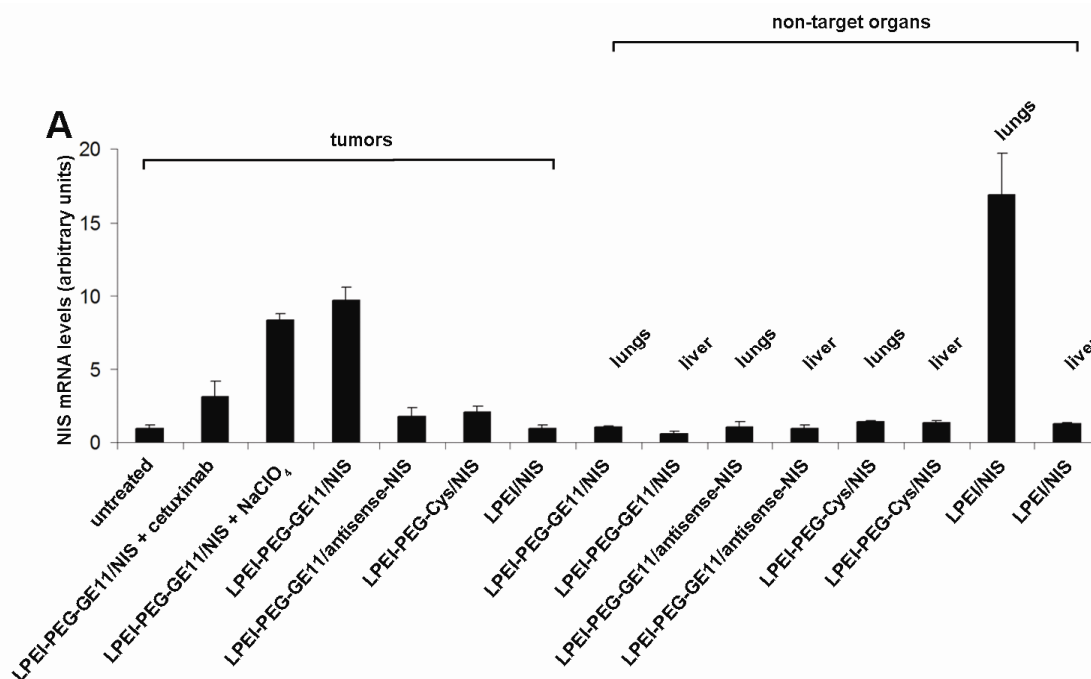
**Fig. 4:** Analysis of human NIS mRNA expression in HuH7 tumors and non-target organs by qPCR (A). A significant level of NIS mRNA expression was induced in HuH7 tumors after systemic NIS gene transfer with or without sodium-perchlorate pretreatment (LPEI-PEG-GE11/NIS). Only a low background level of NIS mRNA expression was detected in untreated tumors, which was set as 1 arbitrary unit. Moreover, no significant NIS expression above background level was found in tumors after application of LPEI-PEG-GE11/antisense-NIS, LPEI-PEG-Cys/NIS, LPEI-PEG-GE11/NIS + cetuximab and LPEI/NIS. After systemic application with LPEI/NIS a high NIS mRNA expression level was detected in the lungs, whereas non-target organs showed no significant NIS mRNA expression after treatment of LPEI-PEG-GE11/NIS, LPEI-PEG-GE11/antisense-NIS, LPEI-PEG-Cys/NIS. Results were reported as NIS/GAPDH ratios.

### *Analysis of NIS protein expression in HuH7 tumors*

Immunohistochemical analysis of HuH7 tumors after systemic application of LPEI-PEG-GE11/NIS revealed a heterogeneous staining pattern with clusters of primarily membrane-associated NIS-specific immunoreactivity (Fig. 4B). In contrast, tumors treated with LPEI-PEG-GE11/antisense-NIS, LPEI-PEG-Cys/NIS and LPEI/NIS (Fig. 4C-E) showed no NIS-specific immunoreactivity. Specificity of staining was confirmed using isotype-matched control immunoglobulin (data not shown).
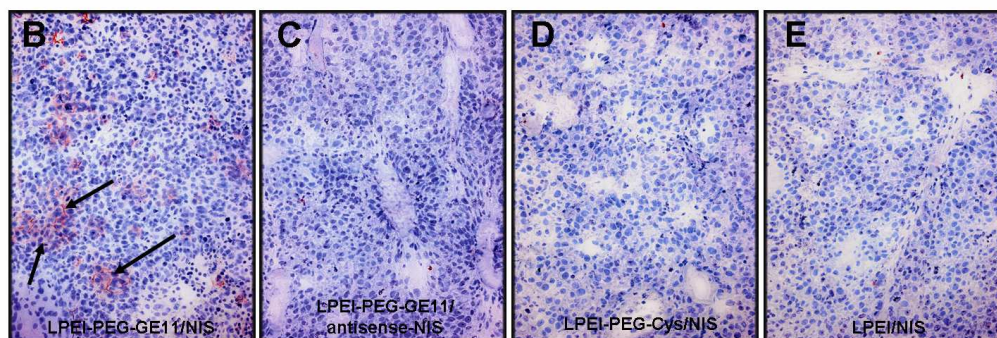
**Fig. 4:** Immunohistochemical staining of HuH7 tumors 24 h after LPEI-PEG-GE11/NIS application using a *h*NIS specific antibody showed clusters of primarily membrane-associated NIS-specific immunoreactivity (B). In contrast, HuH7 tumors treated with the control polyplexes (LPEI-PEG-GE11/antisense-NIS (C), LPEI-PEG-Cys/NIS (D), LPEI/NIS (E)) did not reveal NIS-specific immunoreactivity. Magnification: 100x

### *Radioiodine therapy studies after in vivo NIS gene transfer*

24 h after systemic administration of polyplexes, a therapeutic dose of 55.5 MBq (1.5 mCi) $^{131}$I or saline was administered. The cycle consisting of systemic NIS gene transfer followed by radioiodine was repeated twice on days 3/4 and 7/8. Mice treated with three cycles of LPEI-PEG-GE11/NIS and $^{131}$I showed a significant delay in tumor growth as compared to all control groups (Fig. 5A), tumor growth started again one week after the last treatment. Therefore, in another therapy group a fourth therapy cycle was added at days 14/15, which further delayed tumor growth. In all control groups (LPEI-PEG-GE11/NIS or LPEI-PEG-GE11/antisense-NIS followed by saline, or LPEI-PEG-GE11/antisense-NIS followed by $^{131}$I) mice showed an exponential tumor growth and had to be killed within two weeks after the onset of the experiments due to excessive tumor growth (Fig. 5B). 50% of mice survived 3 - 4 weeks after application of 3 cycles of polyplexes followed by $^{131}$I application; overall survival was further enhanced by addition of another cycle of polyplex/$^{131}$I application (Fig. 5B). Importantly, none of these mice showed major adverse effects due to radionuclide or polyplex treatment in terms of lethargy or respiratory failure. However, a minor body weight loss of 3 - 5% was observed in mice after systemic administration of polyplexes.
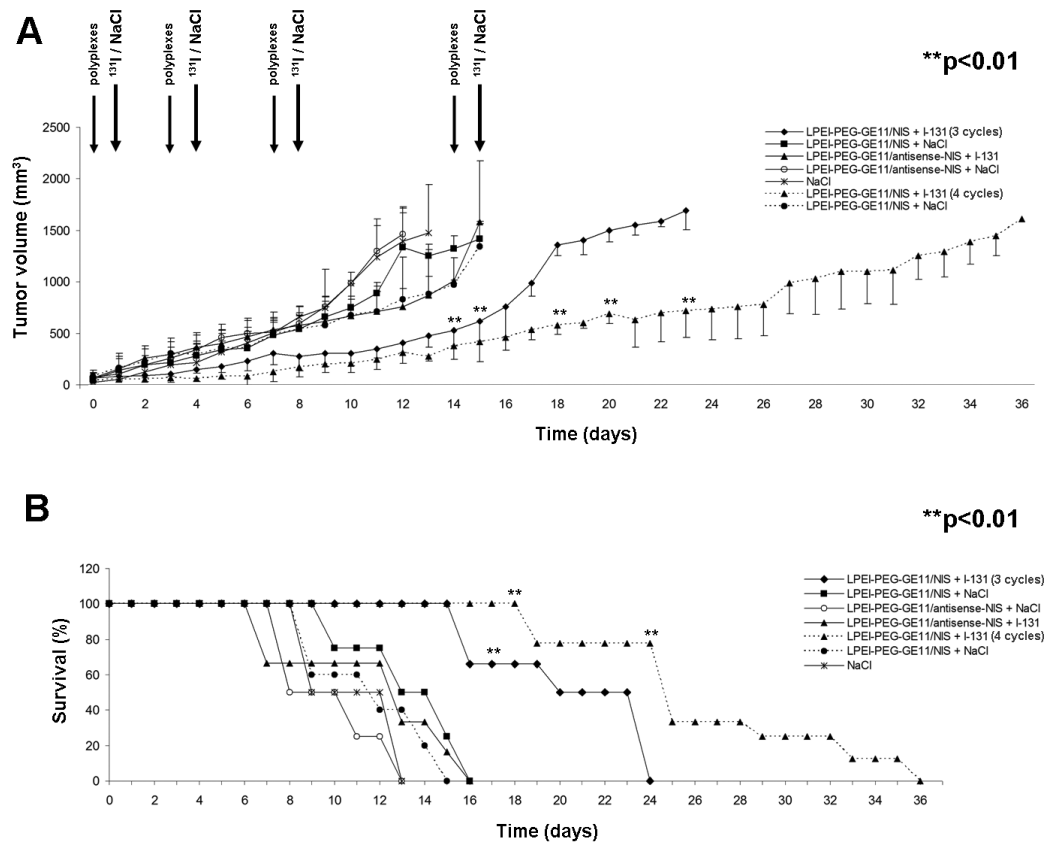
**Fig. 5:** Radioiodine treatment of HuH7 tumors after systemic polyplex-mediated NIS gene transfer *in vivo*. 24 h after i.v. polyplex injection (small arrow), 55.5 MBq $^{131}$I were injected i.p. (big arrow). This treatment cycle was repeated twice on days 3/4 and 7/8 and additionally on days 14/15 (dotted lines). $^{131}$I therapy after systemic LPEI-PEG-GE11/NIS application resulted in a significant delay in tumor growth (A, **p<0.01) which was associated with markedly improved survival (B, Kaplan-Meier-plot (**p<0.01)) as compared to the control groups that were injected with saline only, with LPEI-PEG-GE11/NIS followed by saline application, or with LPEI-PEG-GE11/antisense-NIS followed by saline or $^{131}$I application.

### *Immunofluorescence analysis*

Three to four weeks after treatment, mice were sacrified, and tumors were dissected and processed for immunofluorescence analysis using a Ki67-specific antibody (green) and an antibody against CD31 (red, labelling blood vessels) (Fig. 6). NIS-transduced tumors (LPEI-PEG-GE11/NIS) (Fig. 6B) exhibited a significantly lower intratumoral blood vessel density and proliferation index after $^{131}$I therapy when compared to mock-transduced tumors (LPEI-PEG-GE11/antisense-NIS) tumors (Fig. 6A).
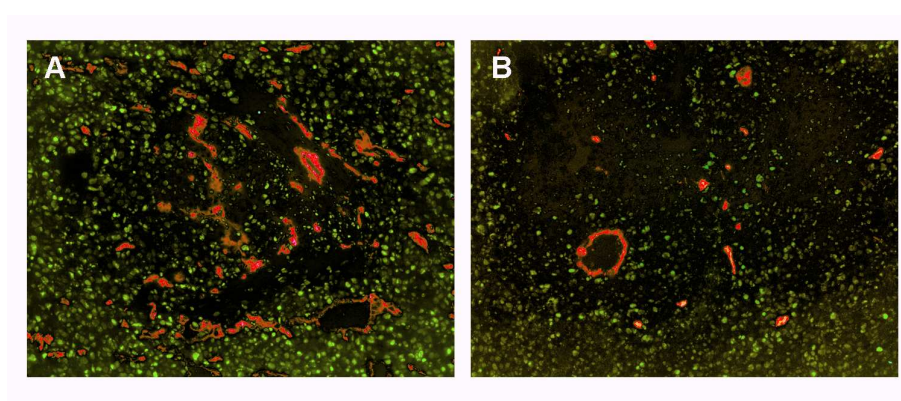


**Fig. 6:** Immunofluorescence analysis using a Ki67-specific antibody (green) and an antibody against CD31 (red, labeling blood vessels) showed significantly decreased proliferation and blood vessel density in NIS-transduced tumors (B) following $^{131}$I treatment as compared to mock-transduced tumors (A). Slides were counterstained with DAPI nuclear stain. Magnification 100x.

# Discussion

In the present study we investigated the efficacy of novel synthetic nanoparticle vectors based on LPEI, shielded by attachment of PEG and coupled with the EGFR-specific ligand GE11 to achieve tumor-selective NIS-mediated radioiodine accumulation in a HCC mouse model. After confirmation of high transduction efficiency of LPEI-PEG-GE11 in human HCC cells *in vitro*, i.v. application of LPEI-PEG-GE11 in nude mice carrying HCC xenografts was demonstrated to result in tumor-selective, EGFR-targeted radioiodine accumulation, which was high enough for a significant therapeutic effect after application of $^{131}$I.

As one of the oldest and most successful targets of molecular imaging and therapy, cloning and characterization of NIS has provided us with a powerful new reporter and therapy gene (Spitzweg and Morris, 2002b; Hingorani *et al.*, 2010a). Many of the characteristics of NIS, which have been confirmed by our work to date, suggest that it represents an ideal therapy gene due to several advantages. NIS as an endogenous human protein implies that its expression in cancer cells is unlikely to be toxic or to elicit a significant immune response that could limit its efficacy. In its dual role as reporter and therapy gene NIS allows direct, non-invasive imaging of functional NIS expression by $^{123}$I-scintigraphy and $^{124}$I-PET-imaging, as well as exact dosimetric calculations before proceeding to therapeutic application of $^{131}$I (Spitzweg and Morris, 2002b; Dingli *et al.*, 2003b).

The capacity of the NIS gene to induce radioiodine accumulation in nonthyroidal tumors has been investigated by several groups including our own, demonstrating the enormous potential of NIS as therapy gene (Spitzweg *et al.*, 1999c; Spitzweg *et al.*, 2000b; Spitzweg *et al.*, 2001a; Spitzweg *et al.*, 2001c; Spitzweg and Morris, 2002b; Kakinuma *et al.*, 2003; Dingli *et al.*, 2004; Cengic *et al.*, 2005; Dwyer *et al.*, 2005a; Scholz *et al.*, 2005; Dwyer *et al.*, 2006a; Spitzweg *et al.*, 2007; Willhauck *et al.*, 2007; Willhauck *et al.*, 2008a; Willhauck *et al.*, 2008b; Peerlinck *et al.*, 2009; Hingorani *et al.*, 2010b; Li *et al.*, 2010; Trujillo *et al.*, 2010). However, only a limited number of studies have investigated systemic NIS gene delivery approaches to address one of the major hurdles on the way to efficient and safe application of the NIS gene therapy concept in the clinical setting in metastatic disease, which is optimal tumor targeting in the presence of low toxicity and high transduction efficiency with the ultimate goal of systemic vector application. In its function as reporter gene NIS provides an elegant means for non-invasive monitoring of vector

biodistribution as well as biodistribution, level and duration of transgene expression after systemic vector application (Dingli *et al.*, 2004; Goel *et al.*, 2007; Chisholm *et al.*, 2009; Liu *et al.*, 2010). We recently reported a systemic non-viral NIS gene delivery approach in a neuroblastoma mouse model (Neuro2A), where biodegradable branched polycations based on OEI-grafted polypropylenimine dendrimers (G2-HD-OEI) for systemic NIS gene application achieved tumor-specific iodide accumulation resulting in a significant therapeutic effect after application of $^{131}$I even in the absence of iodide organification (Klutz *et al.*, 2009). This study showed for the first time a significant therapeutic effect of radioiodine after systemic non-viral NIS gene transfer in an experimental tumor model. The high intrinsic tumor affinity of G2-HD-OEI is based on passive polyplex trapping in the tumor caused by the typically leaky vasculature and inadequate lymphatic drainage in tumors (Maeda, 2001), which can be highly dependent on the tumor type (Navarro *et al.*, 2010).

The "golden standard" of polyethylenimine (PEI)-based gene carriers is LPEI, the linear form of PEI, with a molecular weight of 22 kDa, also known as the commercially available JetPEI®. The major drawback of LPEI is its significant toxicity after systemic application due to acute and long-term toxic effects (Chollet *et al.*, 2002). Transgene expression was demonstrated to be more than 100 times higher in the lung than in the tumor most probably due to pronounced aggregation with erythrocytes that usually results in high transgene expression in the first vascular bed encountered, namely the lung (Russ *et al.*, 2008a; Russ *et al.*, 2008).

A technique to reduce unspecific toxicity and prolong blood circulation time is shielding of polyplexes by PEGylation (polyethylene glycol). Zintchenko *et al*. showed in a previous study with quantoplexes (polyplexes consisting of PEI and DNA with incorporated negatively charged near-infrared-emitting cadmium telluride quantum dots), that PEGylated quantoplexes have a circulation time in the range of several minutes, whereas unshielded PEI polyplexes do not show circulation at all (Zintchenko *et al.*, 2009). The modification of the surface of DNA complexes with PEG can block the interaction with plasma components and erythrocytes and strongly changes the *in vivo* characteristics of particles, resulting in reduced toxicity, prolonged circulation and gene expression in distant tumor tissue after systemic administration (Ogris *et al.*, 1999). However, PEGylation also results in decreased cell binding capacity and subsequently reduced efficacy (Ogris *et al.*, 1999). The addition of specific targeting ligands, such as peptides, proteins and carbohydrates to these shielded

polyplexes can be employed with the aim of active tumor targeting thereby enhancing transfection efficiency and tumor selectivity (De Bruin *et al.*, 2007).

In the current study the EGFR was used as tumor-specific target, a transmembrane receptor with intrinsic tyrosine kinase activity. The upregulation to $2 \times 10^6$ EGFR per cell in numerous solid tumors including lung, liver, breast and bladder cancer, glioblastoma as well as hepatocellular carcinoma makes it an attractive target for cancer gene therapy strategies. EGFR-targeting has been utilized for targeted delivery of neutralizing antibodies (Mendelsohn and Baselga, 2006), toxins (Liu *et al.*, 2005), and nucleid acids (Shir *et al.*, 2006), as well as for targeted gene delivery, either with viral (Dmitriev *et al.*, 2000) or non-viral gene delivery systems (Wolschek *et al.*, 2002). The enhanced uptake of EGF-coupled polyplexes in EGFR-overexpressing tumor cells was shown in several experiments with an up to 300-fold increased transfection efficiency depending on the tumor cell line (Blessing *et al.*, 2001). Studies with HuH7 HCC cells showed that 50% of these "artifical viruses" were already internalised after 5 minutes, whereas untargeted polyplexes reached only approximately 20% after a 20 min incubation (De Bruin *et al.*, 2007). Generating polyplexes with EGF as targeting ligand combined with PEG as shielding moiety lead to rapid internalization via the EGF-receptor and significantly increased transgene expression in subcutaneous hepatoma tumors in mice after systemic administration (Wolschek *et al.*, 2002).

EGF, the natural ligand of the EGFR, however, has strong mitogenic and neoangiogenic activity possibly attenuating the anticancer effect of the therapeutic gene used (Li *et al.*, 2005). For this purpose, Li *et al.* screened a phage display library to discover new EGFR binders and have found a phage clone encoding for a peptide termed GE11, which showed high affinity towards EGFR without activation of the receptor tyrosine kinase. GE11-conjugated PEI polyplexes showed high transfection efficiency in EGFR overexpressing tissues, while no significant activation of EGFR and no mitogenic activity of treated cells was observed (Li *et al.*, 2005)*.*

In our study we used LPEI-PEG-GE11 polymers and complexed them with the human NIS cDNA under the control of the strong human elongation factor 1 alpha promoter. The plasmid used is completely devoid of CpG islands, which has been described to result in prolonged and higher transgene expression in tumor tissue *in vivo* (De Wolf *et al.*, 2008; Navarro *et al.*, 2010). *In vitro* transfection of HuH7 cells with LPEI-PEG-GE11/NIS resulted in a 22-fold increase in iodide uptake activity, which was significantly lower when polyplexes without EGFR-targeting (LPEI-PEG-Cys/NIS) were used.

Following i.v. application of LPEI-PEG-GE11/NIS polyplexes in mice carrying HuH7 xenografts 80% of tumors showed tumor-specific ^{123}I accumulation with approximately 6.5-9% ID/g, a biological half-life of 6 hours and a tumor absorbed dose of 47 mGy / MBq [131]I. In addition, our *in vivo* [123]I scintigraphic imaging studies were confirmed by *ex vivo* biodistribution experiments revealing significant tumoral radioiodine accumulation, whereas no iodide uptake was measured in non-target organs. Significance of EGFR-mediated NIS gene delivery was shown in mice pretreated with the EGFR-specific antibody cetuximab 24 h prior to polyplex application. cetuximab has been shown to inhibit EGFR-mediated tumor cell targeting *in vitro* with EGF-targeted nanoparticles (Diagaradjane *et al.*, 2008) and to downregulate EGFR *in vitro* and *in vivo* (Perez-Torres *et al.*, 2006). Here we demonstrate that cetuximab pretreatment is able to reduce tumor-specific transfection efficiency of EGFR-targeted polyplexes. In line with these results, untargeted LPEI-PEG-Cys/NIS also showed significantly lower iodide uptake, further confirming the EGFR-specificity of LPEI-PEG-GE11. The low, but measurable iodide uptake activity in HCC tumors after LPEI-PEG-Cys/NIS treatment suggests that passive tumor targeting due to the "enhanced permeability and retention-effect" is sufficient for a low level of tumoral NIS transduction (Maeda, 2001), which can be significantly increased after coupling to the EGFR-specific ligand GE11. These data are consistent with the study by Song *et al.* showing enhanced extent and duration of accumulation of fluorescence-labelled liposomes containing GE11 when compared to an unrelated peptide, where accumulation was significant, but less pronounced (Song *et al.*, 2008). In mice treated with LPEI-PEG-GE11/NIS and the specific NIS-inhibitor sodium-perchlorate prior to application of radioiodine or in mice treated with the control vectors (LPEI-PEG-GE11/antisense-NIS) tumors showed no significant iodide uptake demonstrating that tumoral radioiodine accumulation after systemic EGFR-targeted NIS gene transfer was mediated by functional NIS protein.

We further confirmed tumor-specific NIS expression after systemic application of LPEI-PEG-GE11/NIS by real time qPCR, whereas after application of LPEI/NIS high levels of NIS mRNA expression were primarily detected in the lungs of treated animals. Intravenously applied LPEI polyplexes are known to induce high transgene expression activity in the lungs, which is due to aggregation with erythrocytes, but also high cellular toxicity (Chollet *et al.*, 2002). Despite significant mRNA levels, no NIS activity was observed in lungs, which is presumably due to LPEI-mediated cell membrane damage inhibiting proper membrane trafficking of the NIS protein which is required for functional activity. With LPEI-PEG-GE11/NIS or LPEI-PEG-Cys/NIS polyplexes, no pulmonary NIS

mRNA or NIS activity was found suggesting prevention of polyplex aggregation in the lung due to PEG shielding.

In tumor sections NIS-specific immunoreactivity was primarily membrane-associated and occurred in clusters. The patchy staining pattern nicely correlates with experiments using G2-HD-OEI polyplexes for systemic NIS gene transfer in a syngeneic neuroblastoma mouse model (Klutz *et al.*, 2009) and with a study using PEI-based EGF-coupled polymers for targeting the β-galactosidase reporter gene to HCC cells *in vivo* resulting in a heterogeneous and patchy distribution of transgene activity (Wolschek *et al.*, 2002).

Most importantly, systemic EGFR-targeted NIS gene transfer resulted in tumor-specific iodide uptake activity in HCC tumor-bearing mice, which was sufficiently high for a significant therapeutic effect of $^{131}$I. After three to four cycles of systemic polyplex application followed by $^{131}$I injection, tumor-bearing mice showed a significant delay of tumor growth associated with a significantly prolonged survival. In addition, immunoflourescence analysis showed markedly reduced proliferation associated with decreased blood vessel density inside and surrounding the tumor after systemic polyplex-mediated NIS gene transfer followed by $^{131}$I application, suggesting radiation-induced tumor stroma cell damage in addition to tumor cell death. The crossfire effect of $^{131}$I with a maximum path length of up to 2.4 mm might be responsible for stromal cell damage leading to reduced angiogenesis and secretion of growth-stimulatory factors, thereby enhancing therapeutic efficacy.

In conclusion, our data clearly demonstrate the high potential of novel synthetic nanoparticle vectors based on LPEI, shielded by PEG and coupled with the synthetic peptide GE11 as an EGFR-specific ligand for targeting the NIS gene to human HCC overexpressing EGFR. Based on the role of NIS as a potent and well characterized reporter gene allowing non-invasive imaging of functional NIS expression, this study allowed detailed characterization of *in vivo* biodistribution of EGFR-targeted functional NIS expression by gamma camera imaging, which is an essential prerequisite for exact planning and monitoring of clinical gene therapy trials with the aim of individualization of the NIS gene therapy concept in the clinical setting. Tumor-specific iodide accumulation was further demonstrated to be sufficiently high for a significant delay of tumor growth associated with increased survival in HCC xenograft bearing nude mice after three to four cycles of polyplex application followed by $^{131}$I therapy. This study therefore opens the exciting

prospect of NIS-targeted radionuclide therapy of metastatic cancer using EGFR-targeted polyplexes for systemic NIS gene delivery.

## Acknowledgments

# 6.  Summary

Based upon the application of radioiodine that has been used for over 70 years for diagnostic imaging and therapy in the management of thyroid cancer due to endogenous expression of NIS, cloning of NIS has paved the way of a novel cytoreductive gene therapy strategy.

After proof of principle of AFP promoter-mediated NIS gene delivery in a stably NIS-transfected HCC xenograft model (Willhauck *et al.*, 2008b) in this thesis we developed a replication-deficient adenovirus carrying the NIS gene under the control of the AFP promoter (Ad5-AFP-NIS) and applied it in a human HCC (HepG2) xenograft mouse model for local NIS gene delivery. To achieve tumor specificity a mouse AFP-promoter construct consisting of the basal promoter and enhancer I element was used for transcriptional targeting of the NIS gene to liver cancer cells.

HepG2 cells infected with Ad5-AFP-NIS concentrated 50% of the applied activity of $^{125}$I, which was sufficiently high for a therapeutic effect in an *in vitro* clonogenic assay. Four days after intratumoral injection of Ad5-AFP-NIS in HepG2 xenografts, analysis of $^{123}$I or $^{188}$Re accumulation by gamma camera imaging revealed high tumoral radionuclide activity. Tumor-specific NIS expression was further confirmed by immunohistochemistry and real time qPCR. After adenovirus-mediated NIS gene transfer in HepG2 xenografts administration of a therapeutic dose of $^{131}$I or $^{188}$Re resulted in a significant delay in tumor growth and improved survival, with $^{188}$Re being mildly more potent than $^{131}$I.

As a next crucial step towards clinical application of the promising NIS gene therapy concept, we evaluated gene transfer methods that own the potential to achieve sufficient tumor-selective transgene expression levels not only after local but also after systemic application to be able to reach tumor-metastases.

For this purpose, we analyzed the potential of novel biodegradable, branched polycations based on OEI-grafted polypropylenimine dendrimers (G2-HD-OEI) which show high intrinsic tumor affinity to target a NIS-expressing plasmid to neuroblastoma (Neuro2A) and HCC (HuH7) cells *in vitro* and *in vivo*. *In vitro* incubation with NIS-conjugated nanoparticles resulted in a 51-fold increase in perchlorate-sensitive iodide uptake activity in Neuro2A cells and a 44-fold increase in HuH7 cells. *In vivo* NIS-conjugated nanoparticle vectors were injected via the tail vein followed by analysis of radioiodine accumulation using $^{123}$I-scintigraphy, $^{123}$I SPECT-CT imaging and *ex vivo* gamma counting. High levels

of iodide uptake activity were observed in the tumor whereas non-target organs like lungs, liver, kidneys and spleen exhibited only mild or no significant iodide uptake. Tumor-specific NIS expression was further confirmed by immunohistochemistry and real time qPCR. In addition, the achieved tumoral radioiodine uptake was high enough for a significant therapeutic effect of $^{131}$I in Neuro2A and HuH7 tumors, which was associated with significantly improved survival.

To further improve tumor-specific targeting we analyzed the efficacy of novel synthetic nanoparticle vectors based on linear polyethylenimine (LPEI), shielded by attachment of polyethylene glycol (PEG), and coupled with the synthetic peptide GE11 as an EGFR-specific ligand (LPEI-PEG-GE11) for targeting the NIS gene to EGFR-expressing human HCC (Huh7) cells. After systemic application of NIS-polyplexes high tumor-specific iodide activity was demonstrated, which was markedly reduced after application of the EGFR-specific antibody cetuximab confirming the EGFR-specificity of LPEI-PEG-GE11. Further, after three or four cycles of polymer application followed by therapeutic application of $^{131}$I, tumor growth was significantly reduced associated with improved survival.

In conclusion, these data clearly demonstrate the high potential of tumor-specific NIS gene therapy using viral and non-viral gene delivery vectors, which opens the exciting perspective of targeted NIS-mediated radionuclide therapy of extrathyroidal tumors even in the metastatic stage.

# 7. Publications

## Original papers

Klutz K, Russ V, Willhauck MJ, Wunderlich N, Zach C, Gildehaus FJ, Göke B, Wagner E, Ogris M, Spitzweg C: Targeted radioiodine therapy of neuroblastoma tumors following systemic non-viral delivery of the sodium iodide symporter (NIS) gene. Clin Cancer Res. 2009, 15 (19): 6079-86.

Willhauck MJ, Sharif Samani BR, Klutz K, Cengic N, Wolf I, Mohr L, Geissler M, Senekowitsch-Schmidtke R, Göke B, Morris JC, Spitzweg C: Alpha-fetoprotein promoter-targeted sodium iodide symporter gene therapy of hepatocellular carcinoma. Gene Ther. 2008, 15: 214-223.

## Manuscripts in preparation

Klutz K, Willhauck MJ, Wunderlich N, Zach C, Anton M, Senekowitsch-Schmidtke R, Göke B, Spitzweg C: Comparison study of $^{131}$I and $^{188}$Re therapy in liver cancer after tumor-specific *in vivo* sodium iodide symporter (NIS) gene transfer, *submitted.*

Knoop K, Kolokythas M, Klutz K, Willhauck MJ, Wunderlich N, Draganovici D, Zach C, Gildehaus FJ, Böning G, Göke B, Wagner E, Nelson PJ, Spitzweg C: *In vivo* imaging of tumor stoma-selective mesenchymal stem cell recruitment using the sodium iodide symporter as reporter gene, *submitted.*

Klutz K, Willhauck MJ, Dohmen C, Wunderlich N, Knoop K, Zach C, Senekowitsch-Schmidtke R, Gildehaus FJ, Ziegler S, Fürst S, Göke B, Wagner E, Ogris M, Spitzweg C: Image-guided tumor-selective radioiodine therapy of liver cancer following systemic non-viral delivery of the sodium iodide symporter (NIS) gene, *submitted.*

Klutz K, Schaffert D , Willhauck MJ, Grünwald GK, Haase R, Wunderlich N, Zach C, Gildehaus FJ, Senekowitsch-Schmidtke R, Göke B, Wagner E, Ogris M, Spitzweg C:

Epidermal growth factor receptor-targeted radioiodine therapy of hepatucellular cancer following systemic non-viral delivery of the sodium iodide symporter gene, *submitted.*

Klutz K, Grünwald GK, Willhauck MJ, Wunderlich N, Göke B, Senekowitsch-Schmidtke R, Holm PS, Spitzweg C: An alpha-fetoprotein promoter, conditionally replicating adenovirus that expresses the sodium iodide symporter (NIS) for radiovirotherapy of HCC, *in preparation.*

## Poster presentations

Klutz K, Schaffert D , Willhauck MJ, Grünwald GK, Knoop K, Rödl W, Wunderlich N, Zach C, Gildehaus FJ, Göke B, Wagner E, Ogris M, Spitzweg C: Radioiodine therapy of hepatocellular carcinoma following systemic sodium iodide symporter (NIS) gene transfer using EGF receptor-targeted non-viral gene delivery vectors, International Thyroid Congress, 2010, Paris, France.

Klutz K, Schaffert D , Willhauck MJ, Knoop K, Grünwald GK, Rödl W, Wunderlich N, Zach C, Gildehaus FJ, Göke B, Wagner E, Ogris M, Spitzweg C: Systemic sodium iodide symporter (NIS) gene transfer in hepatocellular carcinoma using EGF-receptor targeted non-viral gene delivery, Deutsche Gesellschaft für Innere Medizin, 2010, Wiesbaden, Germany.

Klutz K, Russ V, Willhauck MJ, Wunderlich N, Wagner E, Göke B, Ogris M, Spitzweg C: Comparison of two different non-viral gene delivery vectors for systemic sodium iodide symporter gene transfer in hepatocellular carcinoma, Annual Congress of the European Society of Gene and Cell Therapy, 2009, Hannover, Germany.

Klutz K, Russ V, Willhauck MJ, Wunderlich N, Zach C, Münzing W, Gildehaus FJ, Göke B, Wagner E, Ogris M, Spitzweg C: Radioiodine therapy of neuroblastoma tumors following systemic sodium iodide symporter gene transfer using non-viral gene delivery vectors, Annual Meeting of Endocrine Society, 2009, Washington, USA.

Klutz K, Willhauck MJ, Wunderlich N, Zach C, Senekowitsch-Schmidtke R, Anton M, Göke B, Spitzweg C: Image-guided radioiodine therapy of HCC following AFP-promoter

targeted *in vivo* sodium iodide symporter (NIS) gene transfer, European Congress of Endocrinology, 2009, Istanbul, Turkey.

Klutz K, Russ V, Willhauck MJ, Wunderlich N, Zach C, Münzing W, Gildehaus FJ, Göke B, Wagner E, Ogris M, Spitzweg C: Induction of iodide uptake activity in neuroblastoma tumors following systemic sodium iodide symporter gene transfer using non-viral gene delivery vectors, Deutsche Gesellschaft für Gentherapie, 2008, Berlin, Germany.

## Oral presentations

Klutz K. Schaffert D , Willhauck MJ, Knoop K, Grünwald GK, Rödl W, Wunderlich N, Zach C, Gildehaus FJ, Göke B, Wagner E, Ogris M, Spitzweg C: Systemic sodium iodide symporter (NIS) gene transfer in hepatocellular carcinoma using EGF-receptor targeted non-viral gene delivery vectors, European Congress of Endocrinology, 2010, Prague, Czech Republic.

Klutz K, Russ V, Willhauck MJ, Wunderlich N, Gildehaus FJ, Göke B, Wagner E, Ogris M, Spitzweg C: Comparison of two different non-viral gene delivery vectors for systemic sodium iodide symporter gene transfer in hepatocellular carcinoma, Annual Meeting of American Thyroid Association, 2009, Palm Beach, USA.

Klutz K, Russ V, Willhauck MJ, Wunderlich N, Gildehaus FJ, Göke B, Wagner E, Ogris M, Spitzweg C: Systemic sodium iodide symporter gene therapy in hepatocellular carcinoma using non-viral gene delivery vectors, Annual Meeting of European Thyroid Association, 2009, Lisbon, Portugal.

Klutz K, Russ V, Willhauck MJ, Wunderlich N, Zach C, Münzing W, Gildehaus FJ, Göke B, Wagner E, Ogris M, Spitzweg C: Tumor-specific iodide uptake activity in neuroblastoma tumors following systemic sodium iodide symporter gene transfer using synthetic gene delivery vectors, Annual Meeting of Endocrine Society, 2008, San Fransisco, USA.

## Award

Poster Award 2008, Deutsche Gesselschaft für Gentherapie, Berlin, Germany:

Klutz K, Russ V, Willhauck MJ, Wunderlich N, Zach C, Münzing W, Gildehaus FJ, Göke B, Wagner E, Ogris M, Spitzweg C: Induction of iodide uptake activity in neuroblastoma tumors following systemic sodium iodide symporter gene transfer using non-viral gene delivery vectors, Deutsche Gesselschaft für Gentherapie, 2008, Berlin, Germany.

# 8.   References

Baril*, et al.* (2010). Visualization of gene expression in the live subject using the Na/I symporter as a reporter gene: applications in biotherapy. Br J Pharmacol 159, 761-771.

Blechacz*, et al.* (2006). Engineered measles virus as a novel oncolytic viral therapy system for hepatocellular carcinoma. Hepatology 44, 1465-1477.

Blessing*, et al.* (2001). Different strategies for formation of pegylated EGF-conjugated PEI/DNA complexes for targeted gene delivery. Bioconjug Chem 12, 529-537.

Brunner*, et al.* (2000). Cell cycle dependence of gene transfer by lipoplex, polyplex and recombinant adenovirus. Gene Ther 7, 401-407.

Carlson*, et al.* (2006). In vivo quantitation of intratumoral radioisotope uptake using micro-single photon emission computed tomography/computed tomography. Mol Imaging Biol 8, 324-332.

Carlson*, et al.* (2009). Quantitative molecular imaging of viral therapy for pancreatic cancer using an engineered measles virus expressing the sodium-iodide symporter reporter gene. AJR Am J Roentgenol 192, 279-287.

Castro*, et al.* (1999). Monoclonal antibodies against the human sodium iodide symporter: utility for immunocytochemistry of thyroid cancer. J Endocrinol 163, 495-504.

Cengic*, et al.* (2005). A novel therapeutic strategy for medullary thyroid cancer based on radioiodine therapy following tissue-specific sodium iodide symporter gene expression. J Clin Endocrinol Metab 90, 4457-4464.

Chen*, et al.* (2006). Radioiodine therapy of hepatoma using targeted transfer of the human sodium/iodide symporter gene. J Nucl Med 47, 854-862.

Chisholm*, et al.* (2009). Cancer-Specific Transgene Expression Mediated by Systemic Injection of Nanoparticles. Cancer Res 69, 2655-2662.

Chollet*, et al.* (2002). Side-effects of a systemic injection of linear polyethylenimine-DNA complexes. J Gene Med 4, 84-91.

Dadachova*, et al.* (2002). Rhenium-188 as an alternative to Iodine-131 for treatment of breast tumors expressing the sodium/iodide symporter (NIS). Nucl Med Biol 29, 13-18.

Dadachova*, et al.* (2005). Treatment with rhenium-188-perrhenate and iodine-131 of NIS-expressing mammary cancer in a mouse model remarkably inhibited tumor growth. Nucl Med Biol 32, 695-700.

Dai*, et al.* (1996). Cloning and characterization of the thyroid iodide transporter. Nature 379, 458-460.

De Bruin*, et al.* (2007). Cellular dynamics of EGF receptor-targeted synthetic viruses. Mol Ther 15, 1297-1305.

De*, et al.* (2000). Molecular analysis of the sodium/iodide symporter: impact on thyroid and extrathyroid pathophysiology. Physiol Rev 80, 1083-1105.

De Wolf*, et al.* (2008). Plasmid CpG depletion improves degree and duration of tumor gene expression after intravenous administration of polyplexes. Pharm Res 25, 1654-1662.

Diagaradjane*, et al.* (2008). Imaging epidermal growth factor receptor expression in vivo: pharmacokinetic and biodistribution characterization of a bioconjugated quantum dot nanoprobe. Clin Cancer Res 14, 731-741.

Dingli*, et al.* (2003a). Genetically targeted radiotherapy for multiple myeloma. Blood 102, 489-496.

Dingli*, et al.* (2004). Image-guided radiovirotherapy for multiple myeloma using a recombinant measles virus expressing the thyroidal sodium iodide symporter. Blood 103, 1641-1646.

Dingli*, et al.* (2003b). In vivo imaging and tumor therapy with the sodium iodide symporter. J Cell Biochem 90, 1079-1086.

Dmitriev*, et al.* (2000). Ectodomain of coxsackievirus and adenovirus receptor genetically fused to epidermal growth factor mediates adenovirus targeting to epidermal growth factor receptor-positive cells. J Virol 74, 6875-6884.

Dohan*, et al.* (2003). The sodium/iodide Symporter (NIS): characterization, regulation, and medical significance. Endocr Rev 24, 48-77.

Dufes*, et al.* (2005). Synthetic anticancer gene medicine exploits intrinsic antitumor activity of cationic vector to cure established tumors. Cancer Res 65, 8079-8084.

Dwyer*, et al.* (2005a). In vivo Radioiodide Imaging and Treatment of Breast Cancer Xenografts after MUC1-Driven Expression of the Sodium Iodide Symporter. Clin Cancer Res 11, 1483-1489.

Dwyer, *et al.* (2006a). Adenovirus-mediated and targeted expression of the sodium-iodide symporter permits in vivo radioiodide imaging and therapy of pancreatic tumors. Hum Gene Ther 17, 661-668.

Dwyer, *et al.* (2006b). Sodium iodide symporter-mediated radioiodide imaging and therapy of ovarian tumor xenografts in mice. Gene Ther 13, 60-66.

Dwyer, *et al.* (2005b). A Preclinical Large Animal Model of Adenovirus-Mediated Expression of the Sodium-Iodide Symporter for Radioiodide Imaging and Therapy of Locally Recurrent Prostate Cancer. Mol Ther 12, 835-841.

Everts, and Van Der Poel. (2005). Replication-selective oncolytic viruses in the treatment of cancer. Cancer Gene Ther 12, 141-161.

Faivre, *et al.* (2004). Long-Term Radioiodine Retention and Regression of Liver Cancer after Sodium Iodide Symporter Gene Transfer in Wistar Rats. Cancer Res 64, 8045-8051.

Forrest, *et al.* (2003). A degradable polyethylenimine derivative with low toxicity for highly efficient gene delivery. Bioconjug Chem 14, 934-940.

Gerolami, *et al.* (2003). Gene therapy of hepatocarcinoma: a long way from the concept to the therapeutical impact. Cancer Gene Ther 10, 649-660.

Goel, *et al.* (2007). Radioiodide imaging and radiovirotherapy of multiple myeloma using VSV(Delta51)-NIS, an attenuated vesicular stomatitis virus encoding the sodium iodide symporter gene. Blood 110, 2342-2350.

Goula, *et al.* (1998). Size, diffusibility and transfection performance of linear PEI/DNA complexes in the mouse central nervous system. Gene Therapy 5, 712-717.

Groot-Wassink, *et al.* (2004). Quantitative imaging of Na/I symporter transgene expression using positron emission tomography in the living animal. Mol Ther 9, 436-442.

Hart. (1996). Tissue specific promoters in targeting systemically delivered gene therapy. Semin Oncol 23, 154-158.

Herve, *et al.* (2008). Internal radiotherapy of liver cancer with rat hepatocarcinoma-intestine-pancreas gene as a liver tumor-specific promoter. Hum Gene Ther 19, 915-926.

Hingorani, *et al.* (2010a). The biology of the sodium iodide symporter and its potential for targeted gene delivery. Curr Cancer Drug Targets 10, 242-267.

Hingorani, *et al.* (2010b). Therapeutic Effect of Sodium Iodide Symporter Gene Therapy Combined With External Beam Radiotherapy and Targeted Drugs That Inhibit DNA Repair. Mol Ther

Iyer*, et al.* (2006). Exploiting the enhanced permeability and retention effect for tumor targeting. Drug Discov Today 11, 812-818.

Jelic. (2009). Hepatocellular carcinoma: ESMO clinical recommendations for diagnosis, treatment and follow-up. Ann Oncol 20 Suppl 4, 41-45.

Kakinuma*, et al.* (2003). Probasin promoter (ARR(2)PB)-driven, prostate-specific expression of the human sodium iodide symporter (h-NIS) for targeted radioiodine therapy of prostate cancer. Cancer Res 63, 7840-7844.

Kang*, et al.* (2004). Establishment of a human hepatocellular carcinoma cell line highly expressing sodium iodide symporter for radionuclide gene therapy. J Nucl Med 45, 1571-1576.

Kircheis*, et al.* (2001a). Tumor targeting with surface-shielded ligand-polycation DNA complexes. J Control Release 72, 165-170.

Kircheis*, et al.* (1997). Coupling of cell-binding ligands to polyethylenimine for targeted gene delivery. Gene Ther 4, 409-418.

Kircheis*, et al.* (2001b). Polyethylenimine/DNA complexes shielded by transferrin target gene expression to tumors after systemic application. Gene Ther 8, 28-40.

Kloeckner*, et al.* (2006a). Gene carriers based on hexanediol diacrylate linked oligoethylenimine: effect of chemical structure of polymer on biological properties. Bioconjug Chem 17, 1339-1345.

Kloeckner*, et al.* (2006b). Degradable gene carriers based on oligomerized polyamines. Eur J Pharm 29, 414-425.

Klutz*, et al.* (2009). Targeted radioiodine therapy of neuroblastoma tumors following systemic nonviral delivery of the sodium iodide symporter gene. Clin Cancer Res 15, 6079-6086.

Krasnykh*, et al.* (1996). Generation of recombinant adenovirus vectors with modified fibers for altering viral tropism. J Virol 70, 6839-6846.

Kunath*, et al.* (2003). Integrin targeting using RGD-PEI conjugates for in vitro gene transfer. J Gene Med 5, 588-599.

Lai*, et al.* (1995). Hepatic resection for hepatocellular carcinoma. An audit of 343 patients. Ann Surg 221, 291-298.

Lee*, et al.* (1982). The surgical management of primary carcinoma of the liver. World J Surg 6, 66-75.

Li*, et al.* (2010). Oncolytic measles viruses encoding interferon beta and the thyroidal sodium iodide symporter gene for mesothelioma virotherapy. Cancer Gene Ther 17, 550-558.

Li*, et al.* (2005). Identification and characterization of a novel peptide ligand of epidermal growth factor receptor for targeted delivery of therapeutics. Faseb J 19, 1978-1985.

Liu*, et al.* (2005). Interstitial diphtheria toxin-epidermal growth factor fusion protein therapy produces regressions of subcutaneous human glioblastoma multiforme tumors in athymic nude mice. Clin Cancer Res  11, 329-334.

Liu*, et al.* (2010). Systemic therapy of disseminated myeloma in passively immunized mice using measles virus-infected cell carriers. Mol Ther 18, 1155-1164.

Maeda. (2001). The enhanced permeability and retention (EPR) effect in tumor vasculature: the key role of tumor-selective macromolecular drug targeting. Adv Enzyme Regul 41, 189-207.

Marsee*, et al.* (2004). Imaging of metastatic pulmonary tumors following NIS gene transfer using single photon emission computed tomography. Cancer Gene Ther 11, 121-127.

Matsumura, and Maeda. (1986). A new concept for macromolecular therapeutics in cancer chemotherapy: mechanism of tumoritropic accumulation of proteins and the antitumor agent smancs. Cancer Res 46, 6387-6392.

Mendelsohn, and Baselga. (2006). Epidermal growth factor receptor targeting in cancer. Semin Oncol 33, 369-385.

Merron*, et al.* (2007). SPECT/CT imaging of oncolytic adenovirus propagation in tumours in vivo using the Na/I symporter as a reporter gene. Gene Ther 14, 1731-1738.

Meyer, and Wagner. (2006). Recent developments in the application of plasmid DNA-based vectors and small interfering RNA therapeutics for cancer. Hum Gene Ther 17, 1062-1076.

Navarro*, et al.* (2010). Low generation PAMAM dendrimer and CpG free plasmids allow targeted and extended transgene expression in tumors after systemic delivery. J Control Release 146, 99-105.

Ogris*, et al.* (1999). PEGylated DNA/transferrin-PEI complexes: reduced interaction with blood components, extended circulation in blood and potential for systemic gene delivery. Gene Ther 6, 595-605.

Peerlinck*, et al.* (2009). Targeted radionuclide therapy using a Wnt-targeted replicating adenovirus encoding the Na/I symporter. Clin Cancer Res 15, 6595-6601.

Penheiter, *et al.* (2010). Sodium Iodide Symporter (NIS)-Mediated Radiovirotherapy for Pancreatic Cancer. AJR Am J Roentgenol 195, 341-349.

Perez-Torres, *et al.* (2006). Epidermal growth factor receptor (EGFR) antibody down-regulates mutant receptors and inhibits tumors expressing EGFR mutations. J Biol Chem 281, 40183-40192.

Petrich, *et al.* (2006). Effective Cancer Therapy with the {alpha}-Particle Emitter [211At]Astatine in a Mouse Model of Genetically Modified Sodium/Iodide Symporter-Expressing Tumors. Clin Cancer Res 12, 1342-1348.

Russ, *et al.* (2008a). Oligoethylenimine-grafted polypropylenimine dendrimers as degradable and biocompatible synthetic vectors for gene delivery. Journal Control Release 132, 131-140.

Russ, *et al.* (2008). Novel degradable oligoethylenimine acrylate ester-based pseudodendrimers for in vitro and in vivo gene transfer. Gene Ther 15, 18-29.

Russ, and Wagner. (2007). Cell and Tissue Targeting of Nucleic Acids for Cancer Gene Therapy Pharm Res 24, 1047-1057.

Schaffert, *et al.* (2010). Poly(I:C)-Mediated Tumor Growth Suppression in EGF-Receptor Overexpressing Tumors Using EGF-Polyethylene Glycol-Linear Polyethylenimine as Carrier. Pharm Res.

Scholz, *et al.* (2005). Radioiodine therapy of colon cancer following tissue-specific sodium iodide symporter gene transfer. Gene Ther. 12, 272-80.

Scholz, *et al.* (2004). Dexamethasone enhances the cytotoxic effect of radioiodine therapy in prostate cancer cells expressing the sodium iodide symporter. J Clin Endocrinol Metab 89, 1108-1116.

Schwerdt, *et al.* (2008). Hyperthermia-induced targeting of thermosensitive gene carriers to tumors. Hum Gene Ther 19, 1283-1292.

Shariff, *et al.* (2009). Hepatocellular carcinoma: current trends in worldwide epidemiology, risk factors, diagnosis and therapeutics. Expert Rev Gastroenterol Hepatol 3, 353-367.

Shir, *et al.* (2006). EGF receptor-targeted synthetic double-stranded RNA eliminates glioblastoma, breast cancer, and adenocarcinoma tumors in mice. PLoS Med 3, e6.

Smanik, *et al.* (1996). Cloning of the human sodium Iodide symporter. Biochem Biophys Res Commun 226, 339-345.

Smanik, *et al.* (1997). Expression, exon-intron organization, and chromosome mapping of the human sodium iodide symporter. Endocrinology 138, 3555-3558.

Smrekar, *et al.* (2003). Tissue-dependent factors affect gene delivery to tumors in vivo. Gene Ther 10, 1079-1088.

Song, *et al.* (2008). Peptide ligand-mediated liposome distribution and targeting to EGFR expressing tumor in vivo. Int J Pharm 363, 155-161.

Spitzweg, *et al.* (2007). Image-guided radioiodide therapy of medullary thyroid cancer after carcinoembryonic antigen promoter-targeted sodium iodide symporter gene expression. Hum Gene Ther 18, 916-24.

Spitzweg, *et al.* (2007a) Der Natrium-Iodid-Symporter (NIS): Bedeutung für die Bildgebung und therapeutische Optionen. Nuklearmediziner 30, 1-12.

Spitzweg, *et al.* (2001a). In vivo sodium iodide symporter gene therapy of prostate cancer. Gene Ther 8, 1524-1531.

Spitzweg, *et al.* (2001b). Expression of the sodium iodide symporter in human kidney. Kidney Int 59, 1013-1023.

Spitzweg, *et al.* (2001c). Clinical review 132: The sodium iodide symporter and its potential role in cancer therapy. J Clin Endocrinol Metab 86, 3327-3335.

Spitzweg, *et al.* (2000a). Thyroid iodine transport. Thyroid 10, 321-330.

Spitzweg, *et al.* (1998). Analysis of human sodium iodide symporter gene expression in extrathyroidal tissues and cloning of its complementary deoxyribonucleic acids from salivary gland, mammary gland, and gastric mucosa. J Clin Endocrinol Metab 83, 1746-1751.

Spitzweg, *et al.* (1999a). Regulation of sodium iodide symporter gene expression in FRTL-5 rat thyroid cells. Thyroid 9, 821-830.

Spitzweg, *et al.* (1999b). Analysis of human sodium iodide symporter immunoreactivity in human exocrine glands. J Clin Endocrinol Metab 84, 4178-84.

Spitzweg, and Morris. (2001). Approaches to gene therapy with sodium/iodide symporter. Exp.Clin.Endocrinol.Diabetes 109, 56-59.

Spitzweg, and Morris. (2002a). Sodium iodide symporter (NIS) and thyroid. Hormones (Athens.) 1, 22-34.

Spitzweg, and Morris. (2002b). The sodium iodide symporter: its pathophysiological and therapeutic implications. Clin Endocrinol (Oxf) 57, 559-574.

Spitzweg, *et al.* (2000b). Treatment of prostate cancer by radioiodine therapy after tissue-specific expression of the sodium iodide symporter. Cancer Res 60, 6526-6530.

Spitzweg, *et al.* (2003). Retinoic acid-induced stimulation of sodium iodide symporter expression and cytotoxicity of radioiodine in prostate cancer cells. Endocrinology 144, 3423-32.

Spitzweg, *et al.* (1999c). Prostate-specific antigen (PSA) promoter-driven androgen-inducible expression of sodium iodide symporter in prostate cancer cell lines. Cancer Res 59, 2136-41.

Trujillo, *et al.* (2010). A probasin promoter, conditionally replicating adenovirus that expresses the sodium iodide symporter (NIS) for radiovirotherapy of prostate cancer. Gene Ther

Unterholzner, *et al.* (2006). Dexamethasone stimulation of retinoic Acid-induced sodium iodide symporter expression and cytotoxicity of 131-I in breast cancer cells. J Clin Endocrinol Metab 91, 69-78.

Van Nostrand, and Wartofsky. (2007). Radioiodine in the treatment of thyroid cancer. Endocrinol Metab Clin North Am 36, 807-822.

Verma, and Somia. (1997). Gene therapy - promises, problems and prospects. Nature 389, 239-242.

Wapnir, *et al.* (2004). The Na+/I- Symporter Mediates Iodide Uptake in Breast Cancer Metastases and Can Be Selectively Down-Regulated in the Thyroid. Clin Cancer Res 10, 4294-4302.

Watanabe, *et al.* (2010). Delivery of Na/I symporter gene into skeletal muscle using nanobubbles and ultrasound: visualization of gene expression by PET. J Nucl Med 51, 951-958.

Weiss, *et al.* (1984). Iodide transport in a continuous line of cultured cells from rat thyroid. Endocrinology 114, 1090-1098.

Willhauck, *et al.* (2008a). The potential of (211)Astatine for NIS-mediated radionuclide therapy in prostate cancer. Eur J Nucl Med Mol Imaging 35, 1272-1281.

Willhauck, *et al.* (2007). Application of 188rhenium as an alternative radionuclide for treatment of prostate cancer after tumor-specific sodium iodide symporter gene expression. J Clin Endocrinol Metab 92, 4451-4458.

Willhauck, *et al.* (2008b). Alpha-fetoprotein promoter-targeted sodium iodide symporter gene therapy of hepatocellular carcinoma. Gene Ther 15, 214-223.

Willhauck, *et al.* (2008c). Functional sodium iodide symporter expression in breast cancer xenografts in vivo after systemic treatment with retinoic acid and dexamethasone. Breast Cancer Res Treat 109, 263-272.

Wolf, *et al.* (2004). A phase I study of Adp53 (INGN 201; ADVEXIN) for patients with platinum- and paclitaxel-resistant epithelial ovarian cancer. Gynecol Oncol 94, 442-448.

Wolschek, *et al.* (2002). Specific systemic nonviral gene delivery to human hepatocellular carcinoma xenografts in SCID mice. Hepatology 36, 1106-1114.

Zanta, *et al.* (1997). In vitro gene delivery to hepatocytes with galactosylated polyethylenimine. Bioconjugate Chemistry 8 (6), 839-844.

Zhang, *et al.* (1999). Development and application of a minimal-adenoviral vector system for gene therapy of hemophilia A. Thromb Haemost 82, 562-571.

Zintchenko, *et al.* (2009). Drug nanocarriers labeled with near-infrared-emitting quantum dots (quantoplexes): imaging fast dynamics of distribution in living animals. Mol Ther 17, 1849-1856.

# 9.  Acknowledgments

First of all I would like to thank Prof. Dr. C. Spitzweg for giving me the opportunity to work on this exciting project, for providing me with all the equipment and infrastructure needed for my work as well as for her continuous support, encouragement and excellent supervision throughout my PhD thesis.

I would further like to thank Prof. Dr. E. Wagner for many helpful discussions and for accepting me as an external PhD student at the Department of Pharmacy, Center of Drug Research, Pharmaceutical Biology-Biotechnology, Ludwig-Maximilians-University, Munich.

I am also very grateful to PD Dr. M. Ogris for his scientific support, for his always helpful advice and many fruitful discussions and for a great collaboration. Also all of his lab members are gratefully acknowledged for their help.

Many thanks to all members of the Spitzweg laboratory, Dr. Michael J Willhauck, Nathalie Schwenk, Kerstin Knoop, Geoffrey K Grünwald, Kim Bentrup (ex-member), Alexandra Vetter, Marie Kolokythas, for listening, helping, for all the fun we had and for so much more, I enjoyed working with you.

I would further like to thank the members of the departments of Nuclear Medicine at the Klinikum Großhadern (director: Prof. Dr. P. Bartenstein) and at the Klinikum rechts der Isar (director: Prof. Dr. M. Schwaiger), for the great support and technical assistance during the imaging studies. My personal thanks go to Prof. Dr. Dr. R. Senekowitsch-Schmidtke for her always helpful scientific support.

Moreover, I am grateful to Dr. P. S. Holm and his group members for an excellent collaboration during the studies on adenoviral gene delivery.

I am also grateful to the Members of SFB 824 for their collaboration.

# 10. Curriculum Vitae

**Personal data:**

| | |
|---|---|
| Name: | Kathrin Klutz |
| Date of birth: | February 09th, 1975 |
| Place of birth: | Aalen, Germany |
| Nationality: | German |

**Education:**

12/2006 – 10/2010:  PhD thesis at the Department of Internal Medicine II,
Ludwig-Maximillians-University Munich
in collaboration with the Department of Pharmacy, Center of Drug
Research, Pharmaceutical Biology-Biotechnology,
Ludwig-Maximillians-University, Munich, Germany
supervisor: Prof. Dr. C. Spitzweg, Prof. Dr. Ernst Wagner

04/2002 – 06/2006:  Studies of Biology, University of Technology, Darmstadt, Germany

10/1997 – 03/2002:  Studies of Dentistry at the Medical University Ulm, Germany

08/1996 – 08/1997:  Foreigner University of Perugia, Italia

08/1991 – 06/1995:  Secondary School, Justus von Liebig Gymnasium, Aalen, Germany